The Astrophysical Journal, 703:1696–1724, 2009 October 1 doi:10.1088/0004-637X/703/2/1696

DISCERNING THE PHYSICAL ORIGINS OF COSMOLOGICAL GAMMA-RAY BURSTS BASED ON MULTIPLE OBSERVATIONAL CRITERIA: THE CASES OF $z = 6.7$ GRB 080913, $z = 8.2$ GRB 090423, AND SOME SHORT/HARD GRBs

Bing Zhang[1], Bin-Bin Zhang[1], Francisco J. Virgili[1], En-Wei Liang[2], D. Alexander Kann[3], Xue-Feng Wu[4,5], Daniel Proga[1], Hou-Jun Lv[2], Kenji Toma[4], Peter Mészáros[4,6], David N. Burrows[4], Peter W. A. Roming[4], and Neil Gehrels[7]

[1] Department of Physics and Astronomy, University of Nevada Las Vegas, Las Vegas, NV 89154, USA
[2] Department of Physics, Guangxi University, Guangxi 530004, China
[3] Thüringer Landessternwarte Tautenburg, D-07778, Tautenburg, Germany
[4] Department of Astronomy & Astrophysics, Pennsylvania State University, University Park, PA 16802, USA
[5] Purple Mountain Observatory, Chinese Academy of Sciences, Nanjing 210008, China
[6] Department of Physics, Pennsylvania State University, University Park, PA 16801, USA
[7] NASA Goddard Space Flight Center, Greenbelt, MD 20771, USA
Received 2009 February 13; accepted 2009 August 10; published 2009 September 11

ABSTRACT

The two high-redshift gamma-ray bursts, GRB 080913 at $z = 6.7$ and GRB 090423 at $z = 8.2$, recently detected by *Swift* appear as intrinsically short, hard GRBs. They could have been recognized by BATSE as short/hard GRBs should they have occurred at $z \leqslant 1$. In order to address their physical origin, we perform a more thorough investigation on two physically distinct types (Type I/II) of cosmological GRBs and their observational characteristics. We reiterate the definitions of Type I/II GRBs and then review the following observational criteria and their physical motivations: supernova (SN) association, specific star-forming rate (SFR) of the host galaxy, location offset, duration, hardness, spectral lag, statistical correlations, energetics and collimation, afterglow properties, redshift distribution, luminosity function, and gravitational wave signature. Contrary to the traditional approach of assigning the physical category based on the gamma-ray properties (duration, hardness, and spectral lag), we take an alternative approach to define the Type I and Type II Gold Samples using several criteria that are more directly related to the GRB progenitors (SN association, host galaxy type, and specific SFR). We then study the properties of the two Gold Samples and compare them with the traditional long/soft and short/hard samples. We find that the Type II Gold Sample reasonably tracks the long/soft population, although it includes several intrinsically short (shorter than 1 s in the rest frame) GRBs. The Type I Gold Sample only has five GRBs, four of which are not strictly short but have extended emission. Other short/hard GRBs detected in the *Swift* era represent the BATSE short/hard sample well, but it is unclear whether all of them belong to Type I. We suggest that some (probably even most) high-luminosity short/hard GRBs instead belong to Type II. Based on multiple observational criteria, we suggest that GRB 080913 and GRB 090423 are more likely Type II events. In general, we acknowledge that it is not always straightforward to discern the physical categories of GRBs, and re-emphasize the importance of invoking multiple observational criteria. We cautiously propose an operational procedure to infer the physical origin of a given GRB with available multiple observational criteria, with various caveats laid out.

Key words: gamma rays: bursts

1. INTRODUCTION

Phenomenologically, gamma-ray bursts (GRBs) have been generally classified into the long-duration, soft-spectrum class and the short-duration, hard-spectrum class in the *Compton Gamma Ray Observatory (CGRO)*/BATSE era based on the bimodal distribution of GRBs in the duration-hardness diagram (Kouveliotou et al. 1993).[8] There is no clear boundary line in this diagram to separate the two populations. Traditionally, an observer-frame BATSE-band duration $T_{90} \sim 2$ s has been taken as the separation line: bursts with $T_{90} > 2$s are "long" and bursts with $T_{90} < 2$ s are "short."

The journey was long to uncover the physical origins of these two phenomenologically different classes of GRBs. The discoveries and the routine observations of the broad band afterglows of long GRBs reveal that their host galaxies are typically irregular (in a few cases spiral) galaxies with intense star formation (Fruchter et al. 2006). In a handful of cases these GRBs are firmly associated with Type Ib/c supernovae (SNe; e.g., Hjorth et al. 2003; Stanek et al. 2003; Campana et al. 2006; Pian et al. 2006). This strongly suggests that they are likely related to deaths of massive stars. Theoretically, the "collapsar" model of GRBs has been discussed over the years as the standard scenario for long GRBs (Woosley 1993; Paczýnski 1998; MacFadyen & Woosley 1999; Woosley & Bloom 2006).

The breakthrough to understand the nature of some short GRBs was made in 2005 after the launch of the *Swift* satellite (Gehrels et al. 2004). Prompt localizations and deep afterglow searches for a handful of short GRBs (Gehrels et al. 2005; Bloom et al. 2006; Fox et al. 2005; Villasenor et al. 2005; Hjorth et al. 2005a; Barthelmy et al. 2005a; Berger et al. 2005) suggest that some of them are associated with nearby early-type galaxies with little star formation. Deep searches of associated SNe from these events all led to non-detections (e.g., Kann et al. 2008 and references therein, see also the Appendix for more references).

[8] Several analyses have suggested the existence of an intermediate duration group (Mukherjee et al. 1998; Horvath 1998; Hakkila et al. 2000). However, as discussed in the bulk of the text below, there is so far no strong indication of the existence of a third, physically distinct category of cosmological GRBs based on multiple observational data. So we will focus on the two main phenomenological categories of GRBs in the rest of the paper.

These are in stark contrast to the bursts detected in the pre-*Swift* era (mostly long duration). On the other hand, the observations are consistent with (although not a direct proof of) the long-sought progenitor models that invoke mergers of two compact stellar objects, leading candidates being Neutron Star–Neutron Star (NS–NS) and Neutron Star–Black Hole (NS–BH) systems (Paczýnski 1986; Eichler et al. 1989; Paczýnski 1991; Narayan et al. 1992). Although the sample with secure host galaxies is small, a general trend in the community is to accept that the BATSE short/hard population bursts are of this compact star merger origin.[9]

The clean dichotomy of the two populations (both phenomenological and physical) was soon muddled by the detection of a nearby long-duration GRB without SN association (Gehrels et al. 2006; Gal-Yam et al. 2006; Fynbo et al. 2006; Della Valle et al. 2006a). GRB 060614 has $T_{90} \sim 100$s in the *Swift*/BAT (Barthelmy et al. 2005b) band, which phenomenologically definitely belongs to the long-duration category. On the other hand, the light curve is characterized by a short/hard spike (with a duration ∼5 s) followed by a series of soft gamma-ray pulses. The spectral lag at the short/hard spike is negligibly small, a common feature of the short/hard GRBs (Gehrels et al. 2006). Very stringent upper limits on the radiation flux from an underlying SN have been established (Gal-Yam et al. 2006; Fynbo et al. 2006; Della Valle et al. 2006a). These facts are consistent with the compact star merger scenario. More interestingly, this burst looks like a more energetic version of GRB 050724, the "smoking-gun" burst of the compact star merger population (Barthelmy et al. 2005a; Berger et al. 2005). Zhang et al. (2007a) showed that if one applies the $E_p \propto E_{\gamma,\rm iso}^{1/2}$ relation (Amati et al. 2002; Liang et al. 2004) to GRB 060614 and makes it as energetic as GRB 050724, the pseudo-burst would be detected as a marginal short/hard burst by BATSE, and would be very similar to GRB 050724 if detected by *Swift*/BAT. In particular, the soft gamma-ray tail would appear as the "extended emission" detected in some "short/hard" GRBs including GRB 050724. A second, much shorter (with $T_{90} \sim 4$ s) burst without SN association, GRB 060505, was detected around the same time (Fynbo et al. 2006). However, the physical nature of this burst is subject to intense debate (Ofek et al. 2007; Thöne et al. 2008; McBreen et al. 2008; Kann et al. 2008).

In any case, duration and hardness are not necessarily reliable indicators of the *physical* nature of a GRB any more. In order to determine whether or not a GRB can be associated with a particular physical model, one is forced to appeal to multiple observational criteria (Donaghy et al. 2006). Prompted by the detection of GRB 060614, we (Zhang et al. 2007a; Zhang 2006) suggested naming the bursts that are consistent with the massive-star origin and the compact-star-merger origin models as Type II and Type I, respectively,[10] and attempted to invoke a set of multiple observational criteria to judge the physical category of a GRB. A more developed physical categorization scheme was proposed by Bloom et al. (2008), who also introduced soft gamma-ray repeater (SGR) giant-flare-like (non-destructive and likely repeating) events. Within the destructive events, Bloom et al. (2008) agreed that there are two major *model types* (degenerate and non-degenerate), which correspond to Type I and Type II in the Zhang et al.'s (2007a) classification scheme. Throughout this paper we will adopt the nomenclature of Type I/II to denote the two physically distinct categories of cosmological GRB models.

The recently detected two high-z GRBs, GRB 080913 at $z = 6.7$ (Greiner et al. 2009a) and GRB 090423 at $z = 8.2$ (Tanvir et al. 2009; Salvaterra et al. 2009) introduce a further complication to the scheme associating GRBs with particular theoretical models. Being the two GRBs with the highest redshifts as of the time of writing, these two bursts each have a redshift-corrected duration $[T_{90}/(1+z)]$ shorter than 2 s, with a hard spectrum typical for short/hard GRBs. This naturally raises the interesting question regarding the progenitor system of the burst (Greiner et al. 2009a; Perez-Ramirez et al. 2008; Belczynski et al. 2008; Tanvir et al. 2009; Salvaterra et al. 2009). More generally, it again raises the difficult question regarding how to use the observed properties to judge the physical origin of a GRB. In this paper, we make some attempts to address this difficult problem. The structure of the paper is the following. In Section 2, we present the observational properties of GRB 080913 and GRB 090423, and show that if the identical bursts had occurred at $z < 1$, they could have been recognized as short hard GRBs based on their observed properties. In Section 3, we comment on the strengths and weaknesses of classifying GRBs based on physically motivated criteria. We then reiterate the definitions of Type I/II GRBs in Section 4, and critically review a list of observational criteria as well as their physical motivations as discussed in the literature. In order to address the profound questions of whether "Type I = short/hard/short lag" and "Type II = long/soft/long lag," in Section 5 we take an alternative approach (from the traditional one) to assess the problem. Instead of associating a burst with a particular physical model (massive star core collapses versus compact star mergers) a priori based on its gamma-ray properties (duration, hardness, spectral lag), we use several observational properties that are more directly relevant to the GRB progenitors to define the Gold Samples of Type II and Type I GRBs. We then turn around to evaluate the various observational properties (duration, hardness, spectral lag, afterglow properties, empirical correlations, etc.) of these Gold Samples, and check whether these properties are useful criteria to judge the physical category of the bursts. In Section 6, we discuss the intriguing question whether all short/hard GRBs are of the Type I origin, and raise the possibility that a fraction of (probably even most) high-luminosity short GRBs are of the Type II origin. We then dedicate Section 7 to discuss the possible progenitors of GRB 080913 and GRB 090423, and argue that most likely they are both of the Type II origin. We acknowledge the difficulties of discerning the physical origins of GRBs in Section 8, and cautiously propose an operational procedure to associate a GRB with a specific model based on multiple observational criteria. Our results are summarized in Section 9.

2. GRB 080913 AND GRB 090423: INTRINSICALLY SHORT/HARD GRBS AT HIGH-Z

The light curve of GRB 080913 as detected by *Swift*/BAT is shown as the black solid curve in Figure 1(a). The burst duration T_{90} (the time interval during which 90% of the fluence is measured) in the BAT (15–150 keV) band is 8 ± 1 s. The average BAT band spectrum can be adequately fit by a power law with

[9] It is widely accepted that at least a fraction of short/hard GRBs are the giant flares of SGRs in nearby galaxies (Palmer et al. 2005; Tanvir et al. 2005). The observations suggest that the contribution from such a population is not significant (Nakar et al. 2006), but see Chapman et al. (2009). We do not discuss these bursts in this paper.

[10] The idea was to make a connection to the Type II and Type Ia SNe (not including Type Ib/c), which correspondingly have the massive star and compact star origins, respectively. This is however not related to the original definitions of Type II and Type I SNe, which are based on whether or not there are hydrogen lines in the spectrum.

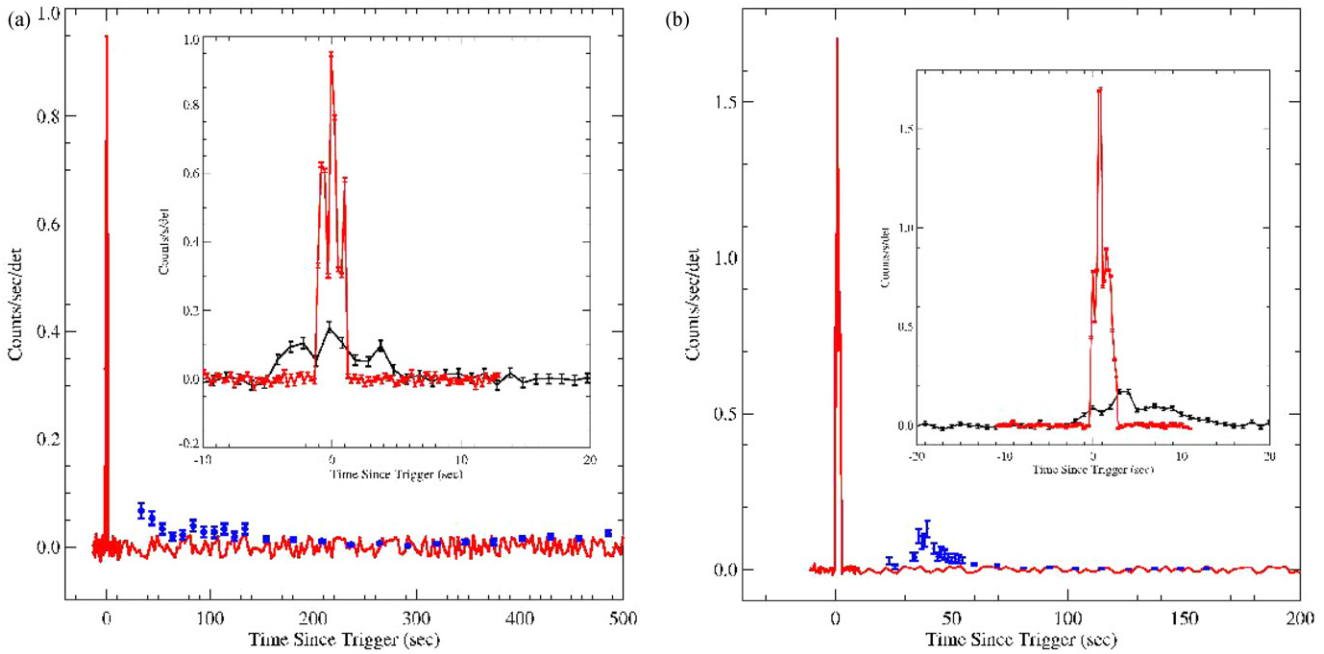

Figure 1. Simulated 15–150 keV light curves of the pseudo-GRBs obtained by placing GRB 080913 and GRB 090423 at $z = 1$. The red curves display the extrapolated BAT data, and the blue data points show the extrapolated XRT data. Inset: a comparison of the light curve of the pseudo-GRBs (red) and the observed GRBs (black). (a) GRB 080913; (b) GRB 090423.

exponential cutoff, with the peak energy $E_p = 93 \pm 56$ keV (Greiner et al. 2009a). A combined *Swift*/BAT and Konus/*Wind* (20–1300 keV) fit using the Band-function spectrum gives $E_p = 121^{+232}_{-39}$ keV (Palshin et al. 2008). Given the measured redshift $z = 6.7$ (Greiner et al. 2009a), this is translated to a rest-frame duration of $T_{90}^{\rm rest} \sim 1$ s, and a best-fit rest-frame peak energy $E_p^{\rm rest} \sim 710$ keV and $E_p^{\rm rest} \sim 930$ keV for the cutoff power law and Band-function spectra, respectively. Although being recognized as a long-duration burst phenomenologically, this burst has an intrinsically short duration and an intrinsically hard spectrum.

In order to compare this burst with other phenomenologically classified short hard GRBs, we simulate a "pseudo" GRB by placing GRB 080913 at $z = 1$. We consider three factors. First, the specific photon flux $N(E_p)$ at E_p is proportional to $(1+z)^2/D_L^2$, where D_L is the luminosity distance. This can be translated to an increase of a factor of ~6.8 of $N(E_p)$ from $z = 6.7$ to $z = 1$. Second, we consider the BAT band (15–150 keV) emission of the pseudo-GRB, which corresponds to an energy band lower by a factor of $(1+6.7)/(1+1) \sim 3.85$ in GRB 080913. We therefore extrapolate the observed BAT spectrum to lower energies and assume a similar light curve in that band. Third, we compress the timescale by a factor of ~3.85 to account for the cosmological time dilation effect. After applying these transformations, we are able to construct the BAT-band light curve of the pseudo-GRB at $z = 1$ as shown in Figure 1(a).

GRB 080913 displays a series of early X-ray flares (Greiner et al. 2009a). It is interesting to check whether they would show up in the BAT band for the pseudo-GRB to mimic the "extended emission" seen in a subgroup of *Swift* "short/hard" GRBs (Norris & Bonnell 2006; Troja et al. 2008).[11] We therefore manipulate

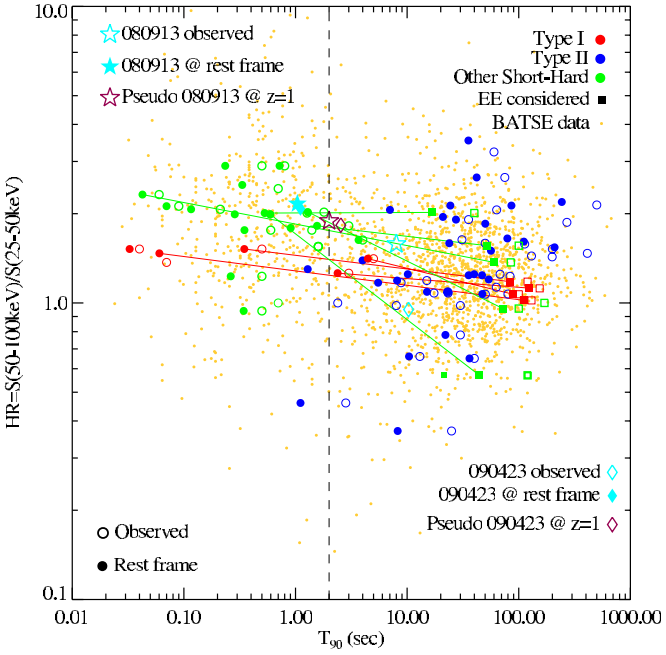

Figure 2. T_{90}–HR diagram of GRBs. The background orange dots are BATSE GRBs. Overplotted are Type II Gold Sample (blue), Type I Gold Sample (red), and other short/hard GRBs (green), mostly detected by *Swift*. Open symbols are for the observed values, while the filled symbols are the rest-frame values. For short GRBs with extended emission, those with the short spike only are denoted as circles, while those including the extended emission are denoted as squares. The same bursts (with different T_{90} with or without extended emission) are connected by lines. GRB 080913, GRB 090423, their pseudo-counterparts at $z = 1$, and their rest-frame counterparts are marked with special colors/symbols.

the X-Ray Telescope (XRT; Burrows et al. 2005b) data of GRB 080913 to simulate the BAT-band-extended emission of the pseudo-burst. We first extrapolate the GRB 080913 XRT data to the BAT band according to the measured XRT photon spectral index. We then follow the three steps mentioned above to shift this BAT-band "virtual" emission to the BAT-band emission

[11] Rigorously based on the T_{90} criterion, the fraction of *Swift* bursts that have $T_{90} < 2$ s is much smaller than that of BATSE bursts. Many display extended emission that extends T_{90} up to several 10 s to even more than 100 s. The current approach in the community is to define a burst "short/hard" if it appears short in the BATSE band. A growing trend is to also include some bursts with extended emission even in the BATSE band to the "short/hard" category.

of the pseudo-burst. This is shown as blue data points in Figure 1(a). By adding the appropriate noise level for the BAT observation, we show that these extrapolated XRT emission components stick out the background, which would appear as the extended emission in the BAT band for the pseudo-burst. We note that our method is based on the assumption of the power-law extension of the X-ray flare spectrum (0.3–10 keV) to the BAT band of the pseudo-burst (1.3–39 keV). On the other hand, since X-ray flares are generally believed to be due to GRB late central engine activities (Burrows et al. 2005a; Zhang et al. 2006; Lazzati & Perna 2007; Chincarini et al. 2007), they may have a Band function or cutoff power-law spectrum (Falcone et al. 2007). If the E_p's of the X-ray flares are within or not far above the XRT window, the extrapolated extended emission would be degraded. We should therefore regard the level of the extended emission of the pseudo-burst as an upper limit. We estimate the BAT-band duration of the pseudo-GRB as $T_{90}(\mathrm{pseudo}) \sim 2.0$ s without extended emission or $T_{90}(\mathrm{pseudo, EE}) \sim 140$ s with extended emission. In any case, the observational properties of this pseudo-burst are very similar to some "short/hard" GRBs detected in the *Swift* era. By comparing the flux level of the pseudo-GRB with other short/hard GRBs, we find that it belongs to the bright end of the short/hard GRB flux distribution, similar to, e.g., GRB 051221A (Burrows et al. 2006; Soderberg et al. 2006b), GRB 060313 (Roming et al. 2006), GRB 060121 (Donaghy et al. 2006), and the recent GRB 090510 detected by Fermi LAT/GBM and *Swift* (Hoversten et al. 2009; Ohno et al. 2009; Guiriec et al. 2009; Rau et al. 2009).

GRB 090423 at $z = 8.2$ is amazingly similar to GRB 080913. It was detected by *Swift*/BAT with a BAT-band $T_{90} \sim 10.3$ s (Tanvir et al. 2009). Given the measured redshift $z = 8.26^{+0.07}_{-0.08}$ (Tanvir et al. 2009), the corresponding rest-frame duration is $\sim T_{90}/(1+z) \sim 1.1$ s. The peak energy measured by BAT is $E_p = 48.6 \pm 6.2$ keV, corresponding to a rest-frame value $E_p^{\mathrm{rest}} = 451 \pm 58$ keV. We performed a similar analysis on GRB 080913. The results are shown in Figure 1(b). Nearly identical conclusions can be drawn from both bursts.

In the above analyses, the intrinsic duration of a burst is defined as $T_{90}/(1+z)$, and the duration of the corresponding pseodo-GRB at $z = 1$ is defined as $2T_{90}/(1+z)$. These calculated durations correspond to different energy bands in the rest frame (the same observed band after redshifting). Strictly speaking, in order to derive the durations of the pseudo-GRBs in the observed energy band, one needs to know the time-dependent spectral information, which is not available for these bursts. Observationally, pulse widths at high energies tend to be narrower than those at low energies (Ford et al. 1995; Romano et al. 2006; Page et al. 2007). An empirical relation $w \propto E^{-a}$ with $a \sim 0.3$ has been suggested (Fenimore et al. 1995; Norris et al. 2005; Liang et al. 2006). For a given observed energy band, this suggests $w \propto (1+z)^{-a}$, which would correspond to a correction factor of $(1+z)^{a-1}$ rather than $(1+z)^{-1}$ to derive the intrinsic duration. However, GRB prompt emission is usually composed of multiple pulses. The separations between the pulses, which are more relevant for the T_{90} definition, may not follow the same energy dependence of the pulse widths. We therefore do not introduce this extra correction factor of T_{90} throughout the paper. For GRB 080913 and GRB 090423, if one takes the $(1+z)^{a-1}$ correction factor, the derived intrinsic durations are in the marginal regime between the phenomenologically defined long and short GRBs.

Figure 2 displays the locations of GRB 080913, GRB 090423, their corresponding pseudo-GRBs at $z = 1$, and their rest-frame counterparts in the traditional T_{90}–hardness ratio (HR) two-dimensional distribution plane. Also plotted are the BATSE GRB sample (orange), the Gold Samples of Type II (blue) and Type I (red) GRBs, and the Other SGRB Sample (green) (see Section 5 for the details of the sample definitions). It is evident that GRB 080913 and GRB 090423 would have been recognized as phenomenologically short/hard GRBs should they have occurred at $z \leqslant 1$.

3. PHENOMENOLOGICAL VS. PHYSICAL CLASSIFICATION SCHEMES: WEAKNESSES AND STRENGTHS

The eventual goal of GRB studies is to identify the physical origins of every observed GRB, including its progenitor system, central engine, energy dissipation mechanism, and radiation mechanism. To achieve this goal, a combination of observations and theoretical modeling is needed. The number of competitive models and the allowed parameter space steadily reduce as more and more observational data are accumulated. This is evident in the history of GRB studies: while more than 100 models were proposed before 1992 (Nemiroff 1994), only two broad categories of progenitor models remain competitive at the time when this paper is written. A group of GRBs are hosted by active star-forming dwarf galaxies (Fruchter et al. 2006), some of which have clear (Type Ic) SN associations (Hjorth et al. 2003; Stanek et al. 2003; Campana et al. 2006; Pian et al. 2006). This points toward a massive star origin of this group of bursts. At least a few bursts were discovered to be associated with galaxies with a very low star-forming rate (SFR; Gehrels et al. 2005; Bloom et al. 2006; Barthelmy et al. 2005a; Berger et al. 2005), which point toward a non-massive-star origin of the bursts, likely due to mergers of compact objects. Therefore it is now justified to discuss at least two physically distinct categories of GRB models as well as how to associate a particular burst with either category based on certain observational criteria.

In the literature, some physical classification schemes of GRBs have been discussed (Zhang et al. 2007a; Bloom et al. 2008). Strictly speaking, these are not classifications of GRBs, but are classifications of models that interpret GRB data. A scientific classification scheme is based on statistical formalisms, which make use of a uniform set of observational data with instrumental biases properly corrected, and classify objects based on statistically significant clustering of some measured properties. Examples include to classify SNe broadly into Type II/I based on whether there are/are not hydrogen lines in the optical spectrum, and to classify GRBs into two (Kouveliotou et al. 1993) or three (Mukherjee et al. 1998; Horvath 1998) classes based on BATSE T_{90} analyses. The classes defined by the phenomenological data do not carry physical meanings, and theoretical modeling is needed to clarify whether different phenomenological classes of objects are of different physical origins. Compared with the SN classification schemes, which are based on the "yes/no" criteria regarding the existence of spectral lines and therefore are relatively insensitive to the instrumental details, the GRB phenomenological classification schemes suffer another major drawback, i.e., every parameter that one can directly measure is strongly instrument dependent. For example, T_{90} is strongly energy dependent, and sensitivity dependent, so that a "short" GRB in a hard energy band would become a "long" GRB in softer bands or if the detector sensitivity is increased. The membership of a particular GRB to a particular category (e.g., long versus short) is not guaranteed. As a

result, such classification schemes cannot be compared from one mission to another, and are of limited scientific value.

A physical classification scheme, on the other hand, is on theoretical models that interpret the data. As a result, it suffers the great difficulty of associating a particular burst with a particular model category. In order to achieve the goal, multiple observational criteria are demanded, but always with non-uniform instrumental selection effects. Ideally, with infinitely sensitive detectors in all wavelengths, it may be possible to derive a set of quantitative observational criteria that can be used to rigorously associate a particular GRB with a particular model category based on statistical properties. However, realistically this is essentially impossible since different criteria rely on completely different observational instruments with different observational bands and sensitivities which are quite non-uniform. Also different criteria could carry different weights in judging the associated model category of a particular burst. The weighting factors of different criteria are also difficult to quantify. Human insights rather than pure statistical analyses are needed. Another drawback of a physical classification scheme of models is that it depends on the models, which are subject to further development as more data are accumulated. The classification criteria are therefore also subject to modification based on data. This can be diminished by invoking model-independent criteria as much as possible. For example, the Type I/II GRB model classification scheme discussed in this paper only appeals to whether the model invokes a degenerate star or a massive star, regardless of the concrete progenitor systems or energy dissipation and radiation mechanisms (see Section 4 for full discussion).

Despite of its weaknesses, a physical classification scheme of models and associating a particular object with a particular model class have the strength to achieve a better understanding of the physical origin of astrophysical objects. For example, in the SN field, there is now a consensus that only a sub-group of Type I SNe (Type Ia) has a distinct physical origin, which is related to explosive disruptions of white dwarfs. The other two sub-types of Type I SNe (Type Ib/Ic) are more closely related to Type II SNe and form together a broad physical category of SN models that invoke massive star core collapses. Such a physical classification scheme of SN models (massive star origin versus white dwarf origin) and the efforts to associate the observed SNe with them reflect a deeper understanding of the physical origins of SNe. The same applies to GRBs. The statistical classification of long-, short- and probably intermediate-duration GRBs has been established in the BATSE era. However, it took several missions and many years of broad-band observations to reveal that there are at least two physically distinct types of models that are associated with these GRBs. Although data are not abundant enough to unambiguously associate every individual GRB with these model categories, current data already revealed some perplexing observational facts (Section 1) that demand more serious investigations of the observational criteria to judge the physical origin of a particular GRB (i.e., the physical model associated with this GRB).

In the rest of the paper, we will discuss Type I/II GRBs, which are defined as the GRBs that are associated with two distinct physical models. This is not a new classification scheme of GRBs to replace the existing long/soft versus short/hard classification scheme, but is a parallel classification of the models that the observed GRBs can be associated with based on multiple criteria data analyses. The two approaches are complementary. As discussed above, T_{90} is energy-band dependent and sensitivity dependent, so that the membership of a particular GRB to a particular duration category is not always guaranteed. On the other hand, if adequate information is retrieved in an ideal observational campaign, the association membership of a particular GRB with a particular physical model category is almost certain regardless of the detector energy band and sensitivity. For example, if an SN is detected to be associated with a GRB, one can safely associate this GRB with the Type II model category regardless of its T_{90} detected by different detectors.

4. TYPE I/II GRBS, THEIR OBSERVATIONAL CRITERIA, AND PHYSICS BEHIND

We reiterate here the definitions of the Type I/II GRBs. Improving upon the descriptions presented in Zhang et al. (2007a), we hereby more rigorously define the following:

1. Type I GRBs (or compact star GRBs) are those GRBs that are associated with the theoretical models invoking destructive explosions in old-population, degenerate, compact stars. The likeliest model candidate is mergers of two compact stars.
2. Type II GRBs (or massive star GRBs) are those GRBs that are associated with the theoretical models invoking destructive explosions in young-population massive stars. The likeliest model candidate is core collapses of massive stars.

Here we do not specify the progenitor systems of each model type. In reality, there could be multiple possible progenitor systems within each model category (see also Bloom et al. 2008). Within the Type I model category, possible progenitor systems include NS–NS mergers (Paczýnski 1986; Eichler et al. 1989; Narayan et al. 1992; Rosswog et al. 2003), NS–BH mergers (Paczýnski 1991; Faber et al. 2006), and possibly Black Hole–White Dwarf (BH–WD) or Neutron Star–White Dwarf (NS–WD) mergers (Fryer et al. 1999; King et al. 2007) (cf. Narayan et al. 2001), see Nakar (2007); Lee & Ramirez-Ruiz (2007) for reviews. On the other hand, within the Type II model category, one may have collapses of single stars (i.e., collapsars; Woosley 1993; MacFadyen & Woosley 1999), or collapses of massive stars in binary systems (Fryer et al. 2007).

The definitions of Type I/II GRBs are based on the physical models that GRBs can be associated with rather than their observational properties. The scheme is therefore not intended to be "operational." The connections between the physical model properties and the observational criteria are not straightforward, and probably very difficult for some GRBs.

In the following, we review a list of observational criteria discussed in the literature that may be applied to differentiate the two physically distinct model categories that GRBs can be associated with (e.g., Donaghy et al. 2006; Zhang et al. 2007a; Zhang 2006), and discuss the physical justifications of each criterion. As justified below, some criteria (e.g., Section 4.1–Section 4.3) are more directly related to the progenitor system of a GRB. On the other hand, the traditional criteria invoking the observed gamma-ray properties (e.g., Section 4.4–Section 4.7) are more related to radiation physics and have less direct connection with the progenitor system. Some afterglow properties (Sections 4.8 and 4.9) do carry information of the progenitor, but theoretical modeling is invoked (and, hence, less definitive because of the uncertainties inherited in the models). The statistical properties (Sections 4.10 and 4.11) can be related to the progenitor system, but again large uncertainties are involved in the identification of

the explicit progenitor system and its cosmological evolutionary scenario. The best clue may be gravitational wave (GW) signals (Section 4.12). However, they are beyond the current detector capability.

4.1. Supernova Association

A positive detection of an SN signature associated with a GRB would undoubtedly establish the association of the burst with Type II. However, the sample of the robust GRB-SN associations is currently small. Non-detections of an SN signature could be due to multiple reasons, e.g., the afterglow is too bright so that the SN light is buried beneath the afterglow level; the follow-up observations were not "deep" enough or not at the right time window; or the lack of an underlying SN is genuine. Only the last case is helpful to judge the physical model category of a burst, although the conclusion is still not clear cut. A genuine SN-less GRB is certainly consistent with the Type-I origin. However, it has been discussed in the literature that some core-collapse GRBs may not eject enough ^{56}Ni to power a SN (Woosley 1993; Heger et al. 2003; Nagataki et al. 2003, 2006; Tominaga et al. 2007), so that the lack of a genuine SN signature may not be evidence completely against the Type II origin. On the other hand, we note that the large uncertainties involved in SN explosion physics prevent the models from having a definite *predictive* power regarding the SN signature. Looking back into the history, the predictions of the SN signature accompanying GRBs have followed a serpentine (and ironic) path. The first core-collapse GRB model was dubbed "failed supernova" (Woosley 1993), which predicts no SN signature associated with a GRB. Driven by the possible GRB 980425/SN 1998bw association, the model was developed to allow an SN associated with a GRB within the "collapsar" scheme. According to MacFadyen & Woosley (1999), the model predicts that "collapsars will always make SNe similar to SN 1998bw." Indeed the statement that "the data and models are consistent with, though not conclusive proof of, the hypothesis that ALL long-soft GRBs are accompanied by SNe of Type Ic" was made right before the discovery of GRB 060614 and GRB 060505 (Woosley & Bloom 2006). Would the discovery of the SN-less long GRBs (060614 and 060505) then beg for a dichotomy of core-collapse GRBs (one group with and another group without the SN association)? Although this is certainly plausible, a simpler picture would be that all genuine SN-less GRBs have the Type I origin. In this paper, we take lacking a genuine SN as a support to the Type I GRB, but do not take this criterion alone to define a Type I GRB. On the other hand, since there is no observational fact that demands the existence of SN-less Type II GRBs,[12] we do not automatically *associate* any genuine SN-less long GRB with the Type II (or Type II candidate) physical model categories unless there are other strong supports to the scenario (see Sections 4.1 and 7 for details).

4.2. Star-forming Rate of the Host Galaxy

Type II GRBs are related to massive star deaths, so they must reside in host galaxies with active star formation. So SFR, or more rigorously, specific star-forming rate (SSFR, i.e., SFR per unit mass) of the host galaxy is a critical parameter to judge the membership of Type II GRBs.

[12] In our opinion, GRB 060614 and GRB 060505 are not solid Type II candidates. As will be discussed in Section 5 (see also Gehrels et al. 2006; Zhang et al. 2007a), GRB 060614 is likely a Type I GRB. GRB 060505 has a much lower overall energetics (including gamma-ray and afterglow) than most other Type II GRBs.

On the other hand, compact star mergers can occur in host galaxies both with and without active star formation (Belczynski et al. 2006; Zheng & Ramirez-Ruiz 2007). If we see a GRB residing in an elliptical or an early-type galaxy, we are more confident that no massive star is involved in the event, and that the burst should be associated with Type I. Those Type I GRBs residing in star-forming galaxies are more difficult to identify. Due to the additional time delay required for the two compact objects to coalesce, a Type I GRB site is expected to be more aged than the site with active star formation. As a result, at least some Type I GRBs should preferentially reside in the regions with relatively low SSFR in the star forming host galaxy. On the other hand, there are channels of fast mergers (Belczynski et al. 2006) that lead to almost "prompt" mergers of compact stars. In such a case, Type I GRBs can reside in high SFR regions within star-forming galaxies.

4.3. Position Offset with Respect to the Host Galaxy

A related criterion is the offset of the GRB location with respect to the center of the host galaxy. The physical motivation is that Type I GRBs invoke mergers of binaries including at least one NS, which likely received a "kick" at birth so that the binary system would migrate from its original birth location. By the time when the two compact stars coalesce, the system should have a large offset from the galaxy center or even be outside of the host galaxy (Bloom et al. 1999). Indeed, several Gold Sample Type I GRBs show such a property (Gehrels et al. 2005; Bloom et al. 2006; Fox et al. 2005; Berger et al. 2005; Barthelmy et al. 2005a; Troja et al. 2008). On the other hand, Type II GRBs explode right at the location where the progenitor stars are formed and therefore should be in the star-forming regions inside the host galaxy (Bloom et al. 2002). This is in general consistent with the observations of long GRBs (Fruchter et al. 2006). Outliers do exist. For example, GRB 070125 is a long GRB whose birth location is in a galactic halo (Cenko et al. 2008b).

Complications arise if a GRB is found not inside any galaxy. It is difficult to judge whether a GRB is "kicked" out from a nearby host galaxy whose projected image is near the location of the GRB, or it is associated with a more distant galaxy at high-z. This problem arises for a good fraction of short/hard GRBs detected in the *Swift* era. For example, GRB 060502B was suggested by Bloom et al. (2007) to be associated with a nearby galaxy at $z = 0.287$ (with a large angular offset), while it is included by Berger et al. (2007) as one of the high-z missing-host short/hard GRBs.

4.4. Duration

Theoretically, we do not know exactly which timescale defines the GRB duration. In principle, there are three timescales that are relevant. The first one is the duration of the central engine activity $t_{\rm engine}$. This corresponds to the accretion timescale of an accretion-powered central engine model (usually invoking a black hole–torus system), or the spindown timescale of a spindown-powered central engine model (usually invoking a rapidly rotating millisecond magnetar or a maximally rotating black hole whose spin energy is tapped via a magnetic torque through the Blandford–Znajek mechanism). The second timescale is the timescale $t_{\rm jet}$ during which a relativistic jet is launched. In principle, there could be epochs during which a jet is launched, but it is not relativistic or not relativistic enough to power the observed gamma-ray emission. The third timescale

is the energy dissipation timescale $t_{\rm dis}$. Current *Swift* observations suggest that the GRB prompt emission is "internal" (Zhang et al. 2006). This requires that the relativistic jet dissipates energy internally before being decelerated by the external circumburst medium. The dissipation could be via internal shocks (Rees & Mészáros 1994) or magnetic reconnection (Usov 1992; Thompson 1994). In principle, one can have an active central engine without launching a relativistic jet, or have a relativistic jet without significant dissipation. In general, the observed GRB duration T_{90} (which also depends on the energy band and the sensitivity limit of the detector) should satisfy[13]

$$T_{90} \leqslant t_{\rm dis} \leqslant t_{\rm jet} \leqslant t_{\rm engine}. \quad (1)$$

In most studies, however, $T_{90} \sim t_{\rm engine} \sim t_{\rm jet} \sim t_{\rm dis}$ has been assumed.

If T_{90} is equal to or at least is proportional to $t_{\rm engine}$, as is assumed by most central engine modelers, then the duration information may be tied to the progenitor properties of GRBs. In particular, Type II GRB progenitors have a massive envelope, which can power a long-duration GRB through accretion. According to the collapsar scenario (MacFadyen & Woosley 1999), the duration of the burst is defined by the envelope fallback timescale, which is typically 10 s of seconds. The model therefore suggests that Type II GRBs should typically have long durations. On the other hand, NS–NS and NS–BH mergers typically have an accretion timescale ~ 0.01–0.1 s (Aloy et al. 2005) if the central engine is a BH-torus system. Therefore, Type I GRBs should typically have short durations. Indeed, a 1 s duration burst is already too long to be accommodated within the simple merger scenarios. One needs to introduce additional ingredients (e.g., an intermediate neutron star phase) to increase the duration (e.g., Rosswog et al. 2003).

This physically motivated clear dichotomy was broken in the *Swift* era. *Swift* discovered that X-ray flares prevail in more than half GRBs, in both long- and short-duration ones (Burrows et al. 2005a; Chincarini et al. 2007; Falcone et al. 2007). This suggests that the GRB central engine activity is not limited to the prompt phase, and is much longer than T_{90} in both long and short GRBs (Zhang et al. 2006; Fan & Wei 2005; Lazzati & Perna 2007). The progenitor and central engine models must then be modified to invoke a much longer accretion timescale (King et al. 2005; Perna et al. 2006; Proga & Zhang 2006), or a non-BH-torus central engine (Dai et al. 2006; Staff et al. 2007). More importantly, several strong Type I GRB candidates (e.g., GRB 050724) are not short, but have softer, extended emission (Villasenor et al. 2005; Barthelmy et al. 2005a; Norris & Bonnell 2006). The merger models therefore must be modified to account for this extended emission (Rosswog 2007). Type I GRBs no longer must be "short."

The discussion above only applies to the case when the line of sight pierces into the relativistic jet, i.e., the on-beam geometry. In this case, the observed timescales reflect the timescales at the central engine (Kobayashi et al. 1997). In the case of an off-beam geometry, i.e., the jet with opening angle θ_j is beaming toward an angle $\theta_v > \theta_j$ with respect to the line of sight, the observed timescale no longer traces that of the central engine. For a discrete pulse, if the pulse duration solely reflects the duration of the emission powered by the central engine, i.e., the rising and falling of the light curve reflects the increase and decrease of the central engine luminosity (in contrast to those models that interpret the decaying wing as the high-latitude emission), the observed duration off-beam is related to the on-beam value through the ratio of the Doppler factor (given the same comoving value), i.e.,

$$\frac{t(\text{offbeam})}{t(\text{onbeam})} = \frac{\mathcal{D}(\theta = 0)}{\mathcal{D}(\theta = \theta_v - \theta_j)} = \frac{1 - \beta\cos(\theta_v - \theta_j)}{1 - \beta}. \quad (2)$$

where the Doppler factor is defined by

$$\mathcal{D} = \frac{1}{\Gamma(1 - \beta\cos\theta)}, \quad (3)$$

and θ is the angle between the line of sight and the velocity vector of the ejecta, which is taken as the closest approach to the jet ($\theta_v - \theta_j$). For multiple emission episodes (i.e., multiple pulses in the light curve), the time interval of the quiescent episodes do not vary with the viewing direction. So Equation (2) applies to the total duration of a GRB only if the prompt emission has one single pulse. Also since the observed flux is lower for a lower $\mathcal{D}$, given a same detector sensitivity, the off-beam T_{90} tends to be shorter than that predicted by Equation (2) due to the limiting flux threshold effect.

The off-beam model predicts that the afterglow light curve should display a rising behavior initially before the $1/\Gamma$ beam enters the line of sight (Panaitescu & Mészáros 1999; Granot et al. 2002). Broadband observations of the majority of GRB afterglows do not show such a signature. So the off-beam geometry, if any, is rare.

4.5. Hardness

The connection between the hardness of spectrum and the GRB progenitor is less direct. It is related to the unknown internal energy dissipation mechanism and radiation mechanism, which in turn depends also on the composition of the GRB ejecta. GRB spectra are usually categorized as a smoothly joined power law, namely, the Band function (Band et al. 1993). The hardness of a GRB is likely related to the location of the E_p, but the flatness of the spectral index below E_p may also play a role. Theoretically, the spectral slope is more closely related to the particle acceleration mechanism (e.g., Sironi & Spitkovsky 2009) and the "compactness" of the emission region (e.g., Pe'er et al. 2006). The spectral peak energy, E_p, can be related to the GRB emission model parameters more directly, although it is model dependent (Zhang & Mészáros 2002a). We will mainly discuss the E_p models more closely in the following.

In general, E_p is a function of the burst luminosity L, the Lorentz factor Γ of the ejecta, and the radius R of the emission site from the central engine. In order to address whether a GRB is hard or soft, one needs to specify a particular emission model. In the following we discuss three internal emission models currently discussed in the literature.

Internal shock model. Within this model, the gamma-ray E_p can be defined either by synchrotron radiation or synchrotron self-Compton (SSC). In general, one can write $E_p \sim \Gamma\hbar\gamma_e^k(eB'/mc)$, where $k = (2, 4)$ for synchrotron and SSC, respectively. Since the comoving magnetic field strength in the ejecta flow satisfies $B' \propto L^{1/2}R^{-1}\Gamma^{-1}$ for both the ordered and the random magnetic field components (Zhang & Mészáros 2002a), one has

$$E_p^{\rm IS} \propto \gamma_e^k L^{1/2} R^{-1}(1+z)^{-1} \propto \gamma_e^k L^{1/2}\Gamma^{-2}\delta t^{-1}(1+z)^{-1}, \quad (4)$$

[13] Here we have assumed that T_{90} records the GRB internal emission only. This is true for most cases. Occasionally the observed prompt emission may also include the emission from the external shocks. T_{90} should be removed from Equation (1) for these cases.

where L is the initial kinetic luminosity of the ejecta, δt is the variability timescale of the unsteady GRB ejecta wind, and the internal shock radius is $R \sim \Gamma^2 \delta t$. Note that E_p is negatively correlated with the bulk Lorentz factor ($\propto \Gamma^{-2}$), which is contrary to the intuition that high-Γ bursts should be hard. Here γ_e is the characteristic Lorentz factor of the electrons that contribute to the emission at E_p. Under the fast cooling condition, which is generally satisfied for internal shocks, γ_e corresponds to the minimum "injection" energy of the electrons, which is related to the "relative" Lorentz factor between the two colliding shells Γ_{fs}, i.e., $\gamma_e \propto \Gamma_{fs} \sim (\Gamma_f/\Gamma_s + \Gamma_s/\Gamma_f)/2$, where Γ_f and Γ_s are the Lorentz factors of the fast and slow shells, respectively. If the Γ variation of a flow is proportional to the average Lorentz factor $\bar{\Gamma}$, i.e., $\Delta\Gamma \propto \bar{\Gamma}$ or $\Gamma_f/\Gamma_s \sim$ const, then γ_e essentially does not depend on $\bar{\Gamma}$, so that a higher E_p should correspond to a lower Γ. On the other hand, it is possible that high-$\bar{\Gamma}$ flows may be more variable, e.g., $\Gamma_f/\Gamma_s \propto \bar{\Gamma}$. If this is the case, then the negative dependence on Γ in Equation (4) is canceled out (for $k = 2$) or reversed (for $k = 4$). In the traditional internal shock model, the variability timescale δt of the ejecta can be derived from the observation. Analyses of power density spectra of GRB light curves (Beloborodov et al. 1998) suggest that the GRB temporal behavior may be self-similar, i.e., lacking a characteristic timescale. In the past, the minimum variability timescale, which can be as small as milliseconds for both short- and some long-duration GRBs, has been adopted to estimate the internal shock radius. Alternatively, it is possible that the rapid variability in GRB light curves may be caused by other mechanisms, such as relativistic turbulence inside the emission region (Narayan & Kumar 2009). Within this latter scenario, the outflow variability timescale relevant to internal shocks can be much longer. Physically, Type I GRB outflows may directly carry the variability information from the inner central engine, i.e., the dynamic timescale of the innermost accretion torus around the black hole, $\delta t \sim t_{\rm dyn} \sim 12\sqrt{3}\pi(GM_{\rm bh}/c^3) \sim 1(M_{\rm bh}/3M_\odot)$ ms (where $M_{\rm bh}$ is the mass of the black hole), or the spin period of the central magnetar or black hole, $\delta t \sim P_{\rm engine} \sim 1$ ms. On the other hand, a Type II jet needs to penetrate through the heavy stellar envelope so that the initial temporal information from the inner central engine may be smeared out and regulated. The observed variability timescale may be related to that of fluid instabilities, and therefore could be much longer. If abundant pairs are produced, it has been argued that the pair photosphere would effectively screen out the variability timescales smaller than a critical value (Kobayashi et al. 2002; Mészáros et al. 2002). This is more relevant to low-Γ events for which the internal shock radii are below the pair photosphere.

With all these complications in mind, one may compare the expected E_p for Type I and Type II GRBs based on Equation (4). On average, Type I GRBs have an isotropic gamma-ray luminosity L 2–3 orders of magnitude smaller than that of Type II GRBs (see the theoretical argument in Section 4.8, and the observational data in Section 4 and Table 1). On the other hand, δt of Type I may be smaller than that of Type II by 2–3 orders of magnitude. This gives

$$\frac{E_p^{\rm IS}({\rm I})}{E_p^{\rm IS}({\rm II})} \sim (10-30)\frac{[\gamma_e^k \Gamma^{-2}(1+z)^{-1}]({\rm I})}{[\gamma_e^k \Gamma^{-2}(1+z)^{-1}]({\rm II})}. \quad (5)$$

This suggests that in a large parameter space Type I GRBs can be harder than Type II GRBs. If γ_e is similar for both types, Type I GRBs can be harder than Type II GRBs as long as their bulk Lorentz factors are not larger than those of Type II by a factor of more than (3–5) times. If $\gamma_e \propto \Gamma$, Type I are generally harder than Type II for both the synchrotron model ($k = 2$, regardless of the value of Γ), and the SSC model ($k = 4$, the E_p ratio is positively dependent on Γ. Theoretically, Type I GRBs should have higher Γ's due to their less baryon loading as compared with Type II GRBs. This favors a harder spectrum of Type I even more for the SSC model. A systematically smaller redshift z for Type I GRBs (due to the merger delay with respect to star formation) also helps to increase the hardness contrast between the two types. In reality, there are large dispersions in L, δt, Γ, γ_e, and z in both types. On the other hand, the HR distribution of the BATSE short/hard versus long/soft dichotomy also shows a large dispersion (Figure 2). In general, the statement that Type I GRBs are harder than Type II GRBs can be made within the internal shock models in the statistical sense. For individual bursts, one cannot draw a firm conclusion regarding the hardness of a particular burst due to the large uncertainties involved in the parameters.

Photosphere model. The possibility that the observed GRB emission has a dominant contribution from the fireball photosphere (Thompson 1994; Mészáros & Rees 2000; Mészáros et al. 2002) has gained increasing attention recently (Rees & Mészáros 2005; Ryde 2005; Pe'er et al. 2007; Thompson et al. 2007; Ioka et al. 2007; Ghisellini et al. 2007; Ryde & Pe'er 2008; Lazzati et al. 2009). In this model, E_p is related to the observed photosphere temperature $T_{\rm ph}$. For a "naked" fireball, i.e., a fireball expanding into a vacuum, the observed photosphere temperature (and hence E_p) depends on whether the photosphere radius $R_{\rm ph}$ is below or above the fireball coasting radius R_c. For a large dimensionless entropy of the fireball $\eta \geqslant \eta_{c2} \sim 10^4[L_{52}R_{0,7}^{-1}]^{1/3}$ (where R_0 is the initial radius of the fireball. Throughout the text the convention $Q_n = Q/10^n$ is adopted in cgs units.),[14] the fireball becomes transparent during the acceleration phase (i.e., $R_{\rm ph} < R_c$). The observed fireball temperature is essentially the temperature at the central engine, i.e., $T_{\rm ph} \sim T_0$, so that

$$E_p^{\rm ph,1} \sim kT_0(1+z)^{-1} \sim L^{1/4}R_0^{-1/2}(1+z)^{-1}. \quad (6)$$

This is the regime discussed in most photosphere models (Thompson 1994; Mészáros & Rees 2000; Ryde 2005). On the other hand, if the fireball becomes transparent beyond the coasting radius ($R_{\rm ph} > R_c$), the photosphere temperature drops with radius due to the decrease of residual internal energy during the expansion, so that $T_{\rm ph} = T_0(R_c/R_{\rm ph})^{2/3}$ (Mészáros & Rees 2000). The detailed parameter dependences are related to whether the opacity is defined by a discrete shell or a continuous outflow wind (Mészáros et al. 2002). For the former ($\eta_{c1} < \eta < \eta_{c2}$, where $\eta_{c1} \sim 250[L_{52}R_{0,7}^{-1}]^{1/5}$), one has (Zhang & Mészáros 2002a)

$$E_p^{\rm ph,2} \sim L^{-1/12}R_0^{-1/6}\Gamma(1+z)^{-1}. \quad (7)$$

For the latter ($\eta < \eta_{c1}$), one has

$$E_p^{\rm ph,3} \sim L^{-5/12}R_0^{1/6}\Gamma^{8/3}(1+z)^{-1}. \quad (8)$$

If additional energy dissipation occurs at small radii, pair production can occur which enhances photon opacity and

[14] This critical entropy is derived (Zhang & Mészáros 2002a) within the discrete shell regime, rather than the continuous wind regime (Mészáros & Rees 2000; Mészáros et al. 2002). This is usually justified, since typically one has $\eta > \eta_{c1}$ in this regime.

Table 1
Samples

GRB Name	z Redshift	log SSFR (Gyr^{-1})	SN?	T_{90} (s)	T_{90} w/ EE (s)	HR[a] $\frac{S(50-100\ \mathrm{keV})}{S(25-50\ \mathrm{keV})}$	Lag[b] (s)	E_p (keV)	$E_{\gamma,\mathrm{iso}}$ 10^{52} erg	$L_{p,\mathrm{iso}}$ 10^{50} erg/s
Type II Gold										
970228	0.695	0.082	?	∼80	n/a	1.07	0[c]	115 ± 38	1.6 ± 0.1	$93.3^{+5.7}_{-6.1}$
970508	0.835	0.534	?	∼23.1	n/a	1.09	$0.384^{+0.090,\mathrm{b}}_{-0.026}$	79 ± 23	0.61 ± 0.13	$14.3^{+0.5}_{-0.6}$
971214	3.418	0.467	?	31.0 ± 1.2	n/a	1.63	$0.066^{+0.026}_{-0.048}$	155 ± 30	21 ± 3	684 ± 65
980425	0.0085	−0.883	Y	23.3 ± 1.4	n/a	1.08	1.46 ± 0.18	119 ± 24	$(6.1 \pm 0.62) \times 10^{-5}$	$4.8^{+7.5}_{-7.8} \times 10^{-4}$
980613	1.0964	1.184	?	50	n/a	1.59	…[d]	93 ± 43	0.59 ± 0.09	$16.7^{+3.9}_{-4.7}$
980703	0.966	0.885	?	411.6 ± 9.3	n/a	1.47	$0.402^{+0.162}_{-0.134}$	254 ± 51	7.2 ± 0.7	166^{+32}_{-31}
990123	1.6	0.340	?	63.4 ± 0.3	n/a	2.06	$0.018^{+0.012}_{-0.012}$	781 ± 62	229 ± 37	3517^{+210}_{-198}
990506	1.30658	−0.081	?	130.0 ± 0.1	n/a	1.44	0.04 ± 0.02	283 ± 57	94 ± 9	930^{+54}_{-52}
990712	0.4331	0.093	?	∼30	n/a	0.98	0.045 ± 0.014	65 ± 11	0.67 ± 0.13	$73.1^{+5.9}_{-6.4}$
991208	0.707	1.121	?	∼68	n/a	1.25	…	183 ± 18	22.3 ± 1.8	110 ± 11
000210	0.846	0.049	?	∼15	n/a	1.19	…	408 ± 14	14.9 ± 1.6	1003^{+80}_{-79}
000418	1.1181	0.757	?	∼30	n/a	?	…	134 ± 10	9.1 ± 1.7	$11.3^{+4.0}_{-4.1}$
000911	1.0585	−0.124	?	∼500	n/a	2.14	…	579 ± 116	67 ± 14	558^{+128}_{-95}
000926	2.0379	−0.165	?	∼25	n/a	0.37	…	101 ± 6.5	27.1 ± 5.9	107 ± 43
011121	0.362	−0.464	Y	∼30	n/a	0.78	…	217 ± 26	7.8 ± 2.1	49.8 ± 4.0
011211	2.14	−0.084	?	∼270	n/a	1.87	…	59 ± 7	5.4 ± 0.6	$21.8^{4.8}_{-5.2}$
020405	0.695	−0.174	Y	∼60	n/a	3.23	…	364 ± 73	10 ± 0.9	$117^{+7.2}_{-6.7}$
020813	1.255	1.167	?	113.0 ± 1.1	n/a	1.58	0.16 ± 0.04	142 ± 13	66 ± 16	450^{+94}_{-86}
020819B	0.41	−0.664	?	∼50.2	n/a	1.07	…	50 ± 15	0.68 ± 0.17	…
020903	0.25	0.555	Y	∼13	n/a	0.66	…	3 ± 1	$(24 \pm 6) \times 10^{-4}$	…
021211	1.006	−0.841	Y	∼8	n/a	0.98	0.32 ± 0.04	46 ± 7	1.12 ± 0.13	155^{+33}_{-29}
030328	1.52	0.680	?	∼199.2	n/a	1.43	0.2 ± 0.2	126 ± 13	47 ± 3	191 ± 38
030329	0.1685	0.304	Y	∼62.9	n/a	1.13	$0.58^{+0.60}_{-0.36}$	68 ± 2	1.5 ± 0.3	22.5 ± 4.5
030528	0.782	1.355	?	∼83.6	n/a	1.23	12.5 ± 0.5	62 ± 3	2.5 ± 0.3	$17.3^{+3.6}_{-3.4}$
031203	0.1055	1.287	Y	∼40	n/a	0.65	0.24 ± 0.12	∼292	∼0.01	$0.12^{+0.03}_{-0.02}$
040924	0.858	0.071	?	2.39 ± 0.24	n/a	1.00	0.3 ± 0.04	67 ± 6	0.95 ± 0.09	191 ± 20
041006	0.716	−0.131	?	17.40 ± 0.25	n/a	1.08	…	63 ± 13	3 ± 0.9	$44^{+1.7}_{-1.8}$
050525A	0.606	?	Y	8.830 ± 0.004	n/a	1.17	$0.0865^{+0.0065}_{-0.008}$	84.1 ± 1.7	2.89 ± 0.57	111.8 ± 2.1
050826	0.297	0.172	?	35.5 ± 1.2	n/a	1.91	…	340^{+790}_{-210}	0.03 ± 0.04	$0.33^{+0.32}_{-0.08}$
051022	0.8	0.142	?	∼200	n/a	1.52	…	418 ± 143	53 ± 5	364^{+48}_{-47}
060218	0.033	−0.061	Y	∼2000	n/a	0.76	218^{+356}_{-140}	4.9 ± 0.3	$(77 \pm 1.4) \times 10^{-4}$	$1.0 \pm 0.6 \times 10^{-3}$
060602A	0.787	?	?	75.0 ± 0.2	n/a	2.65	…	280^{+570}_{-150}	0.91 ± 0.06	$6.14^{+2.54}_{-0.80}$…
080520	1.545	?	?	2.82 ± 0.67	n/a	0.46	…	∼30	0.073 ± 0.019	…

Table 1
(Continued)

GRB Name	z Redshift	log SSFR (Gyr^{-1})	SN?	T_{90} (s)	T_{90} w/ EE (s)	HR[a] $\frac{S(50-100\ \mathrm{keV})}{S(25-50\ \mathrm{keV})}$	Lag[b] (s)	E_p (keV)	$E_{\gamma,\mathrm{iso}}$ 10^{52} erg	$L_{p,\mathrm{iso}}$ 10^{50} erg/s
Type I Gold										
050509B	0.2248	-0.853	N	0.040 ± 0.004	n/a	1.52	0.0043 ± 0.0032	82^{+611}_{-80}	$2.4^{+4.4}_{-1} \times 10^{-4}$	$0.07^{+0.10}_{-0.05}$
050709	0.1606	-0.512	N	0.07 ± 0.01	130 ± 7	1.37/1.02[j]	0 ± 0.002	83^{+18}_{-12}	$(2.7 \pm 1.1) \times 10^{-3}$	$5.4^{+0.67}_{-0.69}$
050724	0.2576	-0.367	N	3 ± 1	154.20 ± 1.12	1.26/1.12	-0.0042 ± 0.0082	110^{+400}_{-45}	$9^{+11}_{-2} \times 10^{-3}$	$0.99^{+0.23}_{-0.10}$
060614	0.1254	-0.863	N	~ 5	106.0 ± 3.3	1.41/1.07	0.003 ± 0.009	302^{+214}_{-85}	0.24 ± 0.04	$1.39^{+0.13}_{-0.07}$
061006	0.4377	-2.189	N	~ 0.5	120.00 ± 0.04	1.52/1.18	...	640^{+144}_{-227}	0.22 ± 0.12	$24.60^{+1.22}_{-0.77}$
Other Short–Hard Bursts										
000607	0.14	?	?	~ 0.008	n/a	2.18	...	...	...	...
050813	~ 0.72	?	N	0.6 ± 0.1	n/a	1.76	-0.0097 ± 0.014	210^{+710}_{-130}	$(1.5^{+2.5}_{-0.8}) \times 10^{-2}$	4.13 ± 2.02
051210[g]	>1.4	?	?	1.27 ± 0.05	40	2.01	-0.0053 ± 0.024	410^{+650}_{-260}	$> 0.191 \pm 0.032$	...
051221A	0.5464	0.804	?	1.4 ± 0.2	n/a	1.74	0 ± 0.004	402^{+72}_{-93}	$0.28^{+0.21}_{-0.1}$	25.8 ± 0.9
060121	1.7/4.6	?	?	1.60 ± 0.07	~ 120	1.55/0.57[h]	0.017 ± 0.009[i]	104^{+134}_{-78}	$4.18^{+3.29}_{-0.39}/22.3^{+17.5}_{-2.07}$	$2445 \pm 162/33574 \pm 2226$
060313	$\leqslant 1.1$	?	?	0.7 ± 0.1	n/a	2.43	$(3 \pm 7) \times 10^{-4}$	922^{+306}_{-177}	$\leqslant 6.24^{+0.43}_{-3.66}$	...
060502B	0.287	?	?	0.09 ± 0.02	n/a	2.12	$(-2 \pm 8) \times 10^{-4}$	340^{+720}_{-190}	$3^{+5}_{-2} \times 10^{-3}$	0.65 ± 0.09
060505	0.0889	-0.777	?	4 ± 1	n/a	1.63	0.36 ± 0.05	~ 223	$(3.39 \pm 0.60) \times 10^{-3}$	$\sim 0.009^{k}$
060801	1.131	?	?	0.5 ± 0.1	n/a	2.89	0.008 ± 0.008	620^{+1070}_{-340}	0.17 ± 0.021	$47.6^{+6.2}_{-1.6}$
061201	0.111?	?	?	0.8 ± 0.1	n/a	2.90	$2.7^{+3.3}_{-2.4} \times 10^{-3}$	873^{+458}_{-284}	$0.018^{+0.002}_{-0.015}$	...
061210	0.4095	?	?	$\sim eq 0.06$	85 ± 5	2.32/1.37	...	540^{+760}_{-310}	$0.09^{+0.16}_{-0.05}$	21.5 ± 1.4
061217	0.8270	?	?	0.212 ± 0.041	n/a	2.07	-0.007 ± 0.009[j]	400^{+810}_{-210}	$0.03^{+0.04}_{-0.02}$	10.8 ± 1.8
070429B	0.9023	?	?	0.5 ± 0.1	n/a	1.23	...	120^{+746}_{-66}	0.03 ± 0.01	24.6 ± 3.8
070714B	0.9225	?	?	~ 3	~ 100	1.82/1.56	0.014 ± 0.007	1120^{+780}_{-380}	$1.16^{+0.41}_{-0.22}$	57.3 ± 3.6
070724A	0.457	?	?	0.50 ± 0.04	n/a	0.94	...	~ 68	0.003 ± 0.001	$1.58^{+0.34}_{-0.14}$
071227	0.3940	?	?	1.8 ± 0.4	~ 100	2.02/0.96	$(0.4 \pm 14) \times 10^{-4,l}$	~ 1000	0.22 ± 0.08	3.34 ± 0.49
080503	...	?	N	~ 0.7	170 ± 40	1.0	-0.013 ± 0.009[m]	...	...	...
080913	6.7	?	?	8 ± 1	n/a	1.58	0 ± 0.42	121^{+232}_{-39}	7 ± 1.81	1200^{+1622}_{-300}
090423	8.2	?	?	10.3 ± 1.1	n/a	1.50	$0.046^{+0.085}_{-0.058}$	48^{+6}_{-5}	10 ± 3	~ 1880

Table 1
(Continued)

Notes. Values of E_p and $E_{\gamma,\rm iso}$ are taken from Amati et al. (2008) and $L_{p,\rm iso}$ are calculated in this work unless otherwise stated below. Further references are: **GRB970228**-z: Tinney et al. (1998); SSFR: Savaglio et al. (2009); T_{90}, spectrum[c]: Frontera et al. (1998); lag: Bernardini et al. (2007); **GRB970508**-z: Metzger et al. (1997); SSFR: Savaglio et al. (2009); T_{90}: Paciesas et al. (1999); spectrum: Djorgovski et al. (1997); lag: Norris et al. (2000). **GRB971214**-z: Kulkarni et al. (1998); SSFR: Savaglio et al. (2009); T_{90}: Paciesas et al. (1999); spectrum: Dal Fiume et al. (2000); lag: Norris et al. (2000). **GRB980425**-z: Tinney et al. (1998); SSFR: Savaglio et al. (2009); T_{90}: Galama et al. (1998); spectrum: Yamazaki et al. (2004); lag: Zhang (2008). **GRB980613**-z: Djorgovski et al. (1999); SSFR: Savaglio et al. (2009); T_{90}: Smith et al. (1998); spectrum: Soffitta et al. (2001); lag: Norris et al. (2000). **GRB980703**-z: Djorgovski et al. (1998); SSFR: Savaglio et al. (2009); T_{90}: Paciesas et al. (1999); spectrum: Ghirlanda et al. (2004); lag: Norris et al. (2000). **GRB990123**-z: Andersen et al. (1999); SSFR: Savaglio et al. (2009); T_{90}: Paciesas et al. (1999); spectrum: Ghirlanda et al. (2004); lag: Norris et al. (2000). **GRB990506**-z: Bloom et al. (2003b); SSFR: Savaglio et al. (2009); T_{90}: Paciesas et al. (1999); spectrum: Ghirlanda et al. (2004); lag: Schaefer (2007). **GRB990712**-z: Vreeswijk et al. (2001); SSFR: Savaglio et al. (2009); T_{90}: Heise et al. (1999); spectrum: Frontera et al. (2001); lag: Hakkila & Giblin (2006). **GRB991208**-z: Dodonov et al. (1999); SSFR: Savaglio et al. (2009); T_{90}: Hurley et al. (2000b); spectrum: Hurley et al. (2000b). **GRB000210**-z: Piro et al. (2002); SSFR: Savaglio et al. (2009); T_{90}: Piro et al. (2002); spectrum: Piro et al. (2002). **GRB000418**-z: Bloom et al. (2003b); SSFR: Savaglio et al. (2009); T_{90}: Hurley et al. (2000a). **GRB000911**-z: Price et al. (2002); SSFR: Savaglio et al. (2009); T_{90}: Price et al. (2002); spectrum: Price et al. (2002). **GRB000926**-z: Castro et al. (2000); SSFR: Savaglio et al. (2009); T_{90}: Hurley et al. (2000c); spectrum: Ulanov et al. (2005). **GRB011121**-z: Greiner et al. (2003a); SSFR: Savaglio et al. (2009); T_{90}: Greiner et al. (2003a); spectrum: Greiner et al. (2003a). **GRB011211**-z: Holland et al. (2002); SSFR: Savaglio et al. (2009); T_{90}: Holland et al. (2002); spectrum: Piro et al. (2005). **GRB020405**-z: Masetti et al. (2002); SSFR: Savaglio et al. (2009); T_{90}: Price et al. (2003); spectrum: Price et al. (2003). **GRB020813**-z: Barth et al. (2003); SSFR: Savaglio et al. (2009); T_{90}, spectrum: Sakamoto et al. (2005); lag: Schaefer (2007). **GRB0208019B**-z: Jakobsson et al. (2005); SSFR: Savaglio et al. (2009); T_{90}, spectrum: Sakamoto et al. (2005). **GRB020903**-z: Soderberg et al. (2004); SSFR: Savaglio et al. (2009); T_{90}, spectrum: Sakamoto et al. (2005). **GRB021211**-z: Vreeswijk et al. (2003); SSFR: Savaglio et al. (2009); T_{90}, spectrum: Sakamoto et al. (2005); lag: Schaefer (2007). **GRB030328**-z: Martini et al. (2003); SSFR: Savaglio et al. (2009); T_{90}, spectrum: Sakamoto et al. (2005); lag: Schaefer (2007). **GRB030329**-z: Greiner et al. (2003b); SSFR: Savaglio et al. (2009); T_{90}, spectrum: Sakamoto et al. (2005); lag: Gehrels et al. (2006). **GRB030528**-z: Rau et al. (2005); SSFR: Savaglio et al. (2009); T_{90}, spectrum: Sakamoto et al. (2005); lag: Schaefer (2007). **GRB031203**-z: Prochaska et al. (2004); SSFR: Savaglio et al. (2009); T_{90}, spectrum: Sazonov et al. (2004); lag: Sazonov et al. (2004); E_p, $E_{\rm iso}$: Ghisellini et al. (2006). **GRB040924**-z: Prochaska et al. (2004); SSFR: Savaglio et al. (2009); T_{90}, spectrum: Sazonov et al. (2004); lag: Schaefer (2007). **GRB041006**-z: Stanek et al. (2005); SSFR: Savaglio et al. (2009); T_{90}: Shirasaki et al. (2008), spectrum: HETE2 website[e]. **GRB050525A**-z: Della Valle et al. (2006b); SSFR: Savaglio et al. (2009); T_{90}: Cummings et al. (2005a); spectrum: this work[f]; Lag: Gehrels et al. (2006); E_p, $E_{\rm iso}$: Golenetskii et al. (2005a) **GRB050826**-z: Halpern & Mirabal (2006); SSFR: Savaglio et al. (2009); T_{90}, spectrum: this work[f]. **GRB051022**-z: Doty et al. (2005); SSFR: Savaglio et al. (2009); T_{90}: Hurley et al. (2005); spectrum: Gal-Yam et al. (2005). **GRB060218**-z: Soderberg et al. (2006a); SSFR: Savaglio et al. (2009); T_{90}: Liang et al. (2006); spectrum: this work[f]; lag: Gehrels et al. (2006). **GRB060602A**-z: Jakobsson et al. (2007); SSFR: n/a; T_{90},spectrum: this work[f]. **GRB050820**-z: Jakobsson et al. (2008); SSFR: n/a; T_{90}, spectrum: this work[f]; E_p, $E_{\rm iso}$: Sakamoto et al. (2008). **GRB050509B**-z: Gehrels et al. (2005); SSFR: Savaglio et al. (2009); T_{90}: Gehrels et al. (2005), spectrum: this work[f]; lag: Gehrels et al. (2006); E_p, $E_{\rm iso}$: Butler et al. (2007). **GRB050709**-z: Fox et al. (2005); SSFR: Savaglio et al. (2009); T_{90}: Villasenor et al. (2005), spectrum: Villasenor et al. (2005); lag: Gehrels et al. (2006); E_p, $E_{\rm iso}$: Butler et al. (2007). **GRB050724**-z: Barthelmy et al. (2005a); SSFR: Savaglio et al. (2009); T_{90}: Barthelmy et al. (2005a); spectrum: this work[f]; lag: Gehrels et al. (2006); E_p, $E_{\rm iso}$: Butler et al. (2007). **GRB060614**-z: Della Valle et al. (2006a); SSFR: Savaglio et al. (2009); T_{90}: Kann et al. (2008); spectrum: Zhang et al. (2007a); lag: Gehrels et al. (2006); E_p, $E_{\rm iso}$: Golenetskii et al. (2006b). **GRB061006**-z: Berger et al. (2007); SSFR: Savaglio et al. (2009); T_{90}, spectrum: this work[f];E_p, $E_{\rm iso}$: Butler et al. (2007). **GRB000607**-z: Nakar et al. (2006); T_{90}, spectrum: Hurley et al. (2002). **GRB050813**-z: Prochaska et al. (2006); T_{90}: Sato et al. (2005), HR: Sato et al. (2005); lag: Ferrero et al. (2007), Gehrels et al. (2006); E_p, $E_{\rm iso}$: Butler et al. (2007). **GRB051210**-z: Berger et al. (2007); T_{90}, spectrum: La Parola et al. (2006); lag: Gehrels et al. (2006); E_p, $E_{\rm iso}$: Butler et al. (2007). **GRB051221A**-z: Soderberg et al. (2006b); SSFR: Savaglio et al. (2009); T_{90}: Cummings et al. (2005b), spectrum: Golenetskii et al. (2005b); lag: Gehrels et al. (2006); E_p, $E_{\rm iso}$: Golenetskii et al. (2005b). **GRB060121**-z: Levan et al. (2006), de Ugarte Postigo et al. (2006); T_{90}, lag, spectrum: Donaghy et al. (2006); E_p, $E_{\rm iso}$: Butler et al. (2007). **GRB060313**-z, T_{90}, spectrum: Roming et al. (2006), Lag: Roming et al. (2006); E_p, $E_{\rm iso}$: Golenetskii et al. (2006a). **GRB060502B**-z: Bloom et al. (2007); T_{90}, spectrum: Sato et al. (2006a); lag: Gehrels et al. (2006); Ep, $E_{\rm iso}$: Butler et al. (2007). **GRB060505**-z: Ofek et al. (2007); SSFR: Savaglio et al. (2009); T_{90}: Palmer et al. (2006); spectrum: Hullinger et al. (2006); lag: McBreen et al. (2008); E_p,$E_{\rm iso}$: Hullinger et al. (2006); L_p: McBreen et al. (2008). **GRB060801**-z: Cucchiara et al. (2006); T_{90}, spectrum: Sato et al. (2006b); lag: Gehrels et al. (2006); E_p,$E_{\rm iso}$: Butler et al. (2007). **GRB061201**-z: Stratta et al. (2007); T_{90}: Markwardt et al. (2006); spectrum: Golenetskii et al. (2006c); lag: Stratta et al. (2007); E_p, $E_{\rm iso}$: Butler et al. (2007). **GRB061210**-z: Berger (2007); T_{90}, spectrum: Cannizzo et al. (2006); E_p, $E_{\rm iso}$: Butler et al. (2007). **GRB061217**-z: Berger (2007); T_{90}, spectrum, lag: Ziaeepour et al. (2006); E_p, $E_{\rm iso}$: Butler et al. (2007). **GRB070429B**-z: Cenko et al. (2008a); T_{90}, spectrum: Markwardt et al. (2007); E_p, $E_{\rm iso}$: Butler et al. (2007) **GRB070714B**-z: Cenko et al. (2008a); T_{90}: Kann et al. (2008); spectrum: this work[f]; lag: Cenko et al. (2008a); E_p, $E_{\rm iso}$: Butler et al. (2007). **GRB070724A**-z: Cucchiara et al. (2007); T_{90}: Kann et al. (2008); spectrum: this work[f]; E_p,$E_{\rm iso}$: estimated with $\Gamma - E_p$ relation. **GRB071227**-z: Berger (2009); T_{90}: Sato et al. (2007), Sakamoto et al. (2007); spectrum: this work[f], Sato et al. (2007); lag: Sakamoto et al. (2007); E_p, $E_{\rm iso}$: Golenetskii et al. (2007). **GRB080503**-T_{90}, spectrum, Lag: Mao et al. (2008). **GRB080913**-z, T_{90}, spectrum: Greiner et al. (2009b); E_p: Palshin et al. (2008), $E_{\rm iso}$: this work. **GRB090423**-z, T_{90}, $E_{\rm iso}$: Tanvir et al. (2009); spectrum: this work; lag: Krimm et al. (2009); L_p: Nava et al. (2009); E_p: Salvaterra et al. (2009).

[a] HR = S(50–100 keV)/S(25–50 keV); [b] Lag between 25–50 keV and 50–100 keV; [c] Absence of lag between 2–26 keV and 40–700 keV; [d] BATSE data are not completed or recorded (Norris et al. 2000); [e] http://space.mit.edu/HETE/Bursts/GRB041006/; [f] http://grb.physics.unlv.edu; [g] We adopted $z = 1.4$ for this burst; [h] Only EE; [i] Lag between 6–40 keV and 80–400 keV; [j] Lag between 25–50 keV and 100–350 keV; [k] Got from $\frac{E_{\gamma,\rm iso}}{t_{90}}$; [l] Lag between 25–50 keV and 100–350 keV; [l] Lag between 15–25 keV and 50–100 keV.

increases the photosphere radius (Mészáros et al. 2002; Rees & Mészáros 2005). We note that the "naked" fireball scenario is more relevant to Type I GRBs.

With the presence of a stellar envelope, the photosphere emission of a Type II GRB is likely modified. Due to continuous energy dissipation and heating inside the envelope, the jet cannot reach the maximum Lorentz factor but instead stores a significant energy in heat before erupting out from the envelope. Effectively, the GRB fireball "central engine" is moved from the central black hole or magnetar to the location slightly below the stellar envelope (Thompson 2006; Thompson et al. 2007; Ghisellini et al. 2007). The jet at this radius $R \sim R_*$ has a moderate Lorentz factor Γ_* and a comoving temperature $T'_* \sim (L/4\pi\Gamma_*^2 R^2\sigma)^{1/4}$, and an observer frame temperature $T_* = \Gamma_* T'_*$. As the jet erupts out from the envelope, it will undergo rapid acceleration under its own thermal pressure. If R_* is greater than the photosphere radius for a naked central engine, the fireball would become transparent shortly after exiting the star due to the rapid fall of density. So the real photosphere radius is essentially $R_{\rm ph} \sim R_*$, and $R_{\rm ph} < R_c$ is always guaranteed. The peak energy E_p is defined by $T_{\rm ph} = T_*$. This leads to a variation of Equation (6) in the form of

$$E_p^{\rm ph,1'} \sim L^{1/4}\Gamma_*^{1/2} R_*^{-1/2}(1+z)^{-1}. \quad (9)$$

Within the photosphere models, it is not obvious why Type I GRBs should be systematically harder than Type II GRBs. The trend, if any, should be opposite. The logic is the following. First, given the same parameters of L, R_0, and z, one typically has $E_p^{\rm ph,1} > E_p^{\rm ph,2} > E_p^{\rm ph,3}$ (e.g., Equation (24) of Zhang & Mészáros 2002a). Next, the stellar envelope effectively "raises" the photosphere for Type II GRBs, so Equations (7) and (8) are usually not relevant. One therefore may only compare the case of Equation (6) for the two types of GRBs, since Equation (9) can be related to Equation (6) through $R_0 = R_*/\Gamma_*$. Equation (6) suggests that Type I GRBs, typically with smaller L, should be softer than Type II GRBs at the same redshift. A smaller z for Type I GRBs may compensate their softness, but in general it is not straightforward to claim that Type I GRBs should be systematically harder than Type II GRBs for the photosphere model. Pairs may lower the photosphere temperatures of some high-L GRBs (especially for Type II), which may help to account for the observed trend, but no handy analytical formula is available to perform direct comparisons.

The recent Fermi-detected GRB 080916C (Abdo et al. 2009) showed a series of featureless Band-function spectra. The expected photosphere emission component is missing, suggesting a Poynting flux dominated flow at the base of the central engine (Zhang & Pe'er 2009). At least for this burst, the observed E_p is not the thermal peak of the photosphere emission.

Magnetic dissipation model. Finally, if the GRB outflow is Poynting flux dominated (Usov 1992; Mészáros & Rees 1997; Spruit et al. 2001; Lyutikov & Blandford 2003; Liang & Noguchi 2009), the characteristic frequency of emission would take a different form and has different dependences on the ejecta parameters. The locations of the magnetic reconnection regions are unknown. If dissipation occurs at small radii, the effect is to modify the photosphere emission through continuous heating (Giannios 2008). This is effectively a photosphere model, which has been discussed above. Alternatively, a Poynting-flux-dominated outflow can reach a global dissipation at a large radius where the MHD approximation is broken (Usov 1994; Spruit et al. 2001; Zhang & Mészáros 2002a; Lyutikov & Blandford 2003).

Lacking a macroscopic reconnection model, E_p, in the reconnection model is difficult to calculate. Under different assumptions, the expression of E_p may take different forms. For example, in a random electric/magnetic field in the magnetic reconnection region, electron acceleration may be balanced by radiation cooling. The typical electron Lorentz factor is therefore $\gamma_e \propto B^{-1/2}$. The synchrotron peak energy may be then expressed in the form of (Zhang & Mészáros 2002a)

$$E_p^{\rm mag} \propto \Gamma(1+z)^{-1}, \quad (10)$$

which depends on Γ and z only. Type I GRBs can then be harder than Type II GRBs, again because Type I GRBs tend to have a cleaner environment, and hence, less baryon loading, than Type II GRBs.

Similar to the duration discussion (Section 4.5), the above discussion applies to the on-beam geometry. For an off-beam geometry, the observed E_p is smaller by a factor of the Doppler factor ratio (Equation (2)). This effect has been discussed by, e.g., Yamazaki et al. (2004b).

4.6. Spectral Lag

Soft GRB emission usually arrives later than hard emission in some GRBs. This "spectral lag" is evident for long-duration GRBs (Norris et al. 2000; Gehrels et al. 2006; Liang et al. 2006), but is typically negligible for short-duration GRBs (Norris & Bonnell 2006; Yi et al. 2006). Usually, the lag may be visualized as the time differences of the peaks of the "same" pulse in different energy bands. Statistically it can be derived through a cross-correlation analysis of the pulse profiles in different energy bands (Norris et al. 2000). Technically, what is usually measured is the lag time Δt between two BATSE (or *Swift*/BAT) bands E and $E + \Delta E$. Mathematically, this corresponds to $|\int_E^{E+\Delta E}(dt/dE)dE|$. It is therefore important to study dt/dE (or dE/dt) in theoretical models.

Theoretically, the leading model of the spectral lag is the "kinetic" effect, i.e., the delay is due to the fact that the observer is looking at the increasing latitudes with respect to the line of sight with time (e.g., Salmonson 2000; Ioka & Nakamura 2001; Norris & Bonnell 2006; Shen et al. 2005; Lu et al. 2006). One can derive the spectral lag within this model as follows. Since the cooling timescale in the GRB emission region is very short, one may assume that the decay of GRB pulses is dominated by this high-latitude "curvature" effect. The comoving emissivity is assumed to be uniform everywhere across the conical jet. Softer emission comes from higher latitudes (due to their smaller Doppler factor) and therefore is delayed by a time $t \sim (1+z)(R_{\rm GRB}/c)(1-\cos\theta)$ with respect to the emission from the line of sight, where θ is the angle from the line of sight. The observed photon energy is related to the comoving one via $E = \mathcal{D}E'$, where $\mathcal{D}$ is the Doppler factor (Equation (3)). One therefore has

$$\frac{dE}{dt} = \frac{cE'}{R_{\rm GRB}(1+z)}\frac{d\mathcal{D}}{d(-\cos\theta)} = -\frac{cE'\beta}{(1+z)R_{\rm GRB}\Gamma(1-\beta\cos\theta)^2}. \quad (11)$$

The negative sign denotes "lag," i.e., increasing E (harder) corresponds to a decreasing arrival time t (earlier). When $\theta \to 0$ (close to the line of sight), this is simplified as

$$\frac{dE}{dt} = -\frac{4cE'\Gamma^3}{(1+z)R_{\rm GRB}} = -\frac{2E'}{(1+z)\tau}\Gamma = -\frac{2}{1+z}\frac{E}{\tau}, \quad (12)$$

where

$$\tau = \frac{R_{\rm GRB}}{2\Gamma^2 c} \quad (13)$$

is the angular spreading time, which could be related to the observed half-width (in the decaying wing) of the GRB pulse.[15] Note that $R_{\rm GRB}$ is a value one cannot directly measure, therefore in the above expression it needs to be combined with Γ^2 to derive τ, leaving only one power in the Γ-dependence in Equation (12). Another comment for this expression is that dE/dt is E-dependent, i.e., for the same GRB pulse, the lag between E_1 and $(E_1+\Delta E)$ should be different from that between E_2 and $(E_2+\Delta E)$. This can be understood with Equation (11) by noticing that different E corresponds to different $\mathcal{D}$, and hence, different θ. For $\theta > 0$, dE/dt takes a different form than Equation (12), which is valid for the hardest (on axis) pulse.

One can immediately draw the following inference from Equation (12). Since $dE/dt \sim E/\tau$, one can get the lag $\Delta t \sim \tau$ if one takes $\Delta E \sim E$. This is to say, the lag time is comparable to the pulse width itself. So spectral lags do not carry direct information of the progenitor. On the other hand, since the pulse width can be related to variability timescale, which may be related to the physical types (Section 4.5), one may speculate the expected spectral lags of the two types by the following way. Type I GRBs have naked central engines, so their pulse widths τ are typically much smaller than those of Type II GRBs, whose variability timescales are longer due to the additional modulation of the stellar envelope. One therefore may expect that Type I GRBs have shorter lags than Type II GRBs. This is consistent with the fact that short-duration GRBs (preferentially Type I) have negligible lags, while long-duration GRBs (preferentially Type II) have long lags.

Another commonly discussed argument is that Type I GRBs may have larger Γ's than Type II GRBs (due to a "cleaner" environment with less baryon loading), and that this might be the origin of short lags (e.g., Norris & Bonnell 2006). According to Equation (12), one can argue[16]

$$\left|\frac{dt}{dE}\right| \propto \frac{1}{\Gamma}. \quad (14)$$

if different bursts have similar τ and E' (see also Shen et al. 2005). However, the two assumptions (same τ and E') lack physical justifications. In particular, E' depends on the dissipation mechanism and the properties (e.g., B field strength) in the dissipation region, which depends on the burst parameters such as L, δt, etc. Although the central engine variability timescales (τ) may be arguably similar within the Type I or Type II category, respectively, they are considerably different between the two types. We therefore conclude that the Lorentz factor argument is not robust. Type I GRBs can have larger Γ's, but it is not the main reason for their short spectral lags.

A major issue of such a kinetic (high-latitude curvature effect) model is that the peak flux of the pulse drops rapidly with angle (Fenimore et al. 1996; Kumar & Panaitescu 2000), so that the flux is expected to be too low in softer bands to interpret the observed flux. None of the previous kinetic modelers (Salmonson 2000; Ioka & Nakamura 2001; Shen et al. 2005; Lu et al. 2006) have seriously confronted the flux predictions with the data (although the timing data have been well interpreted by the models). One way to increase the high-latitude flux is to invoke a non-power-law instantaneous spectrum at the end of internal emission (e.g., at the shock crossing time in the internal shock model), e.g., a power law with exponential cutoff (Zhang et al. 2009) or a Band function (Qin 2008). The curvature effect of these models predicts that the spectral peak sweeps across different energy bands, making the flux not drop as rapidly as in the case of a power-law spectrum. Indeed, GRB 060218 can be modeled by an evolving cutoff power law (Campana et al. 2006), and GRB 050814 can be modeled by the curvature effect model invoking a cutoff power-law spectrum (Zhang et al. 2009). However, the light curve for a given band is always a decay function unless the spectral index before E_p is much flatter than -1. This is not supported by the spectral data of most GRBs. One is then obliged to abandon the hypothesis of a uniform jet. A structured jet with a less energy and/or a lower Lorentz factor at large angles from the jet axis and with the line of sight piercing into the wing of the structured jet (Zhang & Mészáros 2002b; Rossi et al. 2002; Zhang et al. 2004) can be invoked to account for the observed spectral lag data.

In reality, there might be additional mechanisms that are related to the observed spectral lags of GRBs, but the kinetic effect must exist, and may play the dominant role to define spectral lags in most GRBs.

4.7. Statistical Correlations

Observationally, some empirical correlations among several observed quantities have been claimed (see, e.g., Zhang 2007 for a summary). Most of these correlations were discovered for long/soft GRBs. Here we discuss two of them that are potentially related to Type I/II diversity.

Amati (Yonetoku) relation. Statistically, more energetic long GRBs are harder. This is usually expressed in terms of $E_p(1+z) \propto E_{\gamma,\rm iso}^{1/2}$ (Amati et al. 2002) and $E_p(1+z) \propto L_{\gamma,\rm iso}^{1/2}$ (Yonetoku et al. 2004). The dispersions of the correlations are large, and outliers do exist (e.g., the nearby GRB 980425/SN 1998bw is an outlier of the Amati relation). It has been argued that the observed correlations are solely due to some selection effects (Nakar & Piran 2005; Band & Preece 2005; Butler et al. 2007). However, the fact that the correlations are valid for most z-known GRBs which cover five decades in isotropic energy (Sakamoto et al. 2006) suggest that there is likely underlying physics that drives such correlations.

Inspecting the expressions of E_p in various GRB prompt emission models discussed in Section 4.5 (see also Zhang & Mészáros 2002a), one can see that although E_p is indeed generally a function of L, it is usually also a function of other parameters, in particular, the bulk Lorentz factor Γ which is usually not directly measured. In order to interpret the Amati/Yonetoku relations, one needs to introduce a rough dependence between Γ and L. We now again discuss the three prompt emission models and investigate how the correlations may be interpreted within each model.

1. For the internal shock models, the Amati/Yonetoku relations require that $\gamma_e^k r^{-1}$ be roughly constant. If γ_e is roughly constant, then the internal shock radius should be similar

[15] In principle, τ is the upper limit of the observed half-width in the decaying wing, since part of the tail may be buried beneath the next rising pulse.

[16] Note that this is different from Norris & Bonnell (2006) who argued $\Delta t \propto \Gamma^{-1/2}$ based on the expression of the angular spreading time rather than based on the differential property dE/dt as discussed in this paper.

for different bursts. This suggests that Γ is essentially independent of L (since the variability timescale may be similar among Type II GRBs), a requirement not immediately evident based on physical arguments. Alternatively, if $\gamma_e \propto \Gamma$, the relation can be naturally satisfied for the synchrotron model ($k = 2$). This suggests that high-$\bar{\Gamma}$ GRBs are more variable. In other words, while the maximum Lorentz factor of the outflows Γ_M can vary from burst to burst, the minimum Lorentz factors Γ_m for different bursts are similar to each other, so that $\gamma_e \propto (\Gamma_M/\Gamma_m) \propto \bar{\Gamma}$.

2. Within the photosphere model, the most relevant regime for Type II GRBs is the one with a stellar envelope (Equation (9)). An interpretation of the Amati/Yonetoku relation can be made (Thompson 2006; Thompson et al. 2007) by introducing another *assumption* that the total energy of different GRB jets is quasi-universal, a conclusion reached in the pre-*Swift* era (Frail et al. 2001; Bloom et al. 2003a). Recent *Swift* observations suggest that the "achromatic" behavior, the demanded characteristic of a jet break, is not commonly seen (Liang et al. 2008). This raises the issue of interpreting some afterglow temporal breaks as jet breaks. Furthermore, the inferred total energies (after beaming correction) are found to a have larger scatter than the pre-*Swift* sample (Liang et al. 2008; Kocevski & Butler 2008; Racusin et al. 2009). In any case, if one believes $E_\gamma = E_{\gamma,\rm iso}\theta_j^2 \sim$ const, using the argument that baryon sheath near the breakout radius leads to $\Gamma_* \sim \theta_j^{-1} \propto E_{\gamma,\rm iso}^{1/2}$ (Thompson 2006; Thompson et al. 2007), one can translate Equation (9) into $E_p \propto L_{\gamma,\rm iso}^{1/2} \propto E_{\gamma,\rm iso}^{1/2}$ by taking the trivial proportionality $L \propto L_{\gamma,\rm iso} \propto E_{\gamma,\rm iso}$. The first proportionality is based on the fact that the GRB efficiency is not a function of $L_{\gamma,\rm iso}$ (Lloyd-Ronning & Zhang 2004); while the second proportionality is based on the fact that the dispersion of T_{90} is not large and that T_{90} is not correlated to $L_{\gamma,\rm iso}$. In view of the fact that GRB 080916C disfavors the photosphere origin of E_p (Zhang & Pe'er 2009), we regard this interpretation as no longer attractive.
3. The magnetic dissipation model lacks a robust prediction for E_p. In any case, similar to the other two models, the Amati/Yonetoku relation can be satisfied if one assigns a particular $\Gamma - L$ correlation. For example, the specific model described in Equation (10) requires $\Gamma \propto L^{1/2}$.

When the optical afterglow light-curve temporal break ($t_{\rm opt}$) is included, a tighter correlation involving E_p and $E_{\gamma,\rm iso}$ is obtained (Ghirlanda et al. 2004; Liang & Zhang 2005) for some long-duration GRBs. However, the physical connections between the prompt emission properties (E_p and $E_{\gamma,\rm iso}$) and the afterglow properties ($t_{\rm opt}$) or the global collimation degree of the jet are not straightforwardly expected. Furthermore, optical afterglow temporal break data of Type I GRBs are still poor to draw any conclusion. We therefore do not discuss these relations in this paper.

Luminosity-lag relation. Norris et al. (2000) discovered a relation between the gamma-ray peak luminosity $L_{\gamma,\rm iso}^p$ and the spectral lag Δt between the BATSE Channel 1 (25–50 keV) and Channel 3 (100–300 keV), i.e., $L_{\gamma,\rm iso}^p \propto (\Delta t)^{-1.15}$. The relation was refined by Gehrels et al. (2006) who corrected the observed spectral lag to that between two common bands in the cosmic proper rest frame of GRBs. This correction takes two steps. First, the observed spectral lag Δt between the bands from E to $(E + \Delta E)$ can be expressed as $\Delta t = \Delta t_{\rm rest}(E_{\rm rest})(1 + z)$, where $\Delta t_{\rm rest}(E_{\rm rest})$ is the spectral lag between $E_{\rm rest}$ to $(E_{\rm rest} + \Delta E_{\rm rest})$ in the cosmic proper rest frame. Second, what one cares about is the intrinsic spectral lag between a common rest-frame energy interval, e.g., from E to $(E + \Delta E)$. One needs an additional relation between $\Delta t_{\rm rest}(E)$ and $\Delta t_{\rm rest}(E_{\rm rest})$. There is no universal relation for this, but there is an empirical relation between pulse width and energy, i.e., the pulses become narrower with energy with $w \propto E^{-a}$ with $a \sim$ (0.3–0.4) (Fenimore et al. 1995; Norris et al. 2005; Liang et al. 2006; Zhang & Qin 2008). *Assuming that the spectral lag is proportional to the pulse width* (see, e.g., Norris et al. 2005), one may derive $\Delta t_{\rm rest}(E) = \Delta t_{\rm rest}(E_{\rm rest})(E/E_{\rm rest})^{-a} = \Delta t_{\rm rest}(E_{\rm rest})(1 + z)^a$. This finally gives

$$\Delta t_{\rm rest}(E) = \Delta t(E)(1 + z)^{a-1}. \quad (15)$$

In Gehrels et al. (2006), $a \sim 1/3$ was adopted, and a correlation

$$L_{\gamma,\rm iso}^p \propto [\Delta t(1 + z)^{a-1}]^{-\delta} \propto \left[\frac{\Delta t}{(1 + z)^{2/3}}\right]^{-\delta} \quad (16)$$

is found for a sample of long GRBs, with $\delta \sim 1$. Outliers do exist for long GRBs, and short GRBs are noticeably off the track of the correlation.

Is there an underlying physical mechanism that justifies the observed $L_{\gamma,\rm iso}^p \propto (\Delta t_{\rm rest})^{-\delta}$ correlation? It is not obvious based on the theoretical arguments above. According to Equation (12), the intrinsic lag is related to the intrinsic variability timescale of the burst. So a L–lag negative relation may be related to another, probably more intrinsic L–V positive relation, where V is the variability parameter. Technically, there are different definitions of the variability parameter (Fenimore & Ramirez-Ruiz 2000; Reichart et al. 2001; Guidorzi et al. 2006), but in any case, a more variable light curve (high V) would have shorter variability timescales (corresponding to τ), and hence, shorter spectral lags (Δt). Observationally, indeed a positive L–V relation is observed, although with a large scatter (Fenimore & Ramirez-Ruiz 2000; Reichart et al. 2001; Guidorzi et al. 2006). The interpretation of this correlation within the internal shock model invokes several assumptions: (1) The smallest variability timescale is defined by the collisions above the pair photosphere. (2) The true jet energy is quasi-universal (Frail et al. 2001). (3) Narrower jets have higher Γ's (Kobayashi et al. 2002; Mészáros et al. 2002).[17] This is a relevant interpretation to the observed $L_{\gamma,\rm iso}^p \propto (\Delta t_{\rm rest})^{-\delta}$ relation. However, in view of the assumptions invoked in the reasoning (the above three as well as the assumption that the w–E correlation is similar to Δt–E correlation as invoked earlier), we expect that the correlation should not be very tight, and may not follow the same simple power law. This is consistent with the data (see Section 5 for details).

Would Type I GRBs satisfy a similar correlation? In principle, one can expect so if the set of assumptions discussed above is satisfied. In reality, Type I GRBs may not effectively develop a pair photosphere, both because of their preferred higher Lorentz factors (clean environment) and because of their lower total energy. This would make the observed variability timescale trace the central engine variability timescale, which would not vary significantly among bursts.

Another model to interpret the $L_{\gamma,\rm iso}^p \propto (\Delta t_{\rm rest})^{-\delta}$ correlation invokes varying Doppler factors among different bursts (Salmonson 2000; Ioka & Nakamura 2001). These models assume a universal comoving properties of ALL GRBs, and invoke

[17] The third assumption may be in conflict with the explanation of the Amati/Yonetoku relation within the standard internal shock model as discussed in Section 4.5. To interpret that relation, one requires no dependence of Γ on L (and hence, on θ).

the off-beam geometry to interpret longer durations and spectral lags. As already discussed, the comoving properties of GRBs depend on many parameters. The off-beam model is not supported by early afterglow observations. We therefore regard these early models invoking pure geometrical effects as no longer favorable in view of the recent observational progress.

4.8. Energetics and Beaming

Type II GRBs are generally expected to be more energetic than Type I GRBs. In the standard BH-torus central engine model, the total energy of the burst is positively correlated with the total available fuel in the torus. Massive stars are much more abundant in mass, which can reach $\sim 10\,M_\odot$ of fuel in total. On the other hand, a NS–NS merger system has a total energy budget of $\sim 2.8\,M_\odot$. After the prompt collapse, the available fuel in the torus is of order $\sim 0.1\,M_\odot$. A BH–NS merger system has even less fuel to begin with ($\sim 1.4\,M_\odot$). It would reach a similar total energy budget in accretion as the NS–NS system. In these models, Type I GRBs are expected to be 10–100 times less energetic than Type II GRBs. Alternatively, GRBs may be powered by the spin energy of the central object (a rapidly spinning BH or NS). For the case of an NS central engine, Type I GRBs may reach similar energies as Type II GRBs. For the case of a BH engine whose spin energy is extracted via a magnetic torque (Blandford & Znajek 1977; Li 2002), a Type II GRB is again expected to be $\sim$ 10 times more energetic than a Type I GRB if it is powered by a NS–NS merger, again because of the more massive BH in the Type II GRB. A BH–NS merger Type I GRB, on the other hand, may reach the same energetics as Type II GRBs if the initial BH in the binary system is massive enough and has a large enough angular momentum.

In order to relate this theoretically motivated total energy budget to the observed energy, one needs to introduce the beaming factor. The standard GRB jet models invoke a conical jet with uniform energy distribution (Mészáros et al. 1998; Rhoads 1999; Sari et al. 1999). More complicated (maybe more realistic) jet models invoke distributions of jet energy with angle from the jet axis (Mészáros et al. 1998; Zhang & Mészáros 2002b; Rossi et al. 2002; Zhang et al. 2004). Theoretically, it is difficult to model how jets are launched from the central engine. On the other hand, one can speculate about the collimation angle of jets from two types of GRBs from the theoretical point of view: Type II GRBs should tend to have narrower jets than Type I GRBs due to the additional collimation of the stellar envelope (Zhang et al. 2003). Type I GRB jets tend to be broader (Aloy et al. 2005). Observationally this prediction has not been tested statistically. Observations of some individual bursts seem to support this picture. For example, the Type I Gold Sample burst GRB 050724 was found to have a beaming angle wider than $\sim 25^\circ$ (Grupe et al. 2006; Malesani et al. 2007). Type II GRBs on the other hand, have a typical beaming angle of $\sim 5^\circ$ (Frail et al. 2001; Bloom et al. 2003a; Liang et al. 2008; Kocevski & Butler 2008; Racusin et al. 2009). Opposite cases are also observed in some GRBs. For example, the short GRB 051221 (a Type I candidate) has a narrow jet with $\theta_j \sim 4^\circ$–8° (Burrows et al. 2006). This is contrary to the theoretical expectation if it is indeed a Type I GRB. On the other hand, the Type II GRB 060729 (Grupe et al. 2007, 2009a) may have a large opening angle since its X-ray afterglow keeps decaying without a break for hundreds of days.

The observed "isotropic" energy is the total energy divided by the beaming factor ($2 \cdot \pi\theta_j^2/4\pi = \theta_j^2/2$ for uniform jets under the small angle approximation). Considering a factor of $\sim (20/5)^2 \sim 15$ difference in the beaming factor, the isotropic energy of a typical Type I GRB should be a factor $\sim$ 100–1000 times lower than that of a typical Type II GRB. If a Type I GRB has a high isotropic luminosity/energy comparable to that of a typical Type II GRB, one must then demand a very narrow jet, with an opening angle even smaller than that of Type II GRBs. A BH–NS central engine with the Blandford–Znajek mechanism as the engine power can ease the constraint, but a comparable beaming angle to Type II GRBs is nonetheless needed.

4.9. Afterglow Properties

Broadband afterglow emission has been interpreted as the external forward shock emission as the fireball is decelerated by the circumburst medium. An ideal observational campaign can lead to diagnostics of the circumburst medium properties (Panaitescu & Kumar 2002; Yost et al. 2003), which can shed light on the progenitor system of the GRB (e.g., Fan et al. 2005; Greiner et al. 2009a; Xu et al. 2009). In particular, if a stratified stellar-wind-type medium ($n \propto R^{-2}$) (Dai & Lu 1998; Chevalier & Li 2000) is identified, the burst can be identified as a Type II GRB. The case of a constant density medium is, however, less informative. Although Type I GRBs are expected to reside in such a medium, some Gold-Sample Type II GRBs have been found to reside in a constant medium as well (Panaitescu & Kumar 2002; Yost et al. 2003). The mechanism of forming such a medium before the death of the massive star is unknown. In any case, one needs more information to establish the association of a burst with a physical model category if it goes off in a constant density medium. For example, the afterglow luminosity of Type I GRBs should be systematically lower than that of Type II GRBs due to the expectation of both a lower medium density in the merger environment (relevant for $\nu < \nu_c$) and a systematically lower blast wave energy (Panaitescu et al. 2001; Fan et al. 2005; Kann et al. 2008). A Type I GRB can be even "naked" (i.e., no detectable afterglow) if the ambient medium density is low enough. Such GRBs are indeed observed (e.g., GRB 051210; La Parola et al. 2006).

A related issue is the GRB radiative efficiency. Observations and theoretical modeling suggest that the efficiency is similar for both Type I and Type II GRBs (Zhang et al. 2007b; Berger 2007; Gehrels et al. 2008), so that it cannot be regarded as a useful criterion to tell the model category that is associated with a particular GRB.

4.10. Redshift Distribution

Statistically, redshift distributions of Type I and Type II GRBs should be different. Type II GRBs generally trace the star-forming history of the universe.[18] Type I GRBs are expected to be "delayed" with respect to star formation due to the long merger timescale associated with the shrinking of the binary orbits due to gravitational radiation (Belczynski et al. 2006). On average, it is expected that the mean redshift of Type I GRBs is lower than that of Type II GRBs.

4.11. Luminosity Function

The luminosity function of long-duration GRBs is categorized by a broken power law with a break $\sim 10^{52}$ erg s^{-1} (Guetta et al. 2005; Liang et al. 2007; Virgili et al. 2009a). Below the break

[18] Metallicity may play an additional role to select Type II GRBs (e.g., Wolf & Podsiadlowski 2007; Nuzaet al. 2007; Li 2008), but the issue is inconclusive.

the power-law index is > -1, while above the break the power-law index is < -2. Low-luminosity GRBs may form a distinct bump at $L < 10^{49}$ erg s^{-1} (Liang et al. 2007; Virgili et al. 2009a; Dai 2009). As argued below, most long GRBs are Type II GRBs, so this luminosity function may be regarded as that of Type II GRBs. There is however no direct theoretical reason for such a luminosity function. For Type I GRBs, the luminosity function has not been studied in detail due to the limited sample with redshift measurements so far (but see Virgili et al. 2009b). The luminosity function of the BATSE short/hard GRB sample was studied (Guetta & Piran 2006), but as discussed below, it is not justified that this population is identical to the Type I population. This issue will be further discussed in Sections 5.4 and 6 below.

4.12. Gravitation Wave Signals

Probably the most definite criterion to differentiate Type I GRBs from Type II GRBs is through detecting their GW signals. Although the GW signature of a Type II GRB is highly uncertain (e.g., Kobayashi & Mészáros 2003), the wave forms of NS–NS and NS–BH mergers are well predicted (e.g., Dalal et al. 2006). Detections of these signals would unambiguously associate some GRBs with the Type I model category. However, this criterion can only be applied in the future when the GW detectors reach the desired sensitivities.

5. TYPE I AND TYPE II SAMPLES AND THEIR STATISTICAL PROPERTIES

5.1. Sample Selection

The above consideration suggests that theoretically there is no handy, distinct criterion that can be used to immediately determine the physical model category that a burst is associated with. In this section, we attempt to explore the topic further from the observational point of view. The current standard approach is to use three criteria, "duration," "hardness," and (when available) "spectral lag," to categorize bursts as "long" (implicitly assumed to be associated with "Type II") or "short" (implicitly assumed to be associated with "Type I"), and use these samples to explore the statistical properties of other observational properties (e.g., Nakar 2007; Berger 2009). In other words, it is often implicitly assumed that

$$\begin{aligned} \text{Long/soft/long lag} &= \text{Type II} \\ \text{Short/hard/short lag} &= \text{Type I}. \end{aligned} \quad (17)$$

The problem with such an approach is that these criteria may not be always reliable. A notable example was GRB 060614, which is a long GRB but is very likely associated with Type I (Gehrels et al. 2006; Zhang et al. 2007a). Another complication is related to GRB 080913, GRB 090423, and some other intrinsically short GRBs (e.g., Levan et al. 2007). These GRBs can be detected as short/hard GRBs if their redshifts were low enough, but their physical properties are more close to those of Type II GRBs. Some short/hard GRBs (e.g., 060121, de Ugarte Postigo et al. 2006) are very energetic, which are not easy to be accommodated within the Type I progenitor models.

In this paper, we adopt an alternative approach. *Instead of sticking to the observed gamma-ray properties, we adopt the observational criteria that are directly related to the progenitor systems to select the samples, and then go back to investigate the other properties (including duration, hardness, spectral lag, etc.) of the samples.* The advantage of this approach is that we can start with those GRBs whose progenitor systems are more confidently inferred. We can then use them to verify whether the ansatz Equation (17) is justified.

We define the following three samples based on the criteria detailed below.

Type II Gold Sample. This sample is defined such that at least one of the following two criteria are satisfied.

1. There is a spectrally confirmed SN association with the GRB.
2. The SSFR is very high (to be specific, the SSFR satisfies $\log \mathrm{SSFR} > -0.2$ or $\mathrm{SSFR} > 0.63$ Gyr^{-1} in the sample of Savaglio et al. 2009); the GRB location does not have a large offset from the center; and there is no stringent upper limit on the existence of an SN associated with the GRB.

Note that the GRB properties (duration, hardness, and lag) are not the considerations to define the sample. Since not many GRBs have host SSFR information published, this sample is by no means complete, and there should be many more Type II GRBs that are not included. The purpose of selecting this sample is to use the most stringent criteria to investigate how the best Type II GRB candidates look like. As a result, we do not include the GRBs that have a claimed SN bump in the optical light curve but no confirmed SN spectroscopic signature. The threshold of SSFR is arbitrary. This limiting value was chosen because Table 11 of Savaglio et al. (2009) has a mix of long and short GRBs for $\log \mathrm{SSFR(Gpc^{-1})} < -0.3$, which is the regime where confusion arises. The lower bound $\log \mathrm{SSFR} > -0.2$ can be regarded as a safe line above which GRB hosts have very active star formation. One exception is the short-duration GRB 051221A (Soderberg et al. 2006b; Burrows et al. 2006). The SSFR value ($\log \mathrm{SSFR} > 0.804$) is way above the threshold. However, since deep searches have ruled out the association of a 1998bw-like SN (Soderberg et al. 2006b), we do not include it in the Type II sample, and will include it in the "Other short hard sample." We note that many *Swift* long GRBs should be associated with Type II. However, since no published SSFRs are available for most of them, we refrain from including them in the Type II Gold Sample.[19] This sample should be expanded significantly later when the host galaxy information of the *Swift* GRBs is released. Right now the Type II Gold Sample includes 33 GRBs (Table 1, top panel). This is already a large enough sample to study the statistical properties of Type II GRBs.

Type I Gold Sample. The Gold Sample of Type I GRBs is defined by at least one of the following two criteria.

1. The host galaxy is elliptical or early type.
2. The GRB location has a relatively low local SSFR, or a large offset from the center of the host galaxy; and deep searches reveal stringent upper limits on the existence of an underlying SN.

Again the GRB properties (duration, hardness, lag) are not considered. Some arguments (Belczynski et al. 2006; Zheng & Ramirez-Ruiz 2007) have suggested that a fraction of Type I GRBs may be located in the star-forming regions of star-forming galaxies. Our criteria do not select those, since we do not demand the completeness of sample selection. After systematically checking the archival data, we only identify five bursts in the Type I Gold Sample: GRBs 050509B, 050709,

[19] Besides those included in the Savaglio et al. (2009) sample (which covers from GRB 970228 to GRB 061126), we only include GRB 080520 and GRB 060602A based on the SFR criterion. They have a high SFR (though SSFR is not measured) typical for other Type II Gold Sample GRB host galaxies. For example, GRB 080520 has $\sim 15\ M_{\odot}\mathrm{yr}^{-1}$ (Malesani et al. 2008), which is comparable to the highest in the Savaglio et al. (2009) sample.

050724, 060614,[20] and 061006 (Table 1, middle panel). The details of individual GRBs are presented in the Appendix.

Other SGRB Sample. Most short/hard GRBs in the *Swift* era satisfy neither of the two criteria of the Type I Gold Sample. Some of them do not have their host galaxies convincingly identified. Others have host galaxies with active star formation. These GRBs are usually regarded as Type I candidates simply because they are "short/hard." There could be a good fraction of Type I GRBs in this sample, but we are not sure that they can ALL be associated with Type I. Since we define the Gold Samples not based on the GRB properties, we leave these bursts in a separate sample, without specifying whether they are associated with Type I or Type II. There are 20 bursts in this sample (Table 1, bottom panel). The details of individual GRBs are presented in the Appendix.

5.2. Duration-hardness Distribution

Figure 2 presents the traditional T_{90}–HR plot of GRBs. Superimposed on the BATSE data (orange small dots) are the three samples defined above: Type II Gold Sample (blue), Type I Gold Sample (red), and other SGRB sample (green). The HR is defined as the fluence ratio between (50–100) keV and (25–50) keV. For BATSE bursts, this corresponds to the fluence ratio between channel 2 and channel 1. For other detectors (HETE-2, *Swift*/BAT, Konus/*Wind*, INTEGRAL) with different detector energy bands, we perform spectral fits and use the fitted model to derive the HR. Besides the observed points (open symbols), we also plot the corresponding "rest-frame" points (filled symbols) for each burst. The HR is then defined as the flux ratio between the rest-frame (50–100) keV band and (25–50) keV bands, which is again derived from spectral fitting. For a power-law fit, the rest-frame HR is the same as the observed one. For a curved spectrum (e.g., a Band function or an exponential cutoff power law), the two can be different. The T_{90} values are energy- and detector dependent. We do not make efforts to convert all T_{90} to the BATSE band, since this requires time-dependent spectral analyses and extrapolations, and for many bursts the data quality is not sufficient to perform such an analysis. Instead we simply plot T_{90} measured by different detectors (e.g., *Swift* and HETE). The correction to the BATSE-band T_{90} is usually not significant for most long GRBs, but could be significant to those GRBs with soft extended emission. Traditionally, the "rest-frame" T_{90} are not used to define long versus short for a particular GRB. We present them here just to show how the intrinsic distribution may differ from the observed one. To derive the rest-frame $T_{90}^{\rm rest}$, we simply divide the observed value by $(1 + z)$. More rigorously one needs to again take into account the light-curve evolution with energy. This again requires a time-dependent spectral analysis. Since most bursts do not have such detailed information, and since the correction would not be significant for most bursts, we neglect this correction for the sake of simplicity and uniformity. For short GRBs with extended emission, we use circles to denote the short spikes only (excluding the extended emission), while using squares to denote the full emission with extended emission included. These two locations for the same burst with and without extended emission are connected by lines. Since the mean HR is derived, the HRs including extended emission are usually smaller than those without, as the extended emission is typically softer than the initial short spikes.

From Figure 2 one can make the following interesting observations. First, the Type II GRBs are generally long, and they well represent the long/soft population of the BATSE GRBs in the T_{90}–HR plane. However, some Type II GRBs have a duration close to the 2 s separation line, and their intrinsic duration can be shorter than 2 s (e.g., GRB 040924 with $T_{90} = 2.39 \pm 0.24$ s at $z = 0.858$, and GRB 080520 with $T_{90} = 2.82 \pm 0.67$ at $z = 1.545$). Levan et al. (2007) also discussed a sample of apparently long, intrinsically short GRBs. Second, *four out of five Type I Gold Sample GRBs are not strictly "short"*. Except GRB 050509B, all the others have extended emission aside from the initial "short/hard" spike. The spike itself is longer than 2 s for GRB 050724 and GRB 060614. *All 5 Type-I Gold Sample bursts have a moderate HR. None has an extremely hard spectrum.* Third, the Other SGRB Sample fills in the short/hard region in the T_{90}–HR diagram more uniformly, suggesting that it represents the BATSE short/hard sample well. Some bursts in the sample also have extended emission.

5.3. Empirical Correlations

Figure 3(a) displays the E_p–$E_{\gamma,\rm iso}$ (Amati) relation of the three samples. The spectral parameters are collected from the published papers or GCN circular reports (see Table 1 for references). For those GRBs with extended emission (including Type I Gold Sample GRBs 050724, 060614, and 061006), we only consider the short hard spikes. For all the bursts, the isotropic gamma-ray energy ($E_{\gamma,\rm iso}$) is calculated in the GRB rest-frame 1–10^4 keV band through extrapolation based on the spectral parameters. We can see that most GRBs in the Type II Gold Sample indeed follow the $E_p \propto E_{\gamma,\rm iso}^{1/2}$ (Amati) relation. However, there are three noticeable outliers: GRB 980425, GRB 031203, and GRB 050826. The first two are nearby low-luminosity (LL) GRBs, which have been argued to be from a distinct population (e.g., Liang et al. 2007; Virgili et al. 2009a; Dai 2009). Another nearby LL GRB 060218 is a soft burst (Campana et al. 2006) and satisfies the Amati relation well. GRB 050826 with $T_{90} \sim 35$ s is an intermediate Type II GRB between the more "classical" Type II and the nearby LL-GRBs (Kann et al. 2007), and deviates from the relation. We also pay special attention to the two intrinsically short Type II GRBs. Although GRB 040924 is right on the Amati-relation track, GRB 080520 seems to be slightly off the track. The Type I Gold Sample and the other SGRB Samples are populated above the conventional Amati-relation track. Since many short/hard GRBs have E_p outside the BAT band, their E_p error bars are large. The values in our analyses are adopted from Butler et al. (2007). In any case, it seems that they follow a separate track with a shallower slope than the Amati relation. Excluding GRBs 080913, 090423 and 060121 (which are likely Type II, see Section 6.2), a best fit to the Type I Gold and Other SGRB samples lead to a slope 0.34, with the 3σ limits of the slope as (0.15–0.53; see Figure 3(a)). GRB 080913 is marginally within the 3σ regions for the Type II Amati relation, but is also consistent with this new track defined by Type I and other short/hard GRBs within 3σ. GRB 090423 aligns with the Type II Amati relation more closely (see also Lin et al. 2009).

A likely reason that the Type I and the other SGRB Samples deviate from the Amati relation of Type II GRBs is simply because they have shorter durations so that they have smaller $E_{\gamma,\rm iso}$ values than the Type II GRBs with a similar E_p. To test this, we plot the E_p–$L_{\gamma,\rm iso}^{p}$ relation (Yonetoku relation) in Figure 3(b). We can see that the distinction between Type II and Type I

[20] In the literature GRB 060614 is usually taken as a controversial candidate for Type I. This was mainly because of its long duration. We do not consider duration as a criterion when selecting the Gold Sample. This burst satisfies the criterion 2 of the Type I Gold Sample.

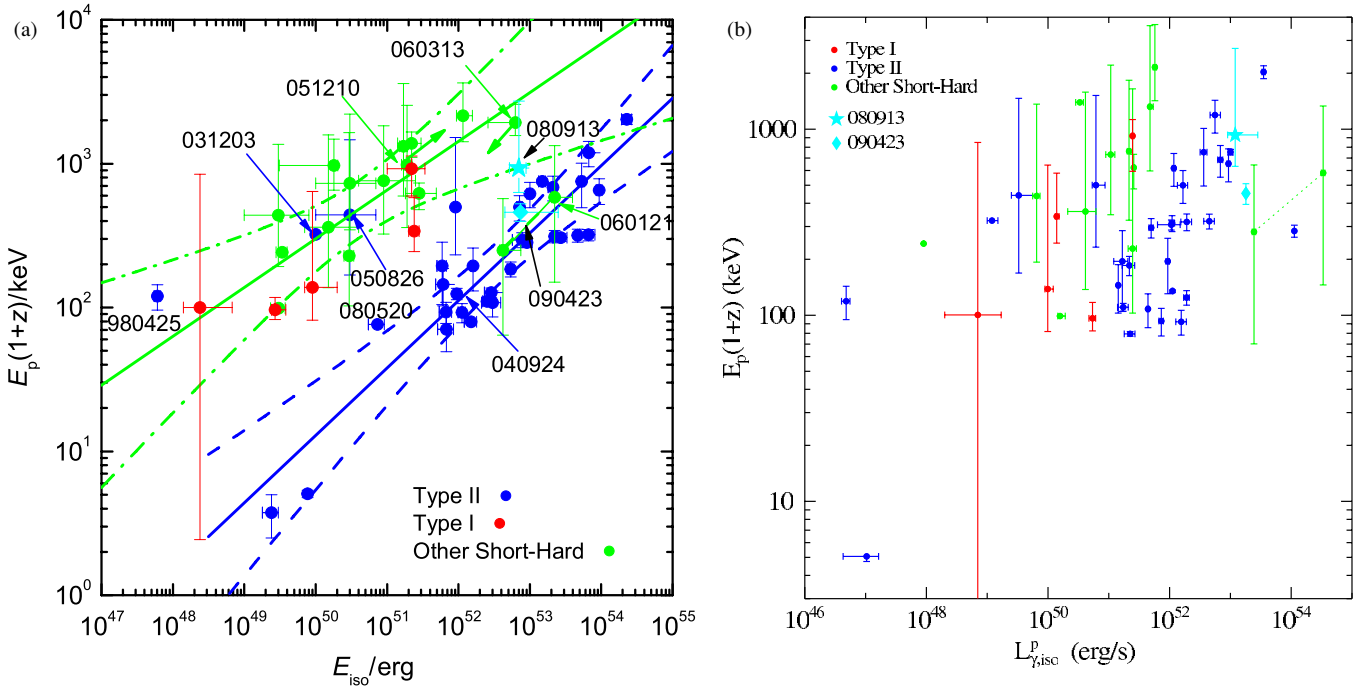

Figure 3. (a) E_p–$E_{\gamma,\rm iso}$ diagram of the three samples of GRB discussed in the paper: Type II Gold Sample (blue), Type I Gold Sample (red), and other short/hard GRBs (green). Two possible redshifts $z = 4.6, 1.7$ for the short GRB 060121 are adopted, which satisfies the relation well (unlike other short/hard GRBs). GRB 080913 and GRB 090423 (cyan) are also plotted for comparison. The best-fit E_p–$E_{\gamma,\rm iso}$ correlations for both Type II and Type I/Other SGRB samples are plotted (solid lines) with the 3σ boundary (dashed line) marked. (b) The E_p–$L^p_{\gamma,\rm iso}$ diagram. The same convention has been used.

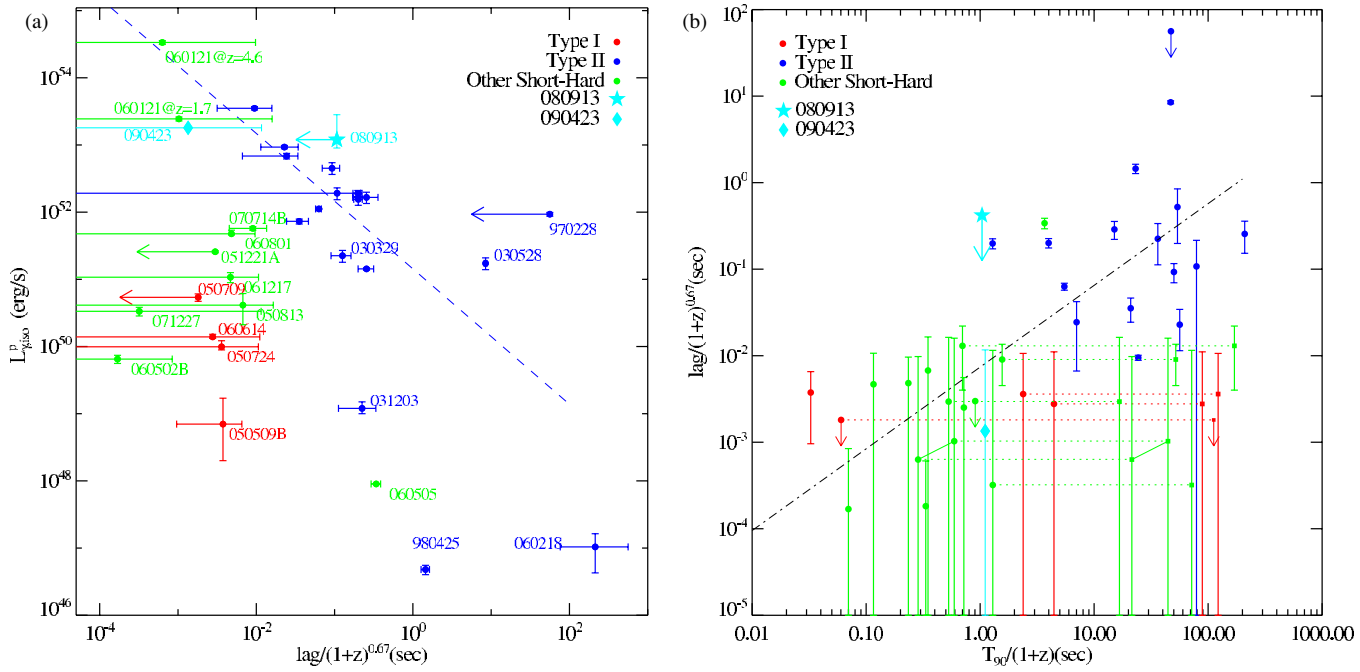

Figure 4. (a) $L^p_{\gamma,\rm iso}$–lag diagram. Same convention as Figure 3 is adopted. GRB 080913 and GRB 090423 satisfy both the correlation defined by Type II GRBs and the "zero lag" trend defined by Type I and Other SGRB Samples. Two possible redshifts $z = 4.6, 1.7$ for the short GRB 060121 are adopted, which satisfies the correlation well (unlike other short/hard GRBs). (b) the lag–T_{90} (intrinsic) diagram of the three samples. The same GRBs with/without extended emission is connected by dotted lines. The spectral lags of these GRBs are for the short/hard spikes only. A positive correlation between duration and spectral lag is derived (dashed line). See text for details.

GRBs becomes less significant, although the correlation now has a much larger scatter. Noticing the large error bars of the Type I and Other SGRB Samples, one may conclude that there is no distinct difference among the three samples as far as the Yonetoku relation is concerned. A similar conclusion was drawn by Ghirlanda et al. (2009) in an analysis of the BATSE GRBs.

Figure 4(a) displays the luminosity-spectral lag diagram of GRBs with the three samples plotted. A group of Gold Sample Type II GRBs indeed defines a $L^p_{\gamma,\rm iso} \propto (\Delta t_{\rm rest})^{-\delta}$ correlation track (Norris et al. 2000; Gehrels et al. 2006), although several low-luminosity, long-lag GRBs lie below the extrapolation of the track (see also Gehrels et al. 2006; Liang et al. 2006).

Gold Sample Type I GRBs are clustered at the lower left corner. This is as expected: short durations define short lags, and smaller energy budgets define lower luminosities. About half of the "Other SGRBs" are clustered close to the Type I Gold Sample, suggesting that they may be associated with Type I as well. Some others fill in the gap between the Type I and Type II Gold Samples. In particular, GRB 060121 lies right on the track for both putative redshifts 1.7 and 4.6 (de Ugarte Postigo et al. 2006). GRB 070714B is also close to the track. The SN-less GRB 060505 clusters with other nearby LL Type II GRBs. Finally, the two high-z GRBs 080913 (note that only the upper limit of spectral lag is derived) and 090423 are consistent with satisfying the $L^p_{\gamma,\rm iso}$–lag correlation of Type II, but are also consistent with the zero-lag trend of Type I/Other SGRB.

As discussed in Section 4.7, the luminosity lag relation may be related to the variability-luminosity relation, and may be more relevant to Type II GRBs. On the other hand, the physical origin of the relation is not clearly understood and is based on many assumptions. Although the correlation may be taken as a reference, it may not be taken as the definite criterion for judging the physical origin of a GRB.

Based on the high-latitude-effect interpretation of spectral lag (Section 4.7), one expects that short spectral lags should be related to short angular spreading times. The latter corresponds to the width of individual pulses. If the number of pulses does not fluctuate significantly among bursts, one would also expect a rough correlation between spectral lags and durations. In Figure 4(b), we display the $T_{90}/(1+z)$ − lag$/(1+z)^{2/3}$ diagram of the three samples of bursts. Again points of the same burst with and without extended emission are connected by lines. We investigate a possible correlation between duration and spectral lag. Since the spectral lags are defined for the short/hard spikes only for those GRBs with the extended emission, we use T_{90} excluding the extended emission for those bursts. A positive correlation between T_{90} and lag with slope 0.94 ± 0.14 is obtained, with the Spearman's rank correlation coefficient $r = 0.735$, corresponding to a chance probability $P < 10^{-4}$. This is consistent with our naive expectation, suggesting that spectral lags are closely related to durations, and may not carry additional information in defining the categories of GRBs.

5.4. Luminosity and Redshift Distributions

Figures 5(a) and (b) display the observed two-dimensional luminosity-redshift ($L^p_{\gamma,\rm iso}$–z) and energy-redshift ($E_{\gamma,\rm iso}$–z) distributions of the three samples. GRBs in the Type I Gold Sample are all at $z < 0.5$. Including the Other SGRB Sample, the upper boundary of z reaches ~ 1 (except GRB 060121). The Type II GRBs have a wider span of redshift distribution, with the peak around $z \sim 1$. In terms of luminosity distribution, the Type II GRBs on average are $\sim$ two orders of magnitude more luminous than the Type I GRBs. Type I GRBs can at least reach a luminosity of $L^p_{\gamma,\rm iso} \sim 2.5 \times 10^{51} \rm erg\,s^{-1}$ (for the Type I Gold GRB 061006). Including the Other SGRB Sample, several short GRBs (070714B, probably 060313, and especially the latest GRB 090510) can reach $L^p_{\gamma,\rm iso} \sim 10^{52}\,\rm erg\,s^{-1}$. GRB 060121 even reaches $L^p_{\gamma,\rm iso} \sim 10^{53}$ –$10^{54}\,\rm erg\,s^{-1}$ for the two fiducial redshifts in discussion. This luminosity is high even for Type II GRBs. GRB 080913 has $L^p_{\gamma,\rm iso} \sim 1.2 \times 10^{53} \rm erg\,s^{-1}$. GRB 090423 has $L^p_{\gamma,\rm iso} \sim 1.88 \times 10^{53}\,\rm erg\,s^{-1}$ (Nava et al. 2009). Both are moderate to high luminosities for Type II GRBs, and are very high when compared with the Type I and Other SGRB Samples (except for GRB 060121). In the $E_{\gamma,\rm iso} - z$ diagram, the separation between Type II and Type I is more distinct, with most SGRB sample bursts lying below the Type II distribution. But GRB 080913 and GRB 090423 become moderate in the Type II Sample due to their intrinsically short durations. The clearer separation between Type II and Type I/Other SGRB Samples is mainly due to the short duration of the SGRB sample, which makes them less energetic. However, GRB 060121 is still as energetic as the average Type II GRBs.

5.5. Afterglow Properties

Figures 6 and 7 present the intrinsic afterglow light curves in the X-ray and optical bands for the three samples. Figure 6 presents the rest-frame 2 keV specific luminosity light curves. Since many Type II Gold Sample GRBs are pre-*Swift*, we do not have many Type II X-ray light curves. Those that are plotted include two LL GRBs (060218 and 050826) and two intermediate-to-high luminosity GRBs (080520 and 050525A). These do not fully represent the Type II GRB X-ray afterglow properties. In order to compensate for this weakness of sample selection, we also overplot the X-ray light curves of a group of early-*Swift* long GRBs in the sample of Nousek et al. (2006). Since we already demonstrated that the Type II Gold Sample represents the BATSE long GRBs well, we assume that the Nousek Sample represents the Type II GRB X-ray afterglows well. We can see that these bursts occupy the upper portion of the light-curve space in Figure 6. By contrast, the Type I Gold Sample occupies the lower portion, and the Other SGRB Sample populates in between with much overlap with both Gold Samples. LL Type II GRBs have luminosities comparable to Type I Gold Sample GRBs.

Figure 7 presents the optical light curves with corrected R_c magnitude by moving all GRBs to $z = 1$ (Kann et al. 2007, 2008). One big difference between these optical light curves and the X-ray light curves (Figure 6) is that most Type II GRBs are represented, exceptions being those GRBs that had negligible optical afterglows but strong SNe signatures (GRBs 980425, 031203, and XRF 060218), dark GRBs, where the optical emission was probably totally suppressed by line-of-sight extinction in the host galaxy (GRBs 990506, 000210, 020819B, 051022), and some with very sparse optical data (XRF 020903, GRBs 030528, 050826, 060602A, 080520). Most data have been taken from Kann et al. (2007, 2008), where the methods of creating the intrinsic light curves are also presented. Similar to the X-ray light curves, the Type II GRB afterglows form a much more luminous group than the Type I GRB afterglows (Kann et al. 2008). The light curves of Type I Gold GRBs and those of most Other SGRBs overlap, indicating that they are likely drawn from the same population. The most prominent exception is again GRB 060121 with an optically luminous afterglow (see Kann et al. 2008, for more details), which is comparable to the afterglows of Type II GRBs.

For both X-ray and optical afterglows, GRB 080913 and GRB 090423 have a luminosity comparable to or higher than the average luminosity of the Type II GRB afterglows (Greiner et al. 2009a; Salvaterra et al. 2009; Tanvir et al. 2009).

6. NATURE OF SHORT/HARD GRBS

Based on the theoretical considerations and the statistical analyses presented above, in this section we attempt to address the question whether the ansatz Equation (17) is valid, i.e., whether Type II GRBs are simply

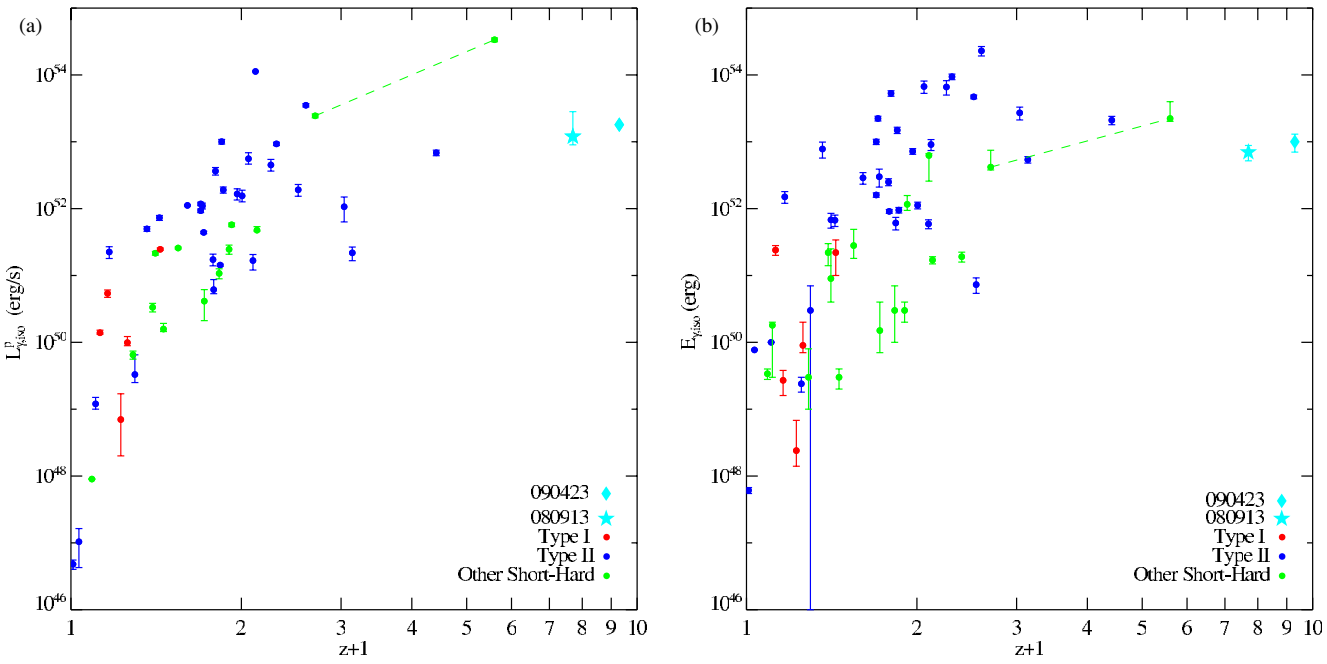

Figure 5. (a) $L^{p}_{\gamma,\rm iso}$–z diagram, and (b) the $E_{\gamma,\rm iso}$–z diagram of the three samples. The same convention as Figure 3 is adopted.

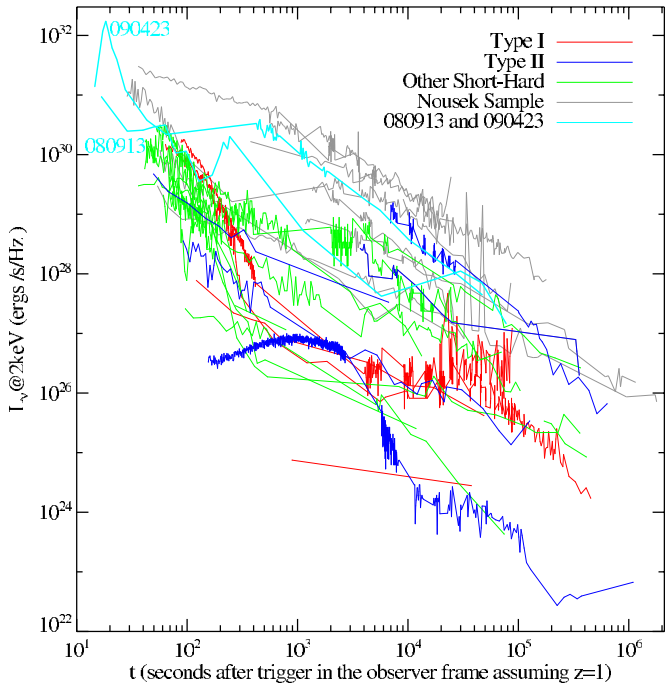

Figure 6. Rest-frame 2 keV X-ray afterglow luminosity light curves of GRB 080913, GRB 090423, and the three samples. All bursts are placed at $z = 1$. The color scheme is the same as in the other figures. Since most Type II Gold Sample bursts are pre-*Swift* ones and have no X-ray light curves, we also add the z-known long GRBs in the sample of Nousek et al. (2006) (gray), which are generally believed to be Type II GRBs. GRB 080913 and GRB 090423 (cyan) both have bright X-ray afterglows typical of Type II GRBs.

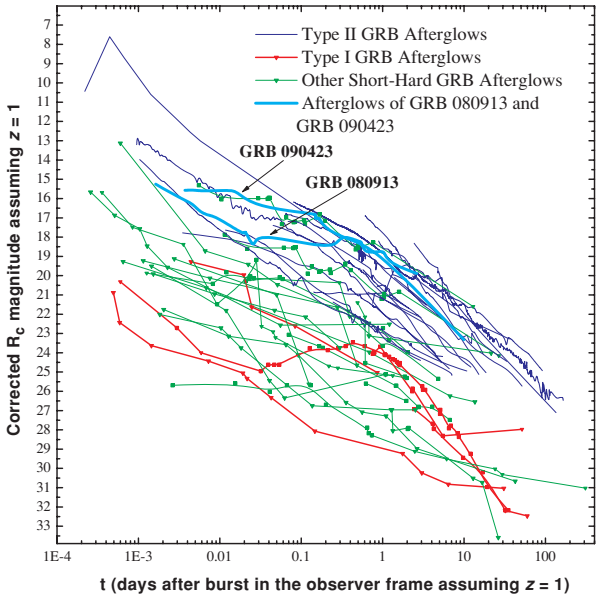

Figure 7. Rest-frame optical light curves of GRB 080913, GRB 090423, and the three samples. The color scheme is the same as in the other figures. Similar to Kann et al. (2007, 2008), they are plotted at a common redshift of $z = 1$. As with the X-ray light curves (Figure 6), the optical afterglows of the Type II Gold Sample GRBs are clearly more luminous than those of the Type I Gold Sample and the Other Short–Hard Sample. The latter two populations are in good agreement with each other. GRB 060121 is the single short-hard GRB which is optically highly luminous. GRB 080913 and GRB 090423 both have bright optical afterglows typical of Type II GRBs.

associated with "long/soft/long lag" GRBs while Type I GRBs are simply associated with "short/hard/short lag" GRBs. In particular, we will address the nature of the Other SGRB Sample. It is likely that some (maybe many) GRBs in the Other SGRB Sample are associated with Type I. The question is whether they are ALL associated with Type I.

6.1. Are All Short/Hard GRBs Associated with Type I?

The most straightforward possibility is to accept that all short/hard GRBs are associated with Type I GRBs. Inspecting the Other SGRB Sample, one may raise the following arguments in support of this suggestion: (1) They indeed occupy the short/hard domain of the BATSE T_{90}–HR diagram, which is in distinct contrast to Type II GRBs that predominantly occupy the long/soft domain. (2) Most of them deviate from the E_p–$E_{\gamma,\rm iso}$ relation

and the $L^{p}_{\gamma,\rm iso}$–lag relation for Type II GRBs. (3) The redshift and luminosity distributions of the observed sample are different from those of Type II, although with much overlap. (4) The afterglow luminosities are systematically lower than those of the Type II majority, although with some overlap. However, as discussed below, there are reasons to be suspicious of this straightforward conclusion.

6.2. Are Some Short/Hard GRBs Associated with Type II?

The fact that some Type II Gold Sample GRBs are intrinsically short naturally raises the possibility that the observed short/hard GRBs are contaminated by Type II GRBs. A small contamination is expected given the overlapping log-normal distributions of T_{90} for the two populations. A more intriguing possibility is that the contamination is not the simple extension of the T_{90} distributions, but accounts for a good fraction of the observed short/hard GRBs.

Conservatively speaking none of the four arguments discussed in Section 5.1 is conclusive. Comparing with the Type I Gold Sample, one cannot straightforwardly demonstrate that the Other SGRB Sample and the Type I Gold Sample come from the same parent sample. In particular, the Type I Gold Sample GRBs are relatively "long" and "soft" within the short/hard population, with four out of five having extended emission. The more "classical" short/hard ones, such as GRBs 051221A, 060313, and 061201, do not satisfy the Gold Sample criteria. After the 2005 revolution of discovering GRB 050509B and GRB 050724, which are associated with elliptical or early-type host galaxies, it is now clear that such associations are not very common. Most short/hard GRBs are found to be associated with star-forming galaxies, some of which have properties close to those of Type II GRBs. According to Berger (2009), the majority of short GRBs appear to occur in star-forming galaxies. Although some compact merger events can have short merger timescales, and therefore appear in star-forming galaxies (Belczynski et al. 2006; Zheng & Ramirez-Ruiz 2007; O'Shaughnessy et al. 2008), the dominance of star-forming host galaxies of short GRBs may raise a concern regarding whether some short GRBs may be associated with Type II. Although there is an observational selection effect that favors redshift identification for star-forming galaxies, the GRBs with bright host galaxies but no redshift identifications (e.g., GRB 051210, La Parola et al. 2006; Berger et al. 2007) are not the predominant population of short/hard GRBs. The fraction of Type II contamination can be small (e.g., $< 1/3$ according to Berger 2009), but may not be negligible. We speculate that some high-L short GRBs in star-forming galaxies may instead be Type II GRBs. For example, GRB 060121 (de Ugarte Postigo et al. 2006) has $E_{\gamma,\rm iso} = 2.2 \times 10^{53}$erg and $L_{\gamma,p,\rm iso} = 3.4 \times 10^{54}\rm erg\,s^{-1}$ for $z = 4.6$ and $E_{\gamma,\rm iso} = 4.2 \times 10^{52}$erg and $L_{\gamma,p,\rm iso} = 2.4 \times 10^{53}\rm erg\,s^{-1}$ for $z = 1.7$. These energy values are typical for Type II GRBs, and the luminosity values even belong to the bright end of the Type II distribution. Its optical afterglow luminosity is also typical for Type II and much brighter than those of the Type I Gold Sample. Given the possible redshifts, this burst lies right on the Amati relation and the luminosity-spectral lag relations of most Type II GRBs (see Figures 3 and 4). GRB 060313 (Roming et al. 2006), whose $z \leqslant 1.1$, can have $E_{\gamma,\rm iso} \sim 3.4 \times 10^{52}\,\rm erg\,s^{-1}$ for $z = 1$. Some afterglow light-curve features (e.g., the very shallow decay of the UVOT, Roming et al. 2005, light curve with flickering features) are hard to accommodate within the merger scenarios. GRB 061201 also shows a very flat early light curve (Stratta et al. 2007) in both X-ray and optical bands, with the first clear X-ray "plateau" appearing in a short GRB. Some models (e.g., Kumar et al. 2008) attribute X-ray plateaus to the signature of massive star accretion. Within such a scenario, GRB 061201 is then a Type II candidate. GRB 060121 also shows strong temporal variability in the afterglow (de Ugarte Postigo et al. 2006), similar to GRB 060313. Even for the not very energetic short/hard GRB 051221A, its identity as a Type I GRB is not unquestionable. Its host galaxy has log(SSFR) = 0.804, which is greater than those of many GRBs in the Type II Gold Sample (Savaglio et al. 2009). A jet break is detected through ToO observations with the *Chandra* XRT (Burrows et al. 2006), which gives a jet corrected gamma-ray energy of $E_\gamma \sim 5 \times 10^{49}$erg. This is smaller than but not far off from the E_γ distribution of Type II GRBs (Frail et al. 2001; Bloom et al. 2003a; Liang et al. 2008; Racusin et al. 2009), and it is also much higher than some other Type I GRBs (e.g., GRB 050509B with $E_{\gamma,\rm iso} \sim 1.1 \times 10^{48}$erg, Gehrels et al. 2005). Although a low density $n \sim 10^{-4} - 10^{-1}\,\rm cm^{-3}$ was inferred from afterglow modeling (Soderberg et al. 2006b; Burrows et al. 2006), it still belongs to the reasonable n-range of other Type II GRBs (Panaitescu & Kumar 2001, 2002; Yost et al. 2003). The recent short/hard GRB 090510 detected by both *Swift* and Fermi (GBM/LAT) (Hoversten et al. 2009; Ohno et al. 2009; Guiriec et al. 2009; Rau et al. 2009) is also located in a star-forming host galaxy, and has an inferred total (collimation-corrected) jet gamma-ray and kinetic energies (assuming $n \sim 1\,\rm cm^{-3}$) $E_\gamma/E_k \sim 10^{50}$ erg. It is again not far-off from the E_γ/E_K distributions of Type II GRBs (Frail et al. 2001; Bloom et al. 2003a; Liang et al. 2008; Racusin et al. 2009), and a Type II origin is possible. Finally, Nysewander et al. (2009) pointed out that the optical-to-X-ray flux ratios of short GRBs are quite similar to those of long GRBs, suggesting a similar circumburst medium density for the two populations. This is consistent with most short GRBs being associated withType II.

Another strong argument for the Type-II association of some (even many) short GRBs is related to luminosity function analyses. Following the similar methodology of modeling L–z distribution of Type II GRBs in Virgili et al. (2009a), Virgili et al. (2009b) have studied the required luminosity function of Type I GRBs in order to reproduce the observed L–z distribution for both Type I and Other SGRB samples. The results suggest that the underlying luminosity function (defined as $N(L)dL \propto L^{-q}$) must be very shallow (e.g., $q \sim 0.5$) in order to reproduce the L–z distribution data. This shallow luminosity function is different from Type II GRBs and other astrophysical objects. A more severe problem is that it cannot reproduce the observed log N–log P distribution of BATSE short/hard GRBs. This apparent conflict disfavors the hypothesis that all short/hard GRBs are associated with Type I.

Theoretically, the duration of a GRB is defined by Equation (1). We now discuss the three relevant timescales in turn and address how a short GRB can in principle be associated with Type II.

First, recent studies of the collapsar model suggest that the engine timescale $t_{\rm engine}$ may not be always long. According to the standard collapsar model (Woosley 1993; MacFadyen & Woosley 1999; Proga et al. 2003), $t_{\rm engine}$ can last as long as the fallback material from the collapsar envelope is available to fuel the accretion disk or torus. However, one should bear in mind that the rotating torus may form only when the specific angular momentum of the accreting gas is higher than the so-called critical specific angular momentum value, i.e., $l_{\rm crit} = 2R_{\rm g}c$, where $R_{\rm g}$ is the gravitational radius. Note that $l_{\rm crit}$ is proportional

to the mass of the BH. During the collapsar evolution the mass accretion rate is very high, therefore the BH mass and consequently the critical angular momentum increase very fast. As a result, the specific angular momentum of the rotating material, which was initially sufficient for the torus formation (i.e., when the BH was just formed), may become insufficient at a later stage of the collapsar evolution when the BH mass increases. Janiuk & Proga (2008) showed that the simple, often cited estimates of the total mass available for torus formation and consequently the duration of a GRB (MacFadyen & Woosley 1999; Proga et al. 2003) are only upper limits. They revised these estimates by taking into account the long-term effect so that as the BH accretes the minimum specific angular momentum needed for torus formation increases. These new estimates predict a significant (an order of magnitude) reduction of the total energy and overall duration of the central engine $t_{\rm engine}$ because only a fraction of the rotating stellar envelope can form a torus.

If a Type II GRB is powered by the black hole spin (Blandford & Znajek 1977) rather than accretion, $t_{\rm engine}$ of a Type II GRB can be also short, since accretion of materials with a very low specific angular momentum would slow down the BH and consequently suppress the jet production. The interplay among the BH mass, BH spin parameter, and the critical specific angular momentum of accreting gas needed for the torus to form have been discussed by Janiuk et al. (2008). They studied several different cases and reached the conclusion that depending on the parameter settings, $t_{\rm engine}$ can be as short as a second.

Second, the timescale during which a relativistic jet is launched ($t_{\rm jet}$) may be in principle shorter than the central engine activity timescale ($t_{\rm engine}$). There is no working baryon-loading model for GRBs, and it is not clear how a clean, high entropy outflow is launched. For example, if the engine power has several episodes and the environment in the earlier episodes is not clean enough, the earlier jet may be choked or be launched but with a heavy baryon loading. The ejecta may therefore become a "dirty" fireball. The GRB episode is then only related to the late "clean" fireball phase when baryon loading is reduced.

Third, energy dissipation is needed to convert other forms (kinetic and magnetic) of energy to radiation (Rees & Mészáros 1992; Mészáros et al. 1993; Rees & Mészáros 1994; Thompson 1994). For a baryonic fireball, a steady outflow may not generate significant internal, non-thermal emission without internal shocks. The energy dissipation timescale ($t_{\rm dis}$) can be smaller than $t_{\rm jet}$. This gives an additional room to reduce the duration of Type II GRBs.

Finally, some other possibilities of producing short GRBs from collapsars have been proposed in the pre-*Swift* era. For example, Zhang et al. (2003) proposed that a short/hard pulse of gamma-ray emission may be associated with eruption of the fireball from the stellar envelope. Yamazaki et al. (2004a) envisioned a geometric model to unify long and short GRBs based on a line-of-sight effect. The original pictures proposed in these papers are no longer supported by the current data, but some ideas may be borrowed to associate short GRBs with Type II model category.

6.3. Is There a "Type III" Model Category?

The current data do not demand the existence of a third type of GRB models to be associated with cosmological GRBs,[21] i.e., those neither associated with massive star deaths nor compact star mergers. However, the possibility is not ruled out by the data, either. Some "hostless" short GRBs (Berger 2009), some long GRBs without X-ray afterglows (Vetere et al. 2008), and the SN-less long-duration, low-energy GRB 060505 (Fynbo et al. 2006; Ofek et al. 2007; Thöne et al. 2008; McBreen et al. 2008; Kann et al. 2008) are oddballs that may hold the clues to identify possible new model categories of GRBs.

[21] Again "cosmological GRBs" do not include SGR giant flares that are believed to account for a small fraction of short/hard GRBs.

7. NATURE OF GRB 080913 AND GRB 090423

We now discuss the possible origin of GRB 080913 at $z = 6.7$ and GRB 090423 at $z = 8.2$. We mainly focus on GRB 080913. The case of GRB 090423 is amazingly similar to GRB 080913, and the conclusion for GRB 080913 can be directly applied to GRB 090423 as well.

7.1. Prompt Properties and Empirical Correlations

As discussed in Section 2 (Figure 2), GRB 080913 and GRB 090423 appear as long GRBs in the observer's frame, but are intrinsically short/hard GRBs in the rest frame. If one applies the criterion for the observed T_{90}, both bursts are "long" and therefore may be associated with Type II according to the ansatz Equation (17). However, the association of a particular GRB to a particular physical model type should not have a z-dependence. The identical burst, if it have occurred at $z < 1$, would be recognized as a short/hard GRB, and hence, a Type I candidate according to the ansatz Equation (17). So it is not straightforward to determine the physical model category a GRB should be associated with based on the observed T_{90}–HR data.

We inspect the compliance of GRB 080913 and GRB 090423 with the empirical correlations. First, they are consistent with the E_p–$E_{\gamma,\rm iso}$ Amati-relation (Figure 3), although GRB 080913 is near the 3σ upper boundary. This has been regarded as one argument in support of the Type II origin of GRB 080913 by Greiner et al. (2009a). On the other hand, GRB 080913 is also consistent with the new track defined by Type I and short/hard GRBs within 3σ. This suggests that the possibility that it is a Type I GRB (or at least similar to other short/hard GRBs) is not ruled out based on this criterion. The compliance of GRB 090423 with the Amati relation is more robust. Second, inspecting the $L^p_{\gamma,\rm iso}$ − lag correlation, it seems that both GRB 080913 and GRB 090423 are consistent with being Type II GRBs—this was another argument by Greiner et al. (2009a). However, both GRBs are also consistent with the "zero-lag" trend of short GRBs.

In conclusion, based on statistical properties, both GRBs can be taken as good Type II candidates. However, the criterion based on empirical correlations is not robust enough to claim the case, and supports from other criteria (see below) are needed to draw firmer conclusions.

7.2. Afterglow Properties

The rest-frame broadband (X-ray and optical) afterglow luminosities of GRB 080913 are moderate, bracketed between those of Type II and Type I Gold Samples (Figures 6 and 7). Although the early luminosities are relatively low, a distinct energy injection episode raises the afterglow luminosity level of this burst to those of Type II at later epochs. Greiner et al. (2009a) have modeled the afterglow and suggested that the light curves are consistent with the deceleration of a relativistic jet by a dense circumburst medium with constant density. The data are consistent with the existence of an achromatic plateau in

X-ray and several optical/IR bands, which can be interpreted within the framework of a continuously fed forward shock. Alternatively, the X-ray rebrightening around 10^5 s may be due to an X-ray flare, whose softer emission may also account for the rebrightening in the IR/optical bands.

Improving upon Greiner et al. (2009a), we have performed a more detailed numerical modeling of the broadband afterglow data. The optical emission can be well modeled by standard synchrotron radiation from the forward shock, while the X-ray emission is likely dominated by the synchrotron self-Compton emission (SSC). The following parameters can fit the optical data well (although we do not apply a parameter search to judge whether this is the best fit): the initial isotropic kinetic energy of the fireball $E_{K,\rm iso} \sim 3.7 \times 10^{52}$ erg, the ambient density $n \sim 3000\,{\rm cm}^{-3}$. the electron equipartition parameter $\epsilon_e \sim 0.04$, the magnetic field equipartition parameter $\epsilon_B \sim 10^{-5}$, and the electron spectral index $p \sim 2.2$. If the late rebrightening is interpreted as an energy injection from the central engine with a time-dependent luminosity $L = L_0(t/t_0)^q$, the data are consistent with $t_0 \sim 6.5 \times 10^3$s, $L_0 \sim 2.9 \times 10^{50}\,{\rm erg\,s^{-1}}$, $q \sim 1$ for $t < t_0$, and $q \leqslant -1$ for $t > t_0$. In any case, a high-density constant medium is needed. This is consistent with the expectation at high-z (Gou et al. 2004) as well as the fitted density of GRB 050904 at $z = 6.3$ (Frail et al. 2006; Gou et al. 2007). The data also demand a jet opening angle $\theta_j > 0.22$ rad, which corresponds to a geometrically corrected total gamma-ray energy $E_\gamma > 1.7 \times 10^{51}$ erg, and a geometrically corrected total kinetic energy $E_K > 9.0 \times 10^{50}$ erg. This value is consistent with those of Type II GRBs (Frail et al. 2001; Bloom et al. 2003a; Liang et al. 2008; Racusin et al. 2009). This is probably the strongest argument in favor of associating the burst with Type II.

GRB 090423 has even brighter X-ray and optical afterglow luminosities than GRB 080913. Although we did not perform detailed afterglow modeling, the afterglow parameters favor those of Type II GRBs, similar to GRB 080913.

7.3. Short Type II or High-z Type I?

Since the discovery of GRB 080913, there has been a debate about its progenitor. As discussed above, data analyses and theoretical modeling suggest that GRB 080913 is very likely a Type II GRB (Greiner et al. 2009a), although a Type I association (Perez-Ramirez et al. 2008; Belczynski et al. 2008) is not ruled out. The evidence in support of the Type II origin of GRB 080913 includes: large values of the geometrically corrected gamma-ray (E_γ) and kinetic (E_K) energies, moderately bright intrinsic afterglow luminosities, a required high density of the circumburst medium, and the marginal compliance of the E_p–$E_{\gamma,\rm iso}$ relation of Type II GRBs.

On the other hand, if GRB 080913 were a high-z Type I GRB, as suggested by its intrinsically short duration, it would have to be an energetic merger event, likely due to a BH–NS merger with a rapidly rotating massive BH. The energy tapping mechanism would have to be the Blandford & Znajek (1977) mechanism (Perez-Ramirez et al. 2008). For this possibility, one requires that during the short age of the universe at $z = 6.7$, i.e., $\tau \sim 8.3 \times 10^8$ yr for the concordance universe, a BH–NS system is formed and merged. Belczynski et al. (2008) have modeled this possibility in detail, and claimed that the event rates for massive star core collapses that give rise to Type II GRBs and for compact star mergers (both NS–NS and BH–NS) are comparable at $z = 6.7$. They concluded that both scenarios are possible. However, there are several factors that would change this conclusion. First, Belczynski et al. (2008) assumed that all the mergers give rise to GRBs. In reality it may be that only a fraction of mergers give rise to GRBs. This fraction factor may be calibrated through confronting the observed number ratio of Type I and Type II GRBs with the model predictions. In the current population synthesis models, this factor is not taken into account (K. Belczynski 2008, private communication). Second, GRB 080913 would be a high-luminosity Type I GRB if it is associated with that category. Considering the power-law luminosity function inferred for Type I GRBs (Virgili et al. 2009b), detecting one high-L event would demand many more low-L events, which would require a significant increase of the required event rate of compact star mergers that is inconsistent with the results of population synthesis. Finally, as we argued above, the large value of the geometrically corrected gamma-ray and afterglow energies do not favor an NS–NS merger model. Only BH–NS mergers with a highly spinning BH should be counted. This would greatly reduce the theoretically predicted event rate that satisfies the constraint.

The detection of GRB 090423, another intrinsically short/hard, high-z, high-L GRB, strongly supports a Type II association of both GRB 080913 and GRB 090423. As argued above, the probability of detecting a high-L Type I event at high-z is much smaller than that of detecting a moderate-L Type II event. With one event, one may still argue for a chance coincidence. With the detection of GRB 090423, the chance probability of detecting two high-L merger events at high-z is greatly reduced, and one can more firmly associate both GRBs with Type II.

With two intrinsically short high-z Type II GRBs detected, one must ask why these events tend to exist at high-z. One possibility would be that it is simply a threshold selection effect. Both events have moderate gamma-ray luminosities, and were detected not far above the threshold. It is possible that there exists other softer pulses that are below the sensitivity threshold of *Swift*/BAT (J. S. Bloom 2009, private communication). On the other hand, such softer emission would be easily detected by *Swift*/XRT if it was indeed there. Both GRB 080913 and GRB 090423 have X-ray flares. However, extrapolating them into the gamma-ray band using a simple spectral model suggests that they would appear as low-level-extended emission of short GRBs (Figure 1). One may still argue for missing soft emission before the XRT slew. This is not ruled out, but the XRT slew time corresponds to a rest-frame time 99.5/7.7=12.9 s for GRB 080913 and 72.5/9.3=7.8 s for GRB 090423. The intrinsic T_{90}'s have to be in any case smaller than these values for these bursts.

A more intriguing possibility would be that this is due to a physical origin and reflects the intrinsic property of the high-z massive stars. These high-z stars may not be spinning as rapidly as their low-z sisters, so that only a smaller mass is left after the prompt collapse. More high-z GRB data are needed to test whether such a scenario is demanded by the data.

8. HOW TO ASSOCIATE A BURST WITH A PHYSICAL MODEL CATEGORY?

The extensive discussion presented above suggests that it is not always easy to associate a particular GRB with a particular physical model category based on observational criteria. The multiple observational criteria discussed in this paper are summarized in Table 2. This is an extension of Figure 2 of Zhang (2006). New criteria are added based on the discussion in this paper. A new column lays out the issues of each criterion. The criteria are sorted by relevant observations. The first six rows (duration, spectrum, spectral lag, $E_{\gamma,\rm iso}$, $E_p - E_{\gamma,\rm iso}$

Table 2
Observational Criteria for Physically Classifying GRBs

Criterion	Type I	Type II	Issues
Duration	Usually short, but can have extended emission.	Long without short/hard spike, can be shorter than 1s in rest frame.	No clear separation line.
Spectrum	Usually hard (soft tail)	Usually soft	Large dispersion, overlapping
Spectral Lag	Usually short	Usually long, can be short.	Related to variability timescale
$E_{\gamma,\rm iso}$	Low (on average)	High (on average)	Wide distribution in both, overlapping
E_p–$E_{\gamma,\rm iso}$	Usually off the track.	Usually on the track.	Some Type II off the track.
$L^p_{\gamma,\rm iso}$–lag	Usually off the track.	Usually on the track.	Some Type II off the track.
SN association	No.	**Yes.**	Some Type II may be genuinely SN-less.
Medium type	Low-n ISM.	**Wind** or High-n ISM.	Large scatter of n distribution.
$E_{K,\rm iso}$	Low (on average)	High (on average)	Large dispersion, overlapping
Jet angle	Wide (on average)	Narrow (on average)	Difficult to identify jet breaks
E_γ and E_K	Low (on average)	High (on average)	Type I BH-NS BZ model ∼ Type II.
Host galaxy type	**Elliptical, early** and late	Late	Deep spectroscopy needed.
SSFR	**Low** or high	High (exception GRB 070125)	overlapping
Offset	Outskirt or outside	Well inside	How to claim association if outside?
z-distribution	Low average z	High average z	overlapping
L-function	Unknown	Broken power law, 2-component	overlapping
GW signals	Precisely modeled	Unknown	No data yet

relation, and $L^p_{\gamma,\rm iso}$-lag relation, are based on the gamma-ray properties only. The next five rows (supernova association, circumburst medium type, $E_{K,\rm iso}$, jet opening angle, and the geometrically corrected energies E_γ and E_K), are based on follow-up broadband observations and afterglow modeling. The next three rows (host galaxy type, specific star forming rate of the host galaxy, and offset of the GRB from the host galaxy) are based on observations of the host galaxies. The next two rows (redshift distribution and luminosity function) are statistical properties. The final row is the gravitational wave criterion. In general, most of these criteria are not "conclusive," i.e., one cannot draw a firm conclusion based on a single criterion. Nonetheless, there are several criteria which, if satisfied, would unambiguously associate a GRB with a certain physical model category. These are marked in bold in Table 2. In particular, if a GRB is found in an elliptical or an early type galaxy, or if the SSFR of its host galaxy is very low, one would be able to associate it with Type I. On the other hand, an SN association or the identification of a wind-type medium in a GRB would establish its association with Type II.

Unfortunately, the above four criteria are usually not satisfied for most GRBs. One is then obliged to use multiple criteria since there are overlapping predicted properties between the two physical model types for each individual criterion. In Figure 8, we cautiously propose an operational procedure to discern the physical origin of a GRB based on the available data.

Several features are worth commenting on in Figure 8. (1) The criteria to define the physical model category a burst is associated with are less stringent compared with those used to define the Gold Samples in Section 5.1. This is because the purpose of the Gold Samples was to allow us to perform statistical analyses. After reviewing the statistical properties in Section 5, we have gained confidence on additional criteria so that more bursts can be analyzed. (2) There are five outcomes in the flowchart. Besides the solid Type I/II identifications, we also define Type I/II "candidates" and the "unknown" category. The Type I/II candidates refer to those with evidence of associating a burst with a particular physical model category, but the evidence is not strong enough to make a firm claim. The unknown category includes the oddball GRBs that do not obviously fit into any criteria discussed in this paper, or the observational data are not adequate for us to make the judgement. They may be associated with Type I, Type II or a completely new type of models. (3) Some qualitative rather than quantitative criteria have been used (e.g., high/low SSFR, large offset, large/small E_γ, E_K). The reason is that it is very difficult to adopt quantitative criteria at the current stage, since the distributions of these quantities predicted by both physical model types and displayed in the statistical analyses of the Type I/II Gold Samples are continuous, without sharp transitions. The "high/low" and "large/small" definitions are based on the statistical properties, and therefore in the relative sense. If confusion occurs (e.g., the quantity is near the boundary and not easy to judge whether it is high/low, large/small, one can follow the "?" sign to go down the flowchart. The flowchart is reasonably operational, i.e., essentially every GRB with reasonable afterglow follow up observations can find a destiny in the chart. For example, the SN-less long-duration GRB 060614 (Gehrels et al. 2006; Gal-Yam et al. 2006; Fynbo et al. 2006; Della Valle et al. 2006a) is associated with Type I (based on low SSFR), and the other SN-less GRB 060505 (Fynbo et al. 2006; Ofek et al. 2007; Thöne et al. 2008; McBreen et al. 2008) can be associated with a Type I candidate based on its small energetics, or an "unknown" burst if one argues that the $L^p_{\gamma,\rm iso}$–lag relation is satisfied for this burst (McBreen et al. 2008). GRB 080913 and GRB 090423 (the main topic of this paper) find their homes as Type II candidates based on the E_p–$E_{\gamma,\rm iso}$ correlation. GRB 060121 (a high-z short GRB) satisfying the E_p–$E_{\gamma,\rm iso}$ is also found to be associated with the "Type II candidate" outcome in the flowchart. (4) It is possible that the procedure and the criteria may be further revised as more data are accumulated. The current procedure only reflects the best knowledge for the time being.

In the flowchart, there are five thick arrows that bridge the short-duration and long-duration GRBs. This suggests that the duration information sometimes is misleading. Some long-duration GRBs can be associated with Type I (e.g., GRB 060614 and probably GRB 080503, Perley et al. 2009), and some short-duration GRBs can be associated with Type II (e.g., GRB 060121, GRB 080913 and GRB 090423). We also present two dashed arrows in the flowchart. These two tracks (a short GRB

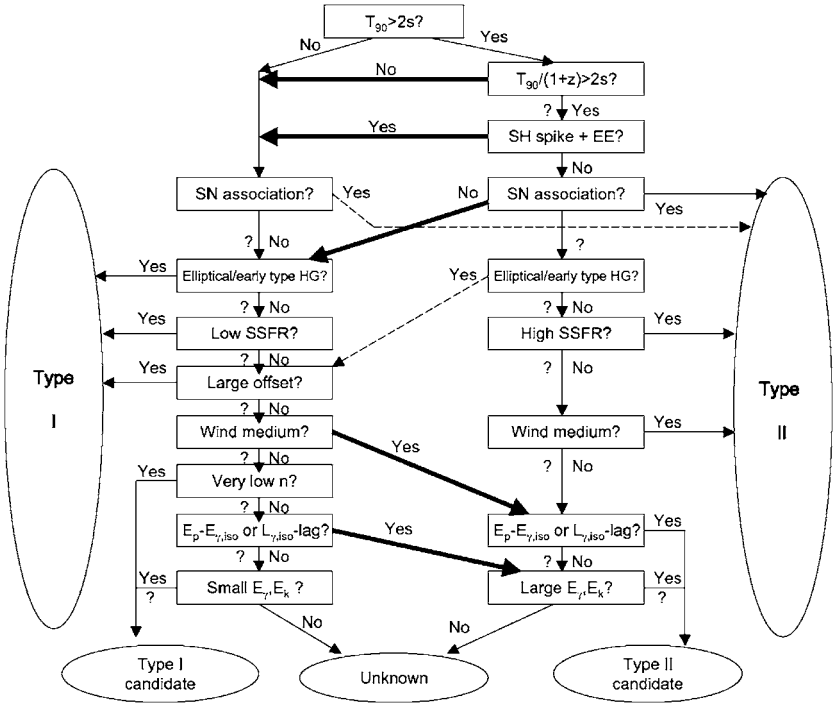

Figure 8. Recommended procedure to judge the association of a particular GRB to a particular physical model category. Multiple observational criteria have been applied. Question marks stand for no information being available to judge the validity of the criterion. The two dotted arrows stand for the possibilities that are in principle possible but have never been observed. Five thick arrows bridge the long-duration and short-duration GRBs, suggesting that the there can be long-duration Type I and short-duration Type II GRBs.

associated with an SN and a long GRB with an elliptical/early-type host galaxy) are in principle possible, but such bursts have never been observed so far.[22] The order of the criteria in Figure 8 is based on the "definiteness" of the criteria, with the higher-level ones carrying more weight than the lower-level ones. Note that "hardness" is generally not regarded as a definitive criterion in the flowchart (except for the relative hardness of the short spike and the extended emission).

9. SUMMARY

Prompted by the interesting question whether the $z = 6.7$ GRB 080913 and $z = 8.2$ GRB 090423 are intrinsically short GRBs associated with the Type II physical model category (Greiner et al. 2009a) or high-z GRBs associated with the Type I physical model category (Perez-Ramirez et al. 2008), we performed a more thorough investigation on the two physically distinct categories of GRB models and their predicted observational characteristics. We further developed the "Type I/II" concept proposed in Zhang et al. (2007a) in the following directions. (1) We have reviewed and expanded the possible multiple observational criteria, and discussed their physical origins from the theoretical point of view. By doing so, we are able to differentiate those criteria that are more closely related to the progenitor types and those that are more directly related to radiation physics. In particular, we argue that SN association, host galaxy properties (type and SSFR), and the offset of the GRB location in the host galaxy are more directly related to the progenitor types. The gamma-ray properties, such as duration, hardness, spectral lag, empirical correlations, are more related to jet dissipation and radiation processes in the emission region, and can only be related to progenitors indirectly. Afterglow and statistical properties can be used to diagnose the GRB progenitor, but theoretical modeling is needed. Gravitational wave signals may be the best criterion to directly probe the progenitor system, but they are too faint for the current detectors to detect. (2) We use several key observational criteria that are directly related to GRB progenitors to define the Gold Samples for Type I and Type II, respectively. These criteria do not involve GRB gamma-ray emission properties such as duration, hardness, spectral lag, etc. We then use these samples to investigate their statistical properties, especially their distribution in the duration-hardness space. We found that the Type II Gold Sample represent the BATSE long/soft population well. The Type I Gold Sample, on the other hand, is not very representative of the short/hard population. The Type I Gold Sample GRBs are typically "long" and not particularly "hard." (3) Although some short/hard GRBs detected in the *Swift* era may share a similar origin as the Type I Gold Sample, we suggest that *some (probably even most) high-L short GRBs may be instead associated with Type II, namely, of a massive star origin*. (3) We summarized the multiple observational criteria needed to discern the physical origin of a GRB in Table 2, with various issues laid out. We emphasize that it is not always straightforward to judge the physical model category a particular GRB is associated with, and we cautiously proposed an operational procedure to discern the physical origin of GRBs (Figure 8). (4) According to this procedure, GRB 080913 and GRB 090423 are Type II candidates. Although a specific Type I scenario invoking the Blandford–Znajek mechanism of a BH–NS merger system is not completely ruled out, the fact that two such GRBs are detected at high-z indeed suggests that a Type I association of these bursts is essentially impossible.

The proposed procedure to associate a particular GRB with a particular physical model category is subject to further test with new observational data. More detailed analyses may allow

[22] The GRB field is full of surprises. If some short/hard GRBs are indeed associated with Type II as argued in this paper, one may someday discover an SN associated with a short/hard GRB. We encourage continuous SN searches for all nearby GRBs, both long and short.

more quantitative criteria to discern the physical origin of GRBs. Based on the past experience, the chances are high that new observations will bring surprises that continuously call for modifications of the criteria, which would further our understanding of the physical origins of cosmological GRBs.

We thank the referee, Jon Hakkila, for insightful comments that significantly improved the presentation of the paper. This work is partially supported by NASA (through grants NAG05GB67G, NNX08AN24G, and NNX08AE57A [BZ], and TM8-9004X [DP] at UNLV, and NNX08AL40G at PSU), the National Natural Science Foundation (Award ID 0908362 for BZ), the National Natural Science Foundation of China (grant 10873002 for EWL, and grants 10503012, 10621303, 10633040 for XFW), and the National Basic Research Program of China ("973" Program 2009CB824800 for both E.W.L. and X.F.W.), and the research foundation of Guangxi University (Grant M30520 for E.W.L.). B.B.Z. acknowledges the President's Fellowship and GPSA Awards from UNLV. F.J.V. acknowledges the Nevada Space Grant Consortium Fellowship. We acknowledge helpful discussion/comments from K. Belczynski, J. S. Bloom, S. Covino, D. B. Fox, A. Fruchter, J. Fynbo, J. Greiner, D. Malesani, P. O'Brien, and S. Savaglio.

APPENDIX A

DETAILS OF THE TYPE I GOLD SAMPLE

1. GRB 050509B. No optical afterglow is detected. The host galaxy is very likely a bright cD elliptical galaxy in a nearby galaxy cluster at $z = 0.2248 \pm 0.0002$. The *Swift* XRT error circle is offset from the elliptical galaxy. A deep upper limit on SN association achieved (Gehrels et al. 2005; Bloom et al. 2006; Hjorth et al. 2005b). Satisfies both criteria 1 and 2 of the Gold Sample.
2. GRB 050709. The host galaxy is identified with the optical afterglow, and is a star-forming galaxy at $z = 0.1606 \pm 0.0001$. The location of the GRB is at the outskirt of the host. Deep upper limit on SN association achieved (Fox et al. 2005). Satisfies criterion 2 for the Gold Sample.
3. GRB 050724. The host is an early-type galaxy at $z = 0.2576 \pm 0.0004$. The afterglow is at the outskirt of the host (Barthelmy et al. 2005a; Berger et al. 2005). A deep upper limit on the SN association achieved (Malesani et al. 2007). Satisfies both criteria 1 and 2 for Gold Sample.
4. GRB 060614. The host galaxy has a low SSFR (Gal-Yam et al. 2006; Savaglio et al. 2009). Very stringent upper limits for any associated SN fainter than any known SN achieved (Gal-Yam et al. 2006; Fynbo et al. 2006; Della Valle et al. 2006a). Satisfies criterion 2 for the Gold Sample.
5. GRB 061006. A faint host galaxy is detected at $z = 0.4377 \pm 0.0002$ (Berger et al. 2007). The SSFR is very low (Berger et al. 2007; Savaglio et al. 2009). Satisfies criterion 1 for the Gold Sample.

APPENDIX B

DETAILS OF OTHER SHORT/HARD GRB SAMPLE

1. GRB 000607. This was an IPN-localized GRB. A putative host galaxy at $z = 0.14$ was proposed (Gal-Yam et al. 2008).
2. GRB 050813. No optical afterglow detected. The X-ray error circle is associated with a galaxy cluster at $z \simeq 0.72$ (Prochaska et al. 2006). Moderately deep SN limit (relevant to this low-z interpretation) was reported by Ferrero et al. (2007).
3. GRB 051210. A *Swift* GRB with X-ray afterglow (La Parola et al. 2006). A galaxy appeared outside the error box, but is likely the host. No lines are observed. It is argued that $z > 1.4$ (Berger et al. 2007).
4. GRB 051221A. Host galaxy is a star forming galaxy at $z = 0.5464$ with a very high SSFR (Soderberg et al. 2006b; Savaglio et al. 2009). A bright SN such as 1998bw is ruled out, but the limit is still consistent with the existence of faint SN 2002ap-like event (Soderberg et al. 2006b). So it does not satisfy the criteria of the Type I Gold Sample.
5. GRB 060121. HETE-2 GRB with a faint optical afterglow, leading to the discovery of an extremely faint host galaxy. The redshift of the afterglow can be estimated as either 4.6 or 1.7 (de Ugarte Postigo et al. 2006; Berger et al. 2007).
6. GRB 060313. Bright short/hard GRB with bright afterglow (Roming et al. 2006). A faint host galaxy is identified whose redshift is unknown (Berger et al. 2007). Spectral analysis of the UVOT data suggests $z \leqslant 1.1$ (Roming et al. 2006).
7. GRB 060502B. No optical afterglow is detected. The XRT position is close to a nearby early type galaxy at $z = 0.287$ (Bloom et al. 2007). The chance probability for the association is 0.03. There is another faint object in the field of view, which could be the host galaxy at a high redshift (Berger et al. 2007).
8. GRB 060801. No optical afterglow is detected. Two possible sources may be considered as the host. One has a redshift $z = 1.131$ (which is slightly outside the XRT error box using the UVOT-aligned XRT position). Another source is within the error box, but is likely even farther away (Berger et al. 2007).
9. GRB 061201. Optical afterglow was detected by UVOT. No host galaxy was identified. Candidates include galaxy cluster Abell 995 ($z = 0.0865$), a star-forming galaxy at $z = 0.111$, or a missing host at an even higher z (Stratta et al. 2007).
10. GRB 061210. A *Swift* GRB with delayed X-ray afterglow detection. No optical afterglow detected. The host galaxy is likely a star-forming galaxy at $z = 0.4095 \pm 0.001$ (Berger et al. 2007).
11. GRB 061217. A faint *Swift* burst without optical afterglow detection. Within the XRT error circle, there is a star-forming galaxy at $z = 0.8270$ (Berger et al. 2007).
12. GRB 070429B. A *Swift* GRB with delayed X-ray afterglow detection. The host galaxy is likely a faint galaxy at $z = 0.9023 \pm 0.0002$ (Perley et al. 2007a; Cenko et al. 2008a).
13. GRB 070707. Detected by INTEGRAL and have X-ray and optical afterglow detected. A very faint host galaxy candidate was reported with no redshift information (Piranomonte et al. 2008).
14. GRB 070714B. A *Swift* GRB with optical afterglow. A secure host galaxy at $z = 0.9225 \pm 0.0001$ is identified (Graham et al. 2009; Cenko et al. 2008a).
15. GRB 070724A. A *Swift* GRB with X-ray afterglow. A potential host galaxy is detected, which is a star-forming galaxy at $z = 0.457$ (Cucchiara et al. 2007).
16. GRB 070729. A *Swift* GRB with faint X-ray afterglow. A putative red host galaxy is identified (Berger & Murray 2007). No redshift is known.

17. GRB 070809. A *Swift* GRB with X-ray and optical afterglow. A nearby, edge-on spiral galaxy may be the host, with $z = 0.2187$ (Perley et al. 2007b).
18. GRB 071227. A *Swift* GRB with X-ray and optical afterglows. A host galaxy is identified as an edge on spiral galaxy. The redshift is $z = 0.3940$ (Berger 2009; D'Avanzo et al. 2009).
19. GRB 080123. A *Swift* GRB with X-ray afterglow. No host galaxy detection is reported.
20. GRB 080503. A *Swift* GRB with short initial spike and very bright extended emission. X-ray and optical afterglows are detected. There is no galaxy directly at the GRB position. There are faint galaxies nearby, but one cannot make firm statements regarding their association with the GRB (Perley et al. 2009).

After this work is finished, two more interesting short/hard GRBs were detected, whose observational properties strengthen the main theme of this paper. We include them here as follows.

1. GRB 090426. This is a rest-frame 0.35 s short/hard GRB at $z = 2.6$ (Levesque et al. 2009). It has a blue, very luminous, star-forming putative host galaxy with a small angular offset of the afterglow location from the center. It is very likely associated with Type II as argued in this paper (Levesque et al. 2009).
2. GRB 090510. This is a bright short/hard GRB detected by both *Swift* and Fermi (GBM/LAT) (Hoversten et al. 2009; Ohno et al. 2009; Guiriec et al. 2009) with bright X-ray and optical afterglows (Grupe et al. 2009b; Kuin et al. 2009; Olivares et al. 2009). With a redshift $z \sim 0.9$ (Rau et al. 2009), the isotropic energy and luminosity of this burst all belong to the high end of the distribution for Other Short/Hard GRBs presented in Figure 5. The afterglow is consistent with a uniform density medium. The X-ray light curve shows an early break at $t \sim 1500$ s since the trigger with a post-break decay index ~ -2.16. If it is interpreted as a jet break, then the total (collimation-corrected) jet gamma-ray and kinetic energies (assuming $n \sim 1\,\mathrm{cm}^{-3}$) are $E_\gamma/E_k \sim 10^{50}$ erg. This is relatively small as compared with (but not far-off from) the E_γ/E_K distributions of Type II GRBs (Frail et al. 2001; Bloom et al. 2003a; Liang et al. 2008; Racusin et al. 2009). Although one may argue for a Type I association based on this, a Type II association is not strongly disfavored.

REFERENCES

Abdo, A. A., et al. 2009, Science, 323, 1688
Aloy, M. A., Janka, H.-T., & Müller, E. 2005, A&A, 436, 273
Amati, L., et al. 2002, A&A, 390, 81
Amati, L., et al. 2008, MNRAS, 391, 577
Andersen, M. I., et al. 1999, Science, 283, 2075
Barth, A. J., et al. 2003, ApJ, 584, L47
Band, D. L., & Preece, R. D. 2005, ApJ, 627, 319
Band, D. L., et al. 1993, ApJ, 413, 281
Barthelmy, S. D., et al. 2005a, Nature, 438, 994
Barthelmy, S. D., et al. 2005b, Space Sci. Rev., 120, 143
Belczynski, K., et al. 2006, ApJ, 648, 1110
Belczynski, K., et al. 2008, ApJ, submitted (arXiv:0812.2470)
Beloborodov, A. M., Stern, B. E., & Svensson, R. 1998, ApJ, 508, L25
Berger, E. 2007, ApJ, 670, 1254
Berger, E. 2009, ApJ, 690, 231
Berger, E., & Murray, D. 2007, GCN Circular, 6686
Berger, E., et al. 2005, ApJ, 634, 501
Berger, E., et al. 2007, ApJ, 664, 1000
Bernardini, M. G., et al. 2007, A&A, 474, L13
Blandford, R. D., & Znajek, R. L. 1977, MNRAS, 179, 433
Bloom, J. S., Butler, N. R., & Perley, D. A. 2008, in AIP Conf. Ser. 1000, Gamma-Ray Bursts 2007: Proceedings of the Santa Fe Conf., ed. M. Galassi, D. Palmer, & E. Fenimore (Melville, NY: AIP), 11
Bloom, J. S., Frail, D. A., & Kulkarni, S. R. 2003a, ApJ, 594, 674
Bloom, J. S., Kulkarni, S. R., & Djorgovski, S. G. 2002, AJ, 123, 1111
Bloom, J. S., et al. 1999, Nature, 401, 453
Bloom, J. S., et al. 2003b, AJ, 125, 999
Bloom, J. S., et al. 2006, ApJ, 638, 354
Bloom, J. S., et al. 2007, ApJ, 654, 878
Burrows, D. N., et al. 2005a, Science, 309, 1833
Burrows, D. N., et al. 2005, Space Sci. Rev., 120, 165
Burrows, D. N., et al. 2006, ApJ, 653, 468
Butler, N. R., Kocevski, D., Bloom, J. S., & Curtis, J. L. 2007, ApJ, 671, 656
Campana, S., et al. 2006, Nature, 442, 1008
Cannizzo, J. K., et al. 2006, GRB Coordinates Network, 20, 1
Castro, S. M., et al. 2000, GRB Coordinates Network, 851, 1
Cenko, S. B., et al. 2008a, ApJ, submitted (arXiv:0802.0874)
Cenko, S. B., et al. 2008b, ApJ, 677, 441
Chapman, Priddey, & Tanvir, N. 2009, MNRAS, 395, 1515
Chevalier, R. A., & Li, Z.-Y. 2000, ApJ, 536, 195
Chincarini, G., et al. 2007, ApJ, 671, 1903
Cucchiara, A., Fox, D. B., Berger, E., & Price, P. A. 2006, GRB Coordinates Network, 5470, 1
Cucchiara, A., et al. 2007, GRB Coordinates Network, 6665, 1
Cummings, J., et al. 2005a, GRB Coordinates Network, 3479, 1
Cummings, J., et al. 2005b, GRB Coordinates Network, 4365, 1
Dai, X. 2009, ApJ, 697, L68
Dai, Z. G., & Lu, T. 1998, MNRAS, 298, 87
Dai, Z. G., Wang, X. Y., Wu, X. F., & Zhang, B. 2006, Science, 311, 1127
Dalal, N., Holz, D., Hughes, S. A., & Jain, B. 2006, Phys. Rev. D, 74, 063006
Dal Fiume, D., et al. 2000, A&A, 355, 454
D'Avanzo, P., et al. 2009, A&A, 498, 711
de Ugarte Postigo, A., et al. 2006, ApJ, 648, L83
Della Valle, M., et al. 2006a, Nature, 444, 1050
Della Valle, M., et al. 2006b, IAU Circ., 8696, 1
Djorgovski, S. G., et al. 1997, IAU Circ., 6660, 1
Djorgovski, S. G., et al. 1998, ApJ, 508, L17
Djorgovski, S. G., et al. 1999, GRB Coordinates Network, 189, 1
Dodonov, S. N., et al. 1999, GRB Coordinates Network, 475, 1
Donaghy, T. Q., et al. 2006, arXiv:astro-ph/0605570
Doty, J., et al. 2005, GRB Coordinates Network, 4145, 1
Eichler, D., Livio, M., Piran, T., & Schramm, D. N. 1989, Nature, 340, 126
Faber, J. A., Baumgarte, T. W., Shapiro, S. L., & Taniguchi, K. 2006, ApJ, 641, L93
Falcone, A. D., et al. 2007, ApJ, 671, 1921
Fan, Y. Z., & Wei, D. M. 2005, MNRAS, 364, L42
Fan, Y. Z., Zhang, B., Kobayashi, S., & Mészáros, P. 2005, ApJ, 628, 867
Fenimore, E. E., Madras, C. D., & Nayakshin, S. 1996, ApJ, 473, 998
Fenimore, E. E., & Ramirez-Ruiz, E. 2000, arXiv:astro-ph/0004176
Fenimore, E. E., et al. 1995, ApJ, 448, L101
Ferrero, P., et al. 2007, AJ, 134, 2118
Ford, et al. 1995, ApJ, 439, 307
Fox, D. B., et al. 2005, Nature, 437, 845
Frail, D. A., et al. 2001, ApJ, 562, L55
Frail, D. A., et al. 2006, ApJ, 646, L99
Frontera, F., et al. 1998, ApJ, 493, L67
Frontera, F., et al. 2001, ApJ, 550, L47
Fruchter, A. S., et al. 2006, Nature, 441, 463
Fryer, C. L., Woosley, S. E., Herant, M., & Davies, M. B. 1999, ApJ, 520, 650
Fryer, C. L., et al. 2007, PASP, 119, 1211
Fynbo, J. P. U., et al. 2006, Nature, 444, 1047
Gal-Yam, A., et al. 2005, GRB Coordinates Network, 4156, 1
Gal-Yam, A., et al. 2006, Nature, 444, 1053
Gal-Yam, A., et al. 2008, ApJ, 686, 408
Galama, T. J., et al. 1998, Nature, 395, 670
Gehrels, N., et al. 2004, ApJ, 611, 1005
Gehrels, N., et al. 2005, Nature, 437, 851
Gehrels, N., et al. 2006, Nature, 444, 1044
Gehrels, N., et al. 2008, ApJ, 689, 1161
Ghirlanda, G., Ghisellini, G., & Lazzati, D. 2004, ApJ, 616, 331
Ghirlanda, G., et al. 2009, A&A, 496, 585
Ghisellini, G., et al. 2006, MNRAS, 372, 1699
Ghisellini, G., et al. 2007, MNRAS, 382, L72
Golenetskii, S., et al. 2005a, GRB Coordinates Network, 3474, 1
Golenetskii, S., et al. 2005b, GRB Coordinates Network, 4394, 1
Golenetskii, S., et al. 2006a, GRB Coordinates Network, 4881, 1

Golenetskii, S., et al. 2006b, GRB Coordinates Network, 5264, 1
Golenetskii, S., et al. 2006c, GRB Coordinates Network, 5890, 1
Golenetskii, S., et al. 2007, GRB Coordinates Network, 7155, 1
Giannios, D. 2008, A&A, 480, 305
Gou, L.-J., Fox, D. B., & Mészáros, P. 2007, ApJ, 668, 1083
Gou, L. J., Mészáros, P., Abel, T., & Zhang, B. 2004, ApJ, 604, 508
Graham, J. F., et al. 2009, ApJ, 698, 1620
Granot, J., Panaitescu, A., Kumar, P., & Woosley, S. E. 2002, ApJ, 570, L61
Greiner, J., et al. 2003a, ApJ, 599, 1223
Greiner, J., et al. 2003b, GRB Coordinates Network, 2020, 1
Greiner, J., et al. 2009a, ApJ, 693, 1610
Greiner, J., et al. 2009b, ApJ, 693, 1912
Grupe, D., et al. 2006, ApJ, 653, 462
Grupe, D., et al. 2007, ApJ, 662, 443
Grupe, D., et al. 2009a, ApJ, submitted (arXiv:0903.1258)
Grupe, D., et al. 2009b, GRB Coordinates Network Circular, 9341, 1
Guetta, D., & Piran, T. 2006, A&A, 453, 823
Guetta, D., Piran, T., & Waxman, E. 2005, ApJ, 619, 412
Guidorzi, C., et al. 2006, MNRAS, 371, 843
Guiriec, S., et al. 2009, GRB Coordinates Network Circular, 9336, 1
Hakkila, J., & Giblin, T. W. 2006, ApJ, 646, 1086
Hakkila, J., et al. 2000, ApJ, 538, 165
Halpern, J. P., & Mirabal, N. 2006, GRB Coordinates Network, 5982, 1
Heger, A., et al. 2003, ApJ, 591, 288
Heise, J., et al. 1999, IAU Circ., 7221, 1
Hjorth, J., et al. 2003, Nature, 423, 847
Hjorth, J., et al. 2005a, Nature, 437, 859
Hjorth, J., et al. 2005b, ApJ, 630, L117
Holland, S. T., et al. 2002, AJ, 124, 639
Horvath, I. 1998, ApJ, 508, 757
Hoversten, E. A., et al. 2009, GRB Coordinates Network Circular, 9331, 1
Hullinger, D., et al. 2006, GRB Coordinates Network, 5142, 1
Hurley, K., Cline, T., & Mazets, E. 2000a, GRB Coordinates Network, 642, 1
Hurley, K., et al. 2000b, ApJ, 534, L23
Hurley, K., et al. 2000c, GRB Coordinates Network, 801, 1
Hurley, K., et al. 2002, ApJ, 567, 447
Hurley, K., et al. 2005, GRB Coordinates Network, 4139, 1
Ioka, K., & Nakamura, T. 2001, ApJ, 554, L163
Ioka, K., et al. 2007, ApJ, 670, L77
Jakobsson, P., et al. 2005, ApJ, 629, 45
Jakobsson, P., et al. 2007, GRB Coordinates Network, 6997, 1
Jakobsson, P., et al. 2008, GRB Coordinates Network, 7757, 1
Janiuk, A., Moderski, R., & Proga, D. 2008, ApJ, 687, 433
Janiuk, A., & Proga, D. 2008, ApJ, 675, 519
Kann, D. A., et al. 2007, ApJ, submitted (arXiv:0712.2186)
Kann, D. A., et al. 2008, ApJ, submitted (arXiv:0804.1959)
King, A., Olsson, E., & Davies, M. B. 2007, MNRAS, 374, L34
King, A., et al. 2005, ApJ, 630, L113
Kobayashi, S., & Mészáros, P. 2003, ApJ, 589, 861
Kobayashi, S., Piran, T., & Sari, R. 1997, ApJ, 490, 92
Kobayashi, S., Ryde, F., & MacFadyen, A. 2002, ApJ, 577, 302
Kocevski, D., & Butler, N. 2008, ApJ, 680, 531
Kouveliotou, C., et al. 1993, ApJ, 413, L101
Krimm, H. A., et al. 2009, GRB Coordinates Network Circular, 9241, 1
Kuin, N. P. M., et al. 2009, GRB Coordinates Network Circular, 9342, 1
Kulkarni, S. R., et al. 1998, Nature, 393, 35
Kumar, P., Narayan, R., & Johnson, J. L. 2008, MNRAS, 388, 1729
Kumar, P., & Panaitescu, A. 2000, ApJ, 541, L51
La Parola, V., et al. 2006, A&A, 454, 753
Lazzati, D., Morsany, B. J., & Begelman, M. 2009, ApJ, 700, L47
Lazzati, D., & Perna, R. 2007, MNRAS, 375, L46
Lee, W. H., & Ramirez-Ruiz, E. 2007, New J. Phys., 9, 17
Levan, A. J., et al. 2006, ApJ, 648, L9
Levan, A. J., et al. 2007, MNRAS, 384, 541
Levesque, E. M., et al. 2009, MNRAS, submitted (arXiv:0907.1661)
Li, L.-X. 2002, ApJ, 567, 463
Li, L.-X. 2008, MNRAS, 388, 1487
Liang, E. W., Dai, Z. G., & Wu, X. F. 2004, ApJ, 606, L29
Liang, E., & Noguchi, K. 2009, ApJ, submitted (arXiv:0905.0160)
Liang, E.-W., Racusin, J. L., Zhang, B., Zhang, B.-B., & Burrows, D. N. 2008, ApJ, 675, 528
Liang, E., & Zhang, B. 2005, ApJ, 633, 611
Liang, E.-W., Zhang, B.-B., Stamatikos, M., Zhang, B., Norris, J., Gehrels, N., Zhang, J., & Dai, Z. G. 2006, ApJ, 653, L81
Liang, E., Zhang, B., Virgili, F., & Dai, Z. G. 2007, ApJ, 662, 1111
Lin, L., Liang, E. W., & Zhang, S. N. 2009, Sci. China G, in press (arXiv: 0906.3057)
Lloyd-Ronning, N. M., & Zhang, B. 2004, ApJ, 613, 477
Lu, R.-J., Qin, Y.-P., Zhang, Z.-B., & Yi, T.-F. 2006, MNRAS, 367, 275
Lyutikov, M., & Blandford, R. 2003, arXiv:astro-ph/0312347
MacFadyen, A. I., & Woosley, S. E. 1999, ApJ, 524, 262
Malesani, D., et al. 2007, A&A, 473, 77
Malesani, D., et al. 2008, GRB Coordinates Network, 7771, 1
Mao, J., et al. 2008, GRB Coordinates Network Circular, 138, 1
Markwardt, C., et al. 2006, GRB Coordinates Network, 5882, 1
Markwardt, C., et al. 2007, GRB Coordinates Network, 51, 1
Martini, P., Garnavich, P., & Stanek, K. Z. 2003, GRB Coordinates Network, 1980, 1
Masetti, N., et al. 2002, GRB Coordinates Network, 1330, 1
McBreen, S., et al. 2008, ApJ, 677, L85
Mészáros, P., Laguna, P., & Rees, M. J. 1993, ApJ, 415, 181
Mészáros, P., Ramirez-Ruiz, E., Rees, M. J., & Zhang, B. 2002, ApJ, 578, 812
Mészáros, P., & Rees, M. J. 1997, ApJ, 482, L29
Mészáros, P., & Rees, M. J. 2000, ApJ, 530, 292
Mészáros, P., Rees, M. J., & Wijers, R. A. M. J. 1998, ApJ, 499, 301
Metzger, M. R., et al. 1997, Nature, 387, 878
Mukherjee, S., et al. 1998, ApJ, 508, 314
Nagataki, S., Mizuta, A., & Sato, K. 2006, ApJ, 647, 1255
Nagataki, S., et al. 2003, ApJ, 596, 401
Nakar, E. 2007, Phys. Rep., 442, 166
Nakar, E., Gal-Yam, A., Piran, T., & Fox, D. B. 2006, ApJ, 640, 849
Nakar, E., & Piran, T. 2005, MNRAS, 360, L73
Narayan, R., & Kumar, P. 2009, MNRAS, 394, L117
Narayan, R., Paczynski, B., & Piran, T. 1992, ApJ, 395, L83
Narayan, R., Piran, T., & Kumar, P. 2001, ApJ, 557, 949
Nava, L., et al. 2009, GRB Coordinates Network Circular, 9325, 1
Nemiroff, R. J. 1994, Comments Astrophys., 17, 189
Norris, J. P., & Bonnell, J. T. 2006, ApJ, 643, 266
Norris, J. P., Marani, G. F., & Bonnell, J. T. 2000, ApJ, 534, 248
Norris, J. P., et al. 2005, ApJ, 627, 324
Nousek, J. A., et al. 2006, ApJ, 642, 389
Nuza, S. E., et al. 2007, MNRAS, 375, 665
Nysewander, M., Fruchter, A. S., & Pe'er, A. 2009, ApJ, 701, 824
Ofek, E. O., et al. 2007, ApJ, 662, 1129
Ohno, M., et al. 2009, GRB Coordinates Network Circular, 9334, 1
Olivares, F., et al. 2009, GRB Coordinates Network Circular, 9352, 1
O'Shaughnessy, R., Belczynski, K., & Kalogera, V. 2008, ApJ, 675, 566
Paciesas, W. S., et al. 1999, ApJS, 122, 465
Paczýnski, B. 1986, ApJ, 308, L43
Paczýnski, B. 1991, Acta Astron., 41, 257
Paczýnski, B. 1998, ApJ, 494, L45
Page, K. L., et al. 2007, ApJ, 663, 1125
Palmer, D. M., et al. 2005, Nature, 434, 1107
Palmer, D., et al. 2006, GRB Coordinates Network, 5076, 1
Pal'shin, V., et al. 2008, GRB Coordinates Network Circular, 8256, 1
Panaitescu, A., & Kumar, P. 2001, ApJ, 560, L49
Panaitescu, A., & Kumar, P. 2002, ApJ, 571, 779
Panaitescu, A., Kumar, P., & Narayan, R. 2001, ApJ, 561, L171
Panaitescu, A., & Mészáros, P. 1999, ApJ, 526, 707
Pe'er, A., Mészáros, P., & Rees, M. J. 2006, ApJ, 642, 995
Pe'er, A., et al. 2007, ApJ, 664, L1
Perez-Ramirez, D., et al. 2008, A&A, submitted (arXiv:0810.2107)
Perley, D. A., et al. 2007a, GRB Coordinates Network Circular, 7140, 1
Perley, D. A., et al. 2007b, GRB Coordinates Network Circular, 7889, 1
Perley, D. A., et al. 2009, ApJ, 696, 1871
Perna, R., Armitage, P. J., & Zhang, B. 2006, ApJ, 636, L29
Pian, E., et al. 2006, Nature, 442, 1011
Piranomonte, S., et al. 2008, A&A, 492, 775
Piro, L., et al. 2002, ApJ, 577, 680
Piro, L., et al. 2005, ApJ, 623, 314
Price, P. A., et al. 2002, ApJ, 573, 85
Price, P. A., et al. 2003, ApJ, 589, 838
Prochaska, J. X., et al. 2004, ApJ, 611, 200
Prochaska, J. X., et al. 2006, ApJ, 642, 989
Proga, D., & Zhang, B. 2006, MNRAS, 370, L61
Proga, D., et al. 2003, ApJ, 599, L5
Qin, Y. 2009, ApJ, 691, 811
Racusin, J. L., et al. 2009, ApJ, 698, 43
Rau, A., Salvato, M., & Greiner, J. 2005, A&A, 444, 425
Rau, A., et al. 2009, GRB Coordinates Network Circular, 9353, 1
Rees, M. J., & Mészáros, P. 1992, MNRAS, 258, 41P
Rees, M. J., & Mészáros, P. 1994, ApJ, 430, L93
Rees, M. J., & Mészáros, P. 2005, ApJ, 628, 847
Reichart, D. E., et al. 2001, ApJ, 552, 57

Rhoads, J. E. 1999, ApJ, 525, 737
Romano, P., et al. 2006, A&A, 456, 917
Roming, P. W. A., et al. 2005, Space Sci. Rev. 2005, 120, 95
Roming, P. W. A., et al. 2006, ApJ, 651, 985
Rossi, E., Lazzati, D., & Rees, M. J. 2002, MNRAS, 332, 945
Rosswog, S. 2007, MNRAS, 376, L48
Rosswog, S., Ramirez-Ruiz, E., & Davies, M. B. 2003, MNRAS, 345, 1077
Ryde, F. 2005, ApJ, 625, L95
Ryde, F., & Pe'er, A. 2008, ApJ, submitted (arXiv:0811.4135)
Sakamoto, T., et al. 2005, ApJ, 629, 311
Sakamoto, T., et al. 2006, ApJ, 636, L73
Sakamoto, T., et al. 2007, GRB Coordinates Network, 7156, 1
Sakamoto, T., et al. 2008, GRB Coordinates Network, 7761, 1
Sato, G., et al. 2005, GRB Coordinates Network, 3793, 1
Sato, G., et al. 2006a, GRB Coordinates Network, 5064, 1
Sato, G., et al. 2006b, GRB Coordinates Network, 5381, 1
Sato, G., et al. 2007, GRB Coordinates Network, 7148, 1
Salmonson, J. D. 2000, ApJ, 544, L115
Salvaterra, R., et al. 2009, Nature, in press (arXiv:0906.1578)
Sari, R., Piran, T., & Halpern, J. P. 1999, ApJ, 519, L17
Savaglio, S., Glazebrook, K., & Le Borgne, D. 2009, ApJ, 691, 182
Sazonov, S. Y., Lutovinov, A. A., & Sunyaev, R. A. 2004, Nature, 430, 646
Shen, R.-F., Song, L.-M., & Li, Z. 2005, MNRAS, 362, 59
Shirasaki, Y., et al. 2008, PASJ, 60, 919
Sironi, L., & Spitkovsky, A. 2009, ApJ, 698, 1523
Smith, M. J. S., et al. 1998, IAU Circ., 6938, 1
Soderberg, A. M., Berger, E., & Schmidt, B. P. 2006a, GRB Coordinates Network, 4804, 1
Soderberg, A. M., et al. 2004, ApJ, 606, 994
Soderberg, A. M., et al. 2006b, ApJ, 650, 261
Soffitta, P., et al. 2001, in Gamma-ray Bursts in the Afterglow Era, ed. E. Costa, F. Frontera, & J. Hjorth (Berlin: Springer), 201
Spruit, H. C., Daigne, F., & Drenkhahn, G. 2001, A&A, 369, 694
Staff, J., Ouyed, R., & Bagchi, M. 2007, ApJ, 667, 340
Stanek, K. Z., et al. 2003, ApJ, 591, L17
Stanek, K. Z., et al. 2005, ApJ, 626, L5
Stratta, G., et al. 2007, A&A, 474, 827
Tanvir, N. R., Chapman, R., Levan, A. J., & Priddey, R. S. 2005, Nature, 438, 991
Tanvir, N. R., et al. 2009, Nature, in press (arXiv:0906.1577)
Thompson, C. 1994, MNRAS, 270, 480
Thompson, C. 2006, ApJ, 651, 333
Thompson, C., Mészáros, P., & Rees, M. J. 2007, ApJ, 666, 1012
Thöne, C. C., et al. 2008, ApJ, 676, 1151
Tinney, C., Stathakis, R., Cannon, R., & Galama, T. 1998, IAU Circ., 6896, 3
Tominaga, N., et al. 2007, ApJ, 657, L77
Troja, E., et al. 2008, MNRAS, 385, L10
Ulanov, M. V., et al. 2005, Nuovo Cimento C, 28, 351
Usov, V. V. 1992, Nature, 357, 472
Usov, V. V. 1994, MNRAS, 267, 1035
Vetere, L., et al. 2008, in AIP Conf. Ser. 1000, Gamma-Ray Bursts 2007: Proceedings of the Santa Fe Symp., ed. M. Galassi, D. Palmer, & E. Fenimore (Melville, NY: AIP), 191
Villasenor, J. S., et al. 2005, Nature, 437, 855
Virgili, F. J., Liang, E.-W., & Zhang, B. 2009a, MNRAS, 392, 91
Virgili, F. J., Zhang, B., O'Brien, P. T., & Troja, E. 2009b, ApJ, submitted
Vreeswijk, P., Fruchter, A., Hjorth, J., & Kouveliotou, C. 2003, GRB Coordinates Network, 1785, 1
Vreeswijk, P. M., et al. 2001, ApJ, 546, 672
Yamazaki, R., Yonetoku, D., & Nakamura, T. 2004, in AIP Conf. Ser. 727, Gamma-Ray Bursts: 30 Years of Discovery, ed. E. Fenimore & M. Galassi (Melville, NY: AIP), 416
Wolf, C., & Podsiadlowski, P. 2007, MNRAS, 375, 1049
Woosley, S. E. 1993, ApJ, 405, 273
Woosley, S. E., & Bloom, J. S. 2006, ARA&A, 44, 507
Xu, D., et al. 2009, ApJ, 696, 971
Yamazaki, R., Ioka, K., & Nakamura, T. 2004a, ApJ, 607, L103
Yamazaki, R., Ioka, K., & Nakamura, T. 2004b, ApJ, 606, L33
Yi, T., Liang, E., Qin, Y., & Lu, R. 2006, MNRAS, 367, 1751
Yonetoku, D., et al. 2004, ApJ, 609, 935
Yost, S. A., Harrison, F. A., Sari, R., & Frail, D. A. 2003, ApJ, 597, 459
Zhang, B. 2006, Nature, 444, 1010
Zhang, B. 2007, Chin. J. Astron. Astrophys., 7, 1
Zhang, B., Dai, X., Lloyd-Ronning, N. M., & Mészáros, P. 2004, ApJ, 601, L119
Zhang, B., & Mészáros, P. 2002a, ApJ, 581, 1236
Zhang, B., & Mészáros, P. 2002b, ApJ, 571, 876
Zhang, B., & Pe'er, A. 2009, ApJ, 700, L65
Zhang, B., Zhang, B.-B., Liang, E.-W., Gehrels, N., Burrows, D. N., & Mészáros, P. 2007a, ApJ, 655, L25
Zhang, B., et al. 2006, ApJ, 642, 354
Zhang, B., et al. 2007b, ApJ, 655, 989
Zhang, B.-B., Zhang, B., Liang, E.-W., & Wang, X.-Y. 2009, ApJ, 690, L10
Zhang, F.-W. 2008, ApJ, 685, 1052
Zhang, F.-W., & Qin, Y.-P. 2008, New Astron., 13, 485
Zhang, W., Woosley, S. E., & MacFadyen, A. I. 2003, ApJ, 586, 356
Zheng, Z., & Ramirez-Ruiz, E. 2007, ApJ, 665, 1220
Ziaeepour, H., et al. 2006, GRB Coordinates Network, 21, 2